UNIVERSITAT ROVIRA I VIRGILI
NUMERICAL AND EXPERIMENTAL STUDY OF TRANSIENT LAMINAR NATURAL CONVECTION OF HIGH PRANDTL NUMBER FLUIDS IN A CUBICAL CAVITY
Obai Younis Taha Elamin
ISBN:978-84-692-9056-9/DL:T-2069-2009

DOCTORAL THESIS

Obai Younis Taha Elamin

NUMERICAL AND EXPERIMENTAL STUDY OF TRANSIENT LAMINAR NATURAL CONVECTION OF HIGH PRANDTL NUMBER FLUIDS IN A CUBICAL CAVITY

Department of Mechanical Engineering

UNIVERSITAT ROVIRA I VIRGILI

UNIVERSITAT ROVIRA I VIRGILI
NUMERICAL AND EXPERIMENTAL STUDY OF TRANSIENT LAMINAR NATURAL CONVECTION OF HIGH PRANDTL NUMBER FLUIDS IN A CUBICAL CAVITY
Obai Younis Taha Elamin
ISBN:978-84-692-9056-9/DL:T-2069-2009

UNIVERSITAT ROVIRA I VIRGILI
NUMERICAL AND EXPERIMENTAL STUDY OF TRANSIENT LAMINAR NATURAL CONVECTION OF HIGH PRANDTL NUMBER FLUIDS IN A CUBICAL CAVITY
Obai Younis Taha Elamin
ISBN:978-84-692-9056-9/DL:T-2069-2009

Obai Younis Taha Elamin

NUMERICAL AND EXPERIMENTAL STUDY OF TRANSIENT LAMINAR NATURAL CONVECTION OF HIGH PRANDTL NUMBER FLUIDS IN A CUBICAL CAVITY

DOCTORAL THESIS

Supervised by
Dr. Jordi Pallarès Curto and
Dr. Francesc Xavier Grau Vidal

Department of Mechanical Engineering

UNIVERSITAT ROVIRA I VIRGILI

Tarragona
2009

UNIVERSITAT ROVIRA I VIRGILI
NUMERICAL AND EXPERIMENTAL STUDY OF TRANSIENT LAMINAR NATURAL CONVECTION OF HIGH PRANDTL NUMBER FLUIDS IN A CUBICAL CAVITY
Obai Younis Taha Elamin
ISBN:978-84-692-9056-9/DL:T-2069-2009

UNIVERSITAT ROVIRA I VIRGILI
NUMERICAL AND EXPERIMENTAL STUDY OF TRANSIENT LAMINAR NATURAL CONVECTION OF HIGH PRANDTL NUMBER FLUIDS IN A CUBICAL CAVITY
Obai Younis Taha Elamin
ISBN:978-84-692-9056-9/DL:T-2069-2009

El Catedràtic d'Universitat Francesc Xavier Grau Vidal i el Professor titular d'Universitat Jordi Pallarès Curto de l'Escola Tècnica Superior d'Enginyeria Química de la Universitat Rovira i Virgili,

Fan constar:

Que el present treball, amb títol:

Numerical and Experimental Study of Transient Laminar Natural Convection of High Prandtl Number Fluids in a Cubical Cavity

que presenta en Obai Younis Taha Elamin per optar al grau de doctor en Enginyeria Química ha estat realitzat sota la nostra immediata direcció i que tots els resultats obtinguts són fruit dels experiments i anàlisis realitzats per l'esmentat doctorand.

I, perquè en prengueu coneixement i tingui els efectes que correspongui, signem aquesta certificació.

Tarragona, octubre de 2009

Dr. Francesc Xavier Grau Vidal Dr. Jordi Pallarès Curto

UNIVERSITAT ROVIRA I VIRGILI
NUMERICAL AND EXPERIMENTAL STUDY OF TRANSIENT LAMINAR NATURAL CONVECTION OF HIGH PRANDTL NUMBER FLUIDS IN A CUBICAL CAVITY
Obai Younis Taha Elamin
ISBN:978-84-692-9056-9/DL:T-2069-2009

UNIVERSITAT ROVIRA I VIRGILI
NUMERICAL AND EXPERIMENTAL STUDY OF TRANSIENT LAMINAR NATURAL CONVECTION OF HIGH PRANDTL NUMBER FLUIDS IN A CUBICAL CAVITY
Obai Younis Taha Elamin
ISBN:978-84-692-9056-9/DL:T-2069-2009

To my parents,
To my wife and sons,
To my brother and sisters,
and
To all my friends

UNIVERSITAT ROVIRA I VIRGILI
NUMERICAL AND EXPERIMENTAL STUDY OF TRANSIENT LAMINAR NATURAL CONVECTION OF HIGH PRANDTL NUMBER FLUIDS IN A CUBICAL CAVITY
Obai Younis Taha Elamin
ISBN:978-84-692-9056-9/DL:T-2069-2009

UNIVERSITAT ROVIRA I VIRGILI
NUMERICAL AND EXPERIMENTAL STUDY OF TRANSIENT LAMINAR NATURAL CONVECTION OF HIGH PRANDTL NUMBER FLUIDS IN A CUBICAL CAVITY
Obai Younis Taha Elamin
ISBN:978-84-692-9056-9/DL:T-2069-2009

Contents

Abstract **v**

Resumen **ix**

Acknowledgements **xiii**

List of Figures **xv**

List of Tables **xviii**

1 Introduction **1**

1.1 Heat transfer 1

1.2 Natural Convection 2

1.3 Previous studies 2

1.3.1 Analytical 3

1.3.2 Experimental 3

1.3.3 Numerical 4

1.4 Motivation and Objective 5

2 Mathematical approach **7**

2.1 Governing equations 7

2.2 Numerical methods 8

2.2.1 Finite volume 8

2.2.2 The central differencing scheme 9

2.2.3 Crank-Nicolson scheme 10

2.2.4 Adams-Bashforth scheme 10

2.2.5 TDMA Solver 10

2.2.6 Fractional step method 12

UNIVERSITAT ROVIRA I VIRGILI
NUMERICAL AND EXPERIMENTAL STUDY OF TRANSIENT LAMINAR NATURAL CONVECTION OF HIGH PRANDTL NUMBER FLUIDS IN A CUBICAL CAVITY
Obai Younis Taha Elamin
ISBN:978-84-692-9056-9/DL:T-2069-2009

3 Experimental approaches **15**

3.1 Experimental setup 15

3.2 Shadowgraph 16

3.2.1 Principle 17

3.2.2 Optical setup 21

4 Results and discussions **23**

4.1 Numerical simulation of transient laminar natural convection in a cubical cavity at $Ra = 10^6$ and $Pr = 4.10^4$: Effect of the variable viscosity and thermal boundary conditions 24

4.1.1 Method validation 27

4.1.2 Instantaneous fields 29

4.1.3 Time Averaged quantities 42

4.2 Experiments and numerical simulation of transient natural convection in a side-cooled cubical cavity: Scaling for variable viscosity fluids 46

4.2.1 Experiments of transient natural convection in a side-cooled cubical cavity 47

4.2.2 Numerical simulation of transient natural convection in a side-cooled cubical cavity 66

5 Conclusions **81**

5.1 Numerical simulation of high Prandtl number fluid in a cavity . 81

5.2 Shadowgraph observations of transient natural convection in a side-cooled cavity 82

5.3 Numerical simulation of transient natural convection in a side-cooled cavity 83

6 Conclusiones **85**

6.1 Simulación numérica de un fluido con elevado número de Prandtl en una cavidad 85

6.2 Observaciones shadowgraph de la convección natural transitoria en una cavidad refrigerada lateralmente 86

6.3 Simulación numérica de la convección natural transitoria en una cavidad refrigerada lateralmente 87

UNIVERSITAT ROVIRA I VIRGILI
NUMERICAL AND EXPERIMENTAL STUDY OF TRANSIENT LAMINAR NATURAL CONVECTION OF HIGH PRANDTL NUMBER FLUIDS IN A CUBICAL CAVITY
Obai Younis Taha Elamin
ISBN:978-84-692-9056-9/DL:T-2069-2009

7 Future work **89**

Nomenclature **91**

Bibliography **93**

UNIVERSITAT ROVIRA I VIRGILI
NUMERICAL AND EXPERIMENTAL STUDY OF TRANSIENT LAMINAR NATURAL CONVECTION OF HIGH PRANDTL NUMBER FLUIDS IN A CUBICAL CAVITY
Obai Younis Taha Elamin
ISBN:978-84-692-9056-9/DL:T-2069-2009

UNIVERSITAT ROVIRA I VIRGILI
NUMERICAL AND EXPERIMENTAL STUDY OF TRANSIENT LAMINAR NATURAL CONVECTION OF HIGH PRANDTL NUMBER FLUIDS IN A CUBICAL CAVITY
Obai Younis Taha Elamin
ISBN:978-84-692-9056-9/DL:T-2069-2009

Abstract

Free convection in enclosed spaces is found widely in natural and industrial systems. It is a topic of primary interest because in many systems it provides the largest resistance to the heat transfer in comparison with other heat transfer modes. In such systems the convection is driven by a density gradient within the fluid, which, usually, is produced by a temperature difference between the fluid and surrounding walls.

For example, in the oil industry, some fuel-oils have Prandtl numbers as high as 10^8. They are usually stored and transported in large tanks at temperatures high enough to keep its viscosity and, thus the pumping requirements, to a reasonable level. In some cases, the tanks have mechanical stirrers or mixers to obtain a better temperature uniformity. In absence of mechanical agitation, a temperature difference between the fluid and the walls of the container may give rise to the unsteady buoyancy force and hence to the unsteady natural convection. As the oil cools down it typically becomes more viscous. At this point the oil viscosity becomes very large and unloading of the tank becomes very difficult. This scenario happened, for example, during the accident of the Prestige tanker [1]. In these situations, it is of primary interest to be able to predict the cooling rate of the oil.

The general objective of this work is to develop and validate a simulation tool able to predict the cooling rates of oil in a tank. This tool has to take into account the variation of the oil viscosity to give detailed information of the cooling rates of the oil under different realistic thermal boundary conditions, as those present in real systems. However, the wide ranges of length, time

[1] On the 19^{th} November 2002 the Prestige tanker carrying about 77000 tones of fuel-oil sunk to the depth of 3600 m some 250 km offshore the coast of Galicia (Spain) with a large quantity of oil remaining on board. The oil was being transported at about 50^oC and the temperature at the depth of 3600 m was estimated to be 3^oC. Predictions of the cooling rates of the fuel can be found in Fernández et al. [1] and in Pallarès et al. [2]

ISBN:978-84-692-9056-9/DL:T-2069-2009

and velocity scales of the cooling process in real systems constitute a serious problem for the complete numerical simulation of the time evolution of the flow and of the temperature distribution.

As a first step towards this general objective, this study analyzes numerically and experimentally the laminar transient natural convection of high Prandlt fluids in cubical cavities. The fluid is considered to be initially hot and at rest. The natural convection flow is initiated by cooling all or some of the walls of the cavity.

First, the influence of different thermal wall boundary conditions, the variation of the viscosity and the wall conductivity on the transient laminar natural convection flow in a cubical cavity with the six walls thermally active is analyzed. In this system the unstable stratification imposed by the top wall of the cavity coexists and interacts with the thermal and velocity boundary layers developed near the side walls of the cavity. It is found that the instantaneous flow field is significantly affected by the effect of the variable viscosity. However this effect is damped out in the averaged quantities (e.g. averaged temperature and heat transfer rate). The consideration of the wall conductivity adds an additional resistance to the heat transfer and delays the convection.

To analyze the individual effect of the side walls of the cavity on the cooling process, the second part of this study considers, numerically and experimentally, the transient laminar natural convection in a cubical cavity with two cold opposite vertical walls. The shadowgraph technique is employed to visualize the development of the transient convective flow. The results indicate that the transient flow development is characterized by the following distinct processes: the initial growth of the vertical boundary layers, the formation and interaction of the horizontal intrusions and the thermal stratification of the cavity. New scaling relations that take into account the viscosity variation with temperature, not reported previously in the literature, are derived for the boundary layer velocities, for the time needed for the boundary layer to reach the steady state and for the velocity and thickness of the horizontal intrusions. These scaling relations are important because they indicate the length and time scales that a complete numerical simulation of the cooling process in a real system has to reproduce. Numerical simulations based on the experiments were carried out. The comparison between the numerical and the experimental results showed good agreement. A time lag between the exper-

UNIVERSITAT ROVIRA I VIRGILI
NUMERICAL AND EXPERIMENTAL STUDY OF TRANSIENT LAMINAR NATURAL CONVECTION OF HIGH PRANDTL NUMBER FLUIDS IN A CUBICAL CAVITY
Obai Younis Taha Elamin
ISBN:978-84-692-9056-9/DL:T-2069-2009

iments and the numerical results is present due to the initial conditions. In addition to the three distinct processes that characterize the flow development; three substages in the initial growth stage are identified: the start-up stage, the transition stage and the steady state stage. The instantaneous flow field is slightly affected by the viscosity variation due to the relatively low Prandtl number and viscosity contrast. Although the magnitude of the convective velocity is larger for higher Prandtl numbers. The results showed that the onset of convection is delayed for high Prandtl numbers.

UNIVERSITAT ROVIRA I VIRGILI
NUMERICAL AND EXPERIMENTAL STUDY OF TRANSIENT LAMINAR NATURAL CONVECTION OF HIGH PRANDTL NUMBER FLUIDS IN A CUBICAL CAVITY
Obai Younis Taha Elamin
ISBN:978-84-692-9056-9/DL:T-2069-2009

UNIVERSITAT ROVIRA I VIRGILI
NUMERICAL AND EXPERIMENTAL STUDY OF TRANSIENT LAMINAR NATURAL CONVECTION OF HIGH PRANDTL NUMBER FLUIDS IN A CUBICAL CAVITY
Obai Younis Taha Elamin
ISBN:978-84-692-9056-9/DL:T-2069-2009

Resumen

La convección natural en espacios cerrados se encuentra ampliamente en sistemas naturales e industriales. Se trata de un tema de interés porque en muchos sistemas ofrece la mayor resistencia dentro de los diferentes modos de transferencia de calor que pueden ocurrir. En tales sistemas, la convección esta impulsada por un gradiente de densidad en el fluido que, generalmente, se produce por una diferencia de temperatura entre el fluido y las paredes de los alrededores.

Por ejemplo, en la industria del petróleo, algunos fuelóleos pueden alcanzar números de Prandtl del orden de 10^8. Por lo general estos fluidos son almacenados y transportados en grandes tanques a temperaturas suficientemente altas para mantener su viscosidad, y por lo tanto los requisitos de bombeo, a un nivel razonable. En algunos casos los tanques tienen agitadores mecánicos o mezcladores para obtener una temperatura más uniforme. En ausencia de agitación mecánica, la diferencia de temperatura entre el fluido y las paredes del recipiente puede dar lugar a una fuerza de flotación inestable y, por ende, a una convección natural inestable. Cuando el aceite se enfría normalmente se vuelve más viscoso. En este punto, la viscosidad del aceite es muy grande y la descarga del tanque se hace muy difícil. Esta situación ocurrió, por ejemplo, durante el accidente del petrolero Prestige [2]. En estas situaciones es de interés primordial la capacidad de predecir la velocidad de enfriamiento del aceite.

El objetivo general de este trabajo es desarrollar y validar una herramienta de simulación capaz de predecir las tasas de enfriamiento de aceite en un

[2] El 19 de noviembre de 2002, el petrolero Prestige transportaba alrededor de 77.000 toneladas de fuel-oil cuando se hundió a una profundidad de 3600 m a unos 250 km de la costa de Galicia (España). Una importante cantidad de aceite quedó a bordo. El aceite se transportaba a unos 50^oC y la temperatura a 3600 m de profundidad se estimó en 3^oC. En Fernández et al. [1] y Pallarès et al. [2] se pueden encontrar predicciones de las velocidades de refrigeración del combustible.

UNIVERSITAT ROVIRA I VIRGILI
NUMERICAL AND EXPERIMENTAL STUDY OF TRANSIENT LAMINAR NATURAL CONVECTION OF HIGH PRANDTL NUMBER FLUIDS IN A CUBICAL CAVITY
Obai Younis Taha Elamin
ISBN:978-84-692-9056-9/DL:T-2069-2009

tanque. Esta herramienta ha de tener en cuenta la variación de la viscosidad del aceite para dar información detallada de las tasas de enfriamiento de éste bajo diferentes condiciones de contorno térmicas realísticas, como las presentes en sistemas reales. Sin embargo, la amplia gama de escalas de longitud, tiempo y velocidad del proceso de enfriamiento en sistemas reales constituyen un grave problema para la completa simulación numérica de la evolución temporal del flujo, y de la distribución de la temperatura.

Como primer paso hacia este objetivo general, este estudio analiza numérica y experimentalmente la convección natural laminar transitoria de fluidos con alto número de Prandlt en cavidades cúbicas. El fluido se considera inicialmente caliente y en reposo. El flujo de convección natural se inicia con el enfriamiento todas o algunas de las paredes de la cavidad.

En primer lugar, se analiza la influencia de diferentes condiciones de contorno térmicas en las paredes, de la variación de la viscosidad y de la conductividad de la pared, en la convección natural del flujo laminar transitorio en una cavidad cúbica con seis paredes térmicamente activas. En este sistema, la estratificación inestable impuesta por la pared superior de la cavidad convive e interactúa con las capas límites térmicas y de velocidad que se desarrollan cerca de las paredes laterales de la cavidad. Se encontró que el campo de flujo se ve afectado significativamente por efecto de la viscosidad variable. No obstante, este efecto se ve amortiguado en las cantidades promedio (e.g. temperatura y tasa de transferencia de calor). Al tener en cuenta la conducción en la pared se añade una resistencia adicional a la transferencia de calor y se retrasa la convección.

Para analizar el efecto individual de las paredes laterales de la cavidad en el proceso de enfriamiento la segunda parte de este estudio considera, numérica y experimentalmente, la convección natural laminar transitoria en una cavidad cúbica con dos paredes verticales opuestas frías. La técnica llamada (shadowgraph) se ha empleado para visualizar el desarrollo del flujo transitorio convectivo. Los resultados indican que el desarrollo del flujo transitorio se caracteriza por los siguientes procesos: el crecimiento inicial de las capas límite verticales, la formación e interacción de las intrusiones horizontales y la estratificación térmica de la cavidad. Se han derivado nuevas relaciones de escala que tienen en cuenta la variación de la viscosidad con la temperatura, no publicadas anteriormente en la literatura, para las velocidades de capa límite, para el tiempo

UNIVERSITAT ROVIRA I VIRGILI
NUMERICAL AND EXPERIMENTAL STUDY OF TRANSIENT LAMINAR NATURAL CONVECTION OF HIGH PRANDTL NUMBER FLUIDS IN A CUBICAL CAVITY
Obai Younis Taha Elamin
ISBN:978-84-692-9056-9/DL:T-2069-2009

que tarda la capa límite en alcanzar el estado estacionario y para la velocidad y el espesor de las intrusiones horizontales. Estas relaciones de escala son importantes porque indican las escalas de longitud y tiempo que tiene que reproducir una simulación numérica completa del proceso de enfriamiento en un sistema real. Se han llevado a cabo simulaciones numéricas basadas en los experimentos. La comparación de los resultados numéricos con los experimentales muestra un buen ajuste. Se observa una diferencia de tiempo entre los experimentos y los resultados numéricos debido a las condiciones iniciales. Además de los tres diferentes procesos que caracterizan el desarrollo del flujo se identifican tres subetapas en la etapa inicial de crecimiento: la etapa de arranque, la etapa de transición y la etapa de estado estacionario. El campo de flujo instantáneo es afectado ligeramente por la variación de la viscosidad pero estas diferencias no son excesivamente altas debido a un número de Prandtl y un contraste de viscosidad relativamente bajos. Aunque la magnitud de la velocidad convectiva es más alta para números de Prandtl más altos, los resultados muestran que la aparición de la convección se retrasa para números de Prandtl altos.

UNIVERSITAT ROVIRA I VIRGILI
NUMERICAL AND EXPERIMENTAL STUDY OF TRANSIENT LAMINAR NATURAL CONVECTION OF HIGH PRANDTL NUMBER FLUIDS IN A CUBICAL CAVITY
Obai Younis Taha Elamin
ISBN:978-84-692-9056-9/DL:T-2069-2009

UNIVERSITAT ROVIRA I VIRGILI
NUMERICAL AND EXPERIMENTAL STUDY OF TRANSIENT LAMINAR NATURAL CONVECTION OF HIGH PRANDTL NUMBER FLUIDS IN A CUBICAL CAVITY
Obai Younis Taha Elamin
ISBN:978-84-692-9056-9/DL:T-2069-2009

Acknowledgements

I would like to acknowledge my supervisors Prof. Francesc Xavier Grau Vidal and Dr. Jordi Pallarès Curto for their guidance, support and for their valuable comments.

I would also like to thank all the PhD students of the ECOMMFIT group for shearing me not only the office but also the knowledge, and for helping me in virtually every thing, especially Roland Blanch.

I am also grateful to Dr. Alexandre Fabregat Tomàs for his great help in LaTeX, Linux and FORTRAN, and for his valuable comments and dissections.

I would also like to express my sincere gratitude to Prof. John C. Patterson, Dr. Feng Xu and Dr. Chengwang Lei, for hosting me in the Natural convection Laboratory of the James Cook University, Townsville, Australia. Their help and discussion on the experimental work is highly appreciated.

I am also grateful to Prof. Serguei Martemianov for hosting me in the Heat transfer Laboratory of Poitiers University, Poitiers, France.

I really appreciate the help from Núria Juanpere Mitjana and Samuel Garcia Mega for taking care of the administrative stuff.

I am pleased to thank Universitat Rovira I Virgili, The Catalan Government, Spanish ministry of education and University of Khartoum (Sudan) who sponsored all of my tuition and living cost as well as research cost during my study.

My thanks extend to the Sudanese community in Catalonia, Arab student community in URV and AIAT members in Tarragona for providing me with the social environment, that I've never felt away from home.

Very Special thanks to Abd Elahmid Tafzi, Abd Elkadir Alkorachi, Khalid Hasani, Saeed Elmotaki, Bou Midian Malah and Abd Elrhman Huikmat and their families for providing spiritual support at critical and opportune times.

Lastly but first in mind, I would like to express my gratitude to my Par-

UNIVERSITAT ROVIRA I VIRGILI
NUMERICAL AND EXPERIMENTAL STUDY OF TRANSIENT LAMINAR NATURAL CONVECTION OF HIGH PRANDTL NUMBER FLUIDS IN A CUBICAL CAVITY
Obai Younis Taha Elamin
ISBN:978-84-692-9056-9/DL:T-2069-2009

ents, my brother, my sisters and in particular my wife and my sons for their unconditional love and support.

Above all, thank Allah the almighty, for his help, care and protection.

UNIVERSITAT ROVIRA I VIRGILI
NUMERICAL AND EXPERIMENTAL STUDY OF TRANSIENT LAMINAR NATURAL CONVECTION OF HIGH PRANDTL NUMBER FLUIDS IN A CUBICAL CAVITY
Obai Younis Taha Elamin
ISBN:978-84-692-9056-9/DL:T-2069-2009

List of Figures

2.1 Grid nomenclature. Small letters denote the faces of the control volume and the capital letters denote the nodes 10

3.1 Sketch of the experimental model 16
3.2 Direct shadowgraph 17
3.3 Focused shadowgraph 18
3.4 Schematic of the optic setup of the focused shadowgraph 20

4.1 The computational domain 25
4.2 Variation of Corn Syrup viscosity with temperature 25
4.3 The mesh 27
4.4 Temperature and stream function contours (continuous line: Lin and Armfield, dashed line: present study),(a)temperature contours at $\tau = 3$,(b)temperature contours at $\tau = 5$,(c)stream function contours at $\tau = 3$,(d)stream function contours at $\tau = 5$, (τ is the nondimensional time). 28
4.5 Velocity vectors and temperature contours at $t = 90$ s, cases 1-4 (see Table (4.1)). 30
4.6 Velocity vectors and temperature contours at $t = 90$ s, cases 5-8 (see Table (4.1)). 31
4.7 Velocity vectors and temperature contours at $t = 1200$ s, cases 1-4 (see Table (4.1)). 33
4.8 Velocity vectors and temperature contours at $t = 1200$ s, cases 5-8 (see Table (4.1)). 35
4.9 Budget of X momentum along Y -axis at $z^* = 0.5, x^* = 0.75$ and $t = 1200$ s. 37

4.10 The isosurfaces of the second largest eigenvalue of the velocity tensor $t = 1200$ s, , cases 1-4 (see Table (4.1)). 38
4.11 Velocity vectors and temperature contours at $t = 1800$ s, cases 1-4 (see Table (4.1)). 40
4.12 Velocity vectors and temperature contours at $t = 1800$ s, cases 5-8 (see Table (4.1)). 41
4.13 Time evolution of the non-dimensional volume averaged temperature 43
4.14 Time evolution of the overall Nusselt number 44
4.15 Time evolution of the overall Nusselt number 44
4.16 Time evolution of the local Nusselt numbers at the top and bottom walls for CV1 45
4.17 Growth of the boundary layer and horizontal intrusions for case 2 ($Ra = 2.6.10^8$, $Pr = 7$, $\frac{\nu_c}{\nu_h} = 1$) (see Table (4.2)), $(a)t = 3$ s, $(b)t = 5$ s, $(c)t = 8$ s, $(d)t = 9$ s, $(e)t = 11$ s, $(f)t = 13$ s, $(g)t = 14$ s, $(h)t = 15s$. 48
4.18 Time evolution of boundary layer thickness 49
4.19 $\delta Ra^{1/4}$ against $\tau^{1/2}$ 50
4.20 The observed time for the thermal boundary layer to reach the maximum thickness plotted against the time scale. J&P stands for Jeevaraj and Patterson [8]. 52
4.21 Development of the horizontal intrusions for case 2 ($Ra = 2.6.10^8$, $Pr = 7$, $\frac{\nu_c}{\nu_h} = 1$)(see Table (4.2)), $(a)t = 18$ s, $(b)t = 20$ s, $(c)t = 28$ s and $(d)t = 33$ s. 54
4.22 Development of the horizontal intrusions at different Rayleigh numbers at $t = 14$ s and $Pr = 7$, $(a)Ra = 0.9.10^8$ case (1), $(b)Ra = 2.6.10^8$ case (2), $(c)Ra = 4.2.10^8$ case (3), $(d)Ra = 5.9.10^8$ case (4). 54
4.23 Observed intrusion velocity plotted against the intrusion velocity scale given in Equation (4.20) and Equation (4.21) 58
4.24 Observed intrusion thickness for cases 1-10 plotted against the intrusion thickness scale given in Equation (4.22) and Equation (4.23). 59

4.25 Development of the horizontal intrusions at different Prandtl numbers at $t = 33$ s and $Ra \approx 5.10^7$ for, $(a)Pr = 21$, $Ra = 6.74.10^7$ case 6, $(b)Pr = 55$, $Ra = 3.1.10^7$ case 7 and $(c)Pr = 190$, $Ra = 4.1.10^7$ case 9. 59

4.26 The observed distance travelled by the intrusion and the scale (Equation (4.20)and Equation (4.21)) plotted against time, $Ra \approx 5.10^7$ 60

4.27 The observed intrusion thickness and the scale (Equation (4.22)and Equation (4.23)) plotted against time, $Ra \approx 5.10^7$ 60

4.28 The development of double-layer structure for case 2, ($Ra = 2.6.10^8$, $Pr = 7$, $\frac{\nu_c}{\nu_h} = 1$) (see Table (4.2)), $(a)t = 58$ s, $(b)t = 68$ s, $(c)t = 96$ s and $(d) = 133$ s. 62

4.29 Double-layer structure at different Rayleigh number at $t = 89$ s and $Pr \approx 7$, $(a)Ra = 9.10^7$ case 1, $(b)Ra = 2.6.10^8$ case 2, $(c)Ra = 4.2.10^8$ case 3 and $(d)Ra = 5.9.10^8$ case 4. 64

4.30 Double-layer structure at different Prandtl number at $t = 143$ s, and $Ra \approx 5.10^7$, $(a)Pr = 21$, $Ra = 6.74.10^7$ case 6, $(b)Pr = 55$, $Ra = 3.1.10^7$ case 7 and $(c)Pr = 190$, $Ra = 4.1.10^7$ case 9, the white arrow indicates the height of the double-layer structure. . 64

4.31 x_s^* against $\tau/Ra^{1/4}$ 65

4.32 Shadowgraph images (experimental) and nondimensional temperature contours (numerical) for case 1 ($Ra = 9.10^7$, $Pr = 8.24$, $\frac{\nu_c}{\nu_h} = 1$) (contours between -1 to -0.1 with an interval of 0.1, and the contour $T^* = -0.01$). 68

4.33 Substages of the initial growth stage, (a) the local temperature at $x^* = 0.05$ and $y^* = 0.5$, (b) local thermal boundary layer thickness at $x^* = 0.5$ and (c) the local Nusselt number at $x^* = 0.5$ for case 1 ($Ra = 9.10^7$, $Pr = 8.24$, $\frac{\nu_c}{\nu_h} = 1$) (see Table (4.2)). 69

4.34 Shadowgraph images (experimental) and nondimensional temperature contours (numerical) for the variable viscosity case 7 ($Ra = 3.1.10^7$, $Pr = 55$, $\frac{\nu_c}{\nu_h} = 1.5$) (see Table (4.2)), (contours between -1 to -0.1 with an interval of 0.1, and the contour $T^* = -0.01$). 71

4.35 The time evolution of observed (experimental) and predicted (numerical) velocity of the horizontal intrusions for case 7 ($Ra = 3.1.10^7$, $Pr = 55$, $\frac{\nu_c}{\nu_h} = 1.5$) (see Table (4.2)). 72
4.36 Non-dimensional temperature contours for case 7 ($Ra = 3.1.10^7$, $Pr = 55$, $\frac{\nu_c}{\nu_h} = 1.5$) (see Table (4.2)), (contours between -1 to -0.1 with an interval of 0.1, and the contour $T^* = -0.01$), solid line: variable viscosity simulation, dashed line: constant viscosity simulation. 73
4.37 Non-dimensional horizontal velocity contours for case 7 ($Ra = 3.1.10^7$, $Pr = 55$, $\frac{\nu_c}{\nu_h} = 1.5$) (see Table (4.2)), solid line: variable viscosity simulation, dashed line: constant viscosity simulation. . 74
4.38 Non-dimensional vertical velocity contours for case 7 ($Ra = 3.1.10^7$, $Pr = 55$, $\frac{\nu_c}{\nu_h} = 1.5$) (see Table (4.2)), solid line: variable viscosity simulation, dashed line: constant viscosity simulation. . 75
4.39 The time evolution of the observed (experimental) and the predicted (numerical) thermal boundary layer thickness for case 1 ($Ra = 9.10^7$, $Pr = 8.24$, $\frac{\nu_c}{\nu_h} = 1$) and case 10 ($Ra = 1.4.10^8$, $Pr = 120$, $\frac{\nu_c}{\nu_h} = 5.87$) (see Table (4.2)). 76
4.40 The time evolution of the predicted (numerical) horizontal intrusion thickness for case 1 ($Ra = 9.10^7$, $Pr = 8.24$, $\frac{\nu_c}{\nu_h} = 1$) and case 10 ($Ra = 1.4.10^8$, $Pr = 120$, $\frac{\nu_c}{\nu_h} = 5.87$) (see Table(4.2)). 77
4.41 The time evolution of the predicted (numerical) horizontal averaged temperature at $x^* = 0.25$ for case 1 ($Ra = 9.10^7$, $Pr = 8.24$, $\frac{\nu_c}{\nu_h} = 1$) and case 10 ($Ra = 1.4.10^8$, $Pr = 120$, $\frac{\nu_c}{\nu_h} = 5.87$) (see Table(4.1)). 78
4.42 Temperature contours for case 1 ($Ra = 9.10^7$, $Pr = 8.24$, $\frac{\nu_c}{\nu_h} = 1$), solid line: thermal boundary layer at point a (see Figure 4.41), dashed line: thermal boundary layer at point b (see Figure 4.41), (only the contour $T^* = -0.01$ is presented to show the boundary layer thickness). 79

UNIVERSITAT ROVIRA I VIRGILI
NUMERICAL AND EXPERIMENTAL STUDY OF TRANSIENT LAMINAR NATURAL CONVECTION OF HIGH PRANDTL NUMBER FLUIDS IN A CUBICAL CAVITY
Obai Younis Taha Elamin
ISBN:978-84-692-9056-9/DL:T-2069-2009

List of Tables

4.1 Studied cases 26
4.2 The experimentally and numerically studied cases 47

UNIVERSITAT ROVIRA I VIRGILI
NUMERICAL AND EXPERIMENTAL STUDY OF TRANSIENT LAMINAR NATURAL CONVECTION OF HIGH PRANDTL NUMBER FLUIDS IN A CUBICAL CAVITY
Obai Younis Taha Elamin
ISBN:978-84-692-9056-9/DL:T-2069-2009

UNIVERSITAT ROVIRA I VIRGILI
NUMERICAL AND EXPERIMENTAL STUDY OF TRANSIENT LAMINAR NATURAL CONVECTION OF HIGH PRANDTL NUMBER FLUIDS IN A CUBICAL CAVITY
Obai Younis Taha Elamin
ISBN:978-84-692-9056-9/DL:T-2069-2009

Chapter 1

Introduction

1.1 Heat transfer

Heat transfer is one of the most observed phenomena in the nature. People have always understood that something flows from hot objects to cold ones. We call that something heat. Simply heat transfer is thermal energy in transient from one body or system due to thermal contact.

The process of heat transfer attracted the researchers, engineers and designers due to its wide applications in industry (Gas turbine, heat exchanger, cooling of electrical components, etc) as well as natural aspects (weather broadcast, green house effects).

There are three different types of heat transfer modes. Conduction heat transfer occurs when there is temperature gradient in stationary medium. Convection is the mode that occurs when heat transfers between a surface and a moving fluid. The third mode is radiation, this mode does not need intervening medium, the heat transfers between two surfaces in the form of electromagnetic waves.

Better understanding of heat transfer would lead directly to great improvements in industry and hence in human life. Only few of the heat transfer problems are simple enough to be solved by analytical methods, however the rest must be tackled either using numerical methods or experimental approaches.

UNIVERSITAT ROVIRA I VIRGILI
NUMERICAL AND EXPERIMENTAL STUDY OF TRANSIENT LAMINAR NATURAL CONVECTION OF HIGH PRANDTL NUMBER FLUIDS IN A CUBICAL CAVITY
Obai Younis Taha Elamin
ISBN:978-84-692-9056-9/DL:T-2069-2009

1.2 Natural Convection

Convection heat transfer is classified according to the nature of the flow. Mainly, convection is divided into two modes. The term forced convection is used when the flow is caused by external means (e.g. using a fan to cool electrical component). While natural convection is used when the main guiding source of the flow is the buoyancy force, which arise from the density difference induced by the temperature gradients. It should be mentioned that not all kinds of the temperature gradients result in natural convection, only when temperature gradient causes the fluid density to decrease within a gravitational field.

Natural convection in cavities is a topic of primary interest, because cavities of different geometries filled with fluid are central components in a long list of engineering and geophysical systems. It is the result of the complex interaction between a finite-size fluid system in thermal communication with all the walls that confine it.

This study is focused in transient natural convection flow in a cubical cavity.

1.3 Previous studies

Transient natural convection in cubical, rectangular or cylindrical cavities has attracted numerous researchers due to its implications in a wide set of technological applications and because its geometric simplicity. The problem of natural convection was studied analytically by Batchelor [3]. Since then great attention was paid to the natural convection in cavities. Fluid properties are in general temperature dependents. For many fluids the variation of viscosity with temperature is larger than the variation of other properties. For this kind of fluids, the impact of the variable viscosity on the natural convection should be addressed. The effect of variable viscosity on the natural convection in cavities has been studied analytically, experimentally and numerically. The following subsections provide a literature review of the previous analytical, experimental and numerical work on natural convection in cavities with variable and constant viscosities. It should be noted that the amount of literature dealing with natural convection in cavities is huge and that the references cited in the next subsections have been selected by its relevance and connection with

ISBN:978-84-692-9056-9/DL:T-2069-2009

the present study.

1.3.1 Analytical

A similarity solution for laminar heat transfer boundary layer for different Prandtl numbers was introduced by Ostrach [4]. His results were in a good agreement with previous experiments. Carey and Mollendorf [5] presented perturbation analysis for three laminar convection flows in fluids with variable viscosity. They concluded that even for moderate values of the viscosity variation, significant effects on the thermal and momentum transport were found. Another analytical study was carried out by Pantokratoras [6] who confirmed the significant influence of the viscosity variation on the heat transfer and wall shear stress.

1.3.2 Experimental

The transient features of natural convection in square cavity with differentially heated side-walls were analyzed experimentally and numerically by Patterson and Armfield [7]. Several features were identified such as the presence of travelling waves instability, the existence of rapid flow divergence in the region of the outflow of the intrusions and the presence of cavity-scale oscillations. Jeevaraj and Patterson [8] investigated experimentally the transient natural convection of glycerol-water mixtures in a side-heated cavity. Recently, Xu et. al. [9] visualized the stages of transition of the transient natural convection in a side-heated cavity. They provided detailed evolution of the corner flow in the entrainment development stage, and they discussed the mechanism of formation of the double-layer structure in the quasi-steady stage. Davaille and Jaupart [10] reported experimental results of transient natural convection at high Rayleigh numbers with large viscosity variation in a tank with the bottom wall insulated and a cold top wall. They studied the effect of the viscosity variation in the unstable boundary layer located near the top wall on the onset of instabilities. They introduced a new viscous temperature scale to compute the heat transfer rate at the cold top wall of the tank and claimed that this scale is sufficient to account for the characteristics of convection. Nelson et al. [11] and Shyu et al. [12] studied the degradation of the thermal stratification in stratified storage tanks and concluded that highly conductive walls

ISBN:978-84-692-9056-9/DL:T-2069-2009

contribute to the degradation of the thermal stratification. Chen and Wu [13] conducted experiments to study the transient natural convection in a vertical slot containing a variable viscosity fluid (glycerine-water solutions). They identified several unsteady vortex processes such as, the merge of secondary vortices, the collapse and degeneration of a tertiary vortex and a sequence of vortex merging and unmerging leading to turbulent flow. They associated the last phenomena to the variable viscosity and the large Prandtl number of the fluid. Recently Oliveski et. al. [14] investigated numerically and experimentally the two dimensional transient natural convection in a tank of oil with constant viscosity. The thermal boundary conditions used in the simulations were determined experimentally.

1.3.3 Numerical

Patterson and Imberger [15] studied the unsteady natural convection in a rectangular cavity with differentially heated side-walls. They introduced scale analysis, flow classification scheme, and described the flow in terms of different stages including the growth of the boundary layer, horizontal intrusions and the steady state. The effect of variation of the physical properties on the natural convection in enclosure was studied numerically by Emry and Lee [16]. In their study, the Prandtl number was ranging from 0.01 to 1. They observed small changes in the temperature and velocity fields, while the overall heat transfer was not affected. Hyun [17] conducted numerical simulations to study the effect of Pr number on the heat up of a stratified fluid in an enclosure. This author showed that the evolution of the flow and temperature fields are influenced by the Pr number. Ogawa et al. [18] carried out three-dimensional steady calculation of natural convection in a fluid with variable viscosity. They classified the flow patterns into two main regimes depending on the behaviour of the upper boundary layer; the stagnant lid regime and the whole layer regime. They concluded that the Nusselt number of the top surface is highly dependent on the viscosity in the whole layer regime. Cotter and Michael [19] numerically studied the influence of the external heat transfer coefficient and aspect ratio of the enclosure on the transient natural convection of a warm crude oil in a vertical cylindrical storage tank located in a cold environment.

All the above mentioned studies initiate the convective flow by heating

UNIVERSITAT ROVIRA I VIRGILI
NUMERICAL AND EXPERIMENTAL STUDY OF TRANSIENT LAMINAR NATURAL CONVECTION OF HIGH PRANDTL NUMBER FLUIDS IN A CUBICAL CAVITY
Obai Younis Taha Elamin
ISBN:978-84-692-9056-9/DL:T-2069-2009

one side-wall and cooling the opposite one (e.g. Xu et. al. [9]), or by cooling/heating the top/ bottom wall (e.g. Davaille and Jaupart [10]). In the literature, it was found that the number of numerical and experimental studies that consider the cooling or heating of both side-walls or only one side-wall is rare. An example is the experimental work done by Lin and Akins [20] who studied three dimensional flow patterns inside a cubical cavity suddenly immersed in hot water. These authors found that the inclusion of the time and/or Pr number does not improve the correlation between the Nusselt and the Rayleigh numbers and that the use of the conventional correlations is accurate enough for prediction purposes. Nicolette and Yang [21] investigated numerically and experimentally the transient natural convection in two dimensional square enclosures with only one side-wall cooled and the other three walls insulated. Lin and Armfiled [22] & [23] introduced a detailed scale analysis of the natural convection cooling in rectangular and cylindrical container in which the both side-walls were cooled. They were able to identify different transient flow development processes, and obtained very good agreement between their scalings and their numerical results. Lin et.al. [24] carried out scaling analysis of cooling of a low fluid in a rectangular container and validated the scalings using direct numerical simulations.

1.4 Motivation and Objective

In the oil industry, the oil, which has Prandtl numbers of about 10^8, usually is thermally stored and transported in large tanks at high temperature. A temperature difference between the fluid and the ambient may give rise to the unsteady buoyancy force and hence the unsteady natural convection. In the initial period of cooling the natural convection regime dominates over the conduction contribution but as the oil cools it typically becomes more viscous, and this increase of viscosity inhibits the convection. At this point the oil viscosity becomes very large and unloading of the tank becomes very difficult. For this reason it is of primary interest to be able to predict the cooling rate of the oil. As discussed in the previous sections, the numerical and/or experimental study of transient natural convection cooling is rare. The lack of the experimental and numerical data for cooling of fluid with variable viscosity

UNIVERSITAT ROVIRA I VIRGILI
NUMERICAL AND EXPERIMENTAL STUDY OF TRANSIENT LAMINAR NATURAL CONVECTION OF HIGH PRANDTL NUMBER FLUIDS IN A CUBICAL CAVITY
Obai Younis Taha Elamin
ISBN:978-84-692-9056-9/DL:T-2069-2009

in cavities has motivated this study. The general objective of this work is to develop and validate a simulation tool able to predict the cooling rates of oil tank. This tool should take in to account the variation of the oil viscosity and the influence of the tank walls conductivity. As a first step towards this objective, a set of experiments were carried out for code validation in laminar regime. Another objective of this study is to provide scaling relations taking into account the variable viscosity of the fluid. These scaling were developed by studying the balance of the transport equations at different stages of the flow. Such scales are of great interest because they indicate the relevant length and time scales that have to be reproduced by a complete numerical simulation of the cooling process in real systems.

UNIVERSITAT ROVIRA I VIRGILI
NUMERICAL AND EXPERIMENTAL STUDY OF TRANSIENT LAMINAR NATURAL CONVECTION OF HIGH PRANDTL NUMBER FLUIDS IN A CUBICAL CAVITY
Obai Younis Taha Elamin
ISBN:978-84-692-9056-9/DL:T-2069-2009

Chapter 2

Mathematical approach

2.1 Governing equations

The natural convection problem considered is governed by the three-dimensional unsteady Navier - Stokes equations and the energy equation along with the Boussinesq approximation. The governing equations in non-dimensional form in Cartesian coordinates system can be written as:

$$\frac{\partial u_i^*}{\partial x_i^*} = 0 \tag{2.1}$$

$$\frac{\partial u_i^*}{\partial t^*} + \frac{\partial (u_i^* u_j^*)}{\partial x_j^*} = -\frac{\partial P^*}{\partial x_i^*} + \frac{\partial}{\partial x_j^*}\left[Pr(T^*)\left(\frac{\partial u_i^*}{\partial x_j^*} + \frac{\partial u_j^*}{\partial x_i^*}\right)\right] + \delta_{i1}\, Ra_o\, Pr_o\, T^* \tag{2.2}$$

$$\frac{\partial T^*}{\partial t^*} + \frac{\partial (u_j^* T^*)}{\partial x_j^*} = \frac{\partial^2 T^*}{\partial x_j^* \partial x_j^*} \tag{2.3}$$

The non-dimensional form the governing equations are obtained by using the following scales:

$$x_i^* = \frac{x_i}{H} \;,\; u_i^* = \frac{u_i H}{\alpha} \;,\; t^* = \frac{t\alpha}{H^2} \;,\; P^* = \frac{P}{\rho(\frac{\alpha}{H})^2} \;,\; T^* = \frac{T - T_c}{T_h - T_c} \tag{2.4}$$

UNIVERSITAT ROVIRA I VIRGILI
NUMERICAL AND EXPERIMENTAL STUDY OF TRANSIENT LAMINAR NATURAL CONVECTION OF HIGH PRANDTL NUMBER FLUIDS IN A CUBICAL CAVITY
Obai Younis Taha Elamin
ISBN:978-84-692-9056-9/DL:T-2069-2009

Where H is the dimension of the cubical cavity, and T_h and T_c are the initial and the wall temperature, respectively.

The Prandtl and Rayleigh number are defined as:

$$Ra_0 = \frac{\beta g(T_h - T_c)H^3}{\nu_0 \alpha} \tag{2.5}$$

$$Pr_0 = \frac{\nu_0}{\alpha} \tag{2.6}$$

2.2 Numerical methods

The in-house three-dimensional finite volume code named 3DINAMICS is employed to solve the discretized equations along with the associated boundary conditions. The code utilizes the staggered variable arrangement. The spatial discretization of both the diffusive and convective terms is carried out by the central differencing scheme. The time discretization for all terms is performed with the second order Crank-Nicolson scheme, except for the buoyancy term which is discretized using the Adams-Bashforth scheme. The Tri-Diagonal Matrix solver (TDMA) is employed to solve the resulting system of algebraic equations. The link between the velocity and pressure field is handled with the Fractional Step Method, and the resulting Poisson equation is solved with the Conjugate Gradient Method (see Van Der Vost [25]). This code has been validated and tested in numerical simulation of turbulent and laminar natural convection flows by Pallarès et. al. [26] and Valencia et. al. [27]. The complete mathematical formulation and the associated numerical methods of the code can be found in Cuesta [28]. In the following subsections the main characteristics of the numerical methods used are briefly described, the interested reader can find a complete description in Versteeg and Malalasekera [29] and Ferziger [30].

2.2.1 Finite volume

Let Φ be any dependent scalar variable. The transport equation of Φ reads

$$\frac{\partial}{\partial t}(\rho\Phi) + \frac{\partial}{\partial x_i}\left(\rho u_i \Phi - \Gamma_\Phi \frac{\partial \Phi}{\partial x_i}\right) = S_\Phi \tag{2.7}$$

ISBN:978-84-692-9056-9/DL:T-2069-2009

Where S_Φ is a source term and Γ_Φ is the diffusive coefficient. Defining the convective and diffusive flux as

$$I_i = \rho u_i \Phi - \Gamma_\Phi \frac{\partial \Phi}{\partial x_i} \tag{2.8}$$

For steady state the term involving time derivative vanishes. Using Equation (2.8), Equation (2.7) can be written as

$$\frac{\partial I_i}{\partial x_i} = S_\Phi \tag{2.9}$$

Integration of Equation (2.9) over a control volume in the physical space, using Gauss' theorem

$$\int_V \frac{\partial I_i}{\partial x_i} dV = \int_A I_i A_i$$

yields

$$\int_A I_i dA_i = \int_V S dV \tag{2.10}$$

The integral above yields the discretized equation.

$$\sum_{faces} (I_i A_i)_{face} \quad = S\delta V \tag{2.11}$$

Equation (2.11) is rearranged using the differencing scheme for I_i, to the standard form.

$$a_p \Phi_p = \sum_{NB} a_{NB} \Phi_{NB} + S\delta V \tag{2.12}$$

Equation (2.12) is solved with the iterative methods to obtain the approximate solution of the transport equation (Equation (2.7)).

2.2.2 The central differencing scheme

The central differencing scheme approximates the face value by using linear interpolation. For example, for the east face of the control volume:

$$\Phi_e = (1 - f_e)\Phi_P + f_e \phi_E$$

UNIVERSITAT ROVIRA I VIRGILI
NUMERICAL AND EXPERIMENTAL STUDY OF TRANSIENT LAMINAR NATURAL CONVECTION OF HIGH PRANDTL NUMBER FLUIDS IN A CUBICAL CAVITY
Obai Younis Taha Elamin
ISBN:978-84-692-9056-9/DL:T-2069-2009

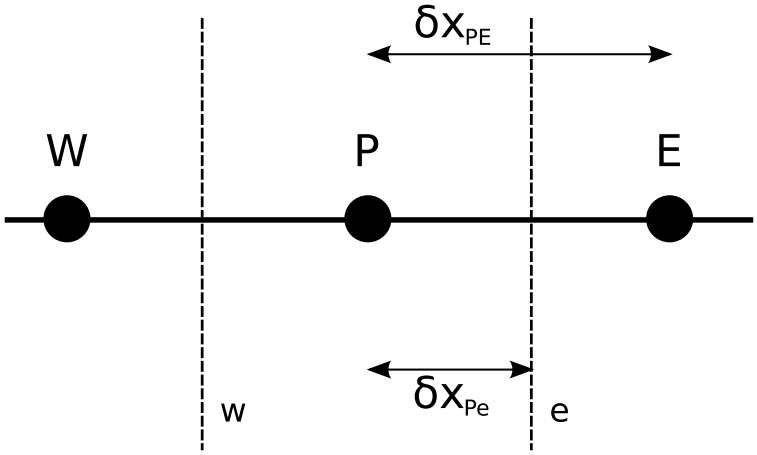

Figure 2.1: Grid nomenclature. Small letters denote the faces of the control volume and the capital letters denote the nodes

where

$$f_e = \frac{\delta x_{Pe}}{\delta x_{PE}}$$

See Figure 2.1 for the grid nomenclature.

2.2.3 Crank-Nicolson scheme

The Crank-Nicolson scheme in time is like central differencing scheme in space.

$$\Phi_i^n = 0.5\Phi_i^n + 0.5\phi_i^{(n-1)}$$

2.2.4 Adams-Bashforth scheme

The best known multipoint methods are derived by fitting a polynomial to the derivatives at a number of points in time. The second order Adams-Bashforth reads:

$$\Phi^{n+1} = \Phi^n + \frac{\Delta t}{2}\left[3f(t_n, \Phi^n) - f(t_{n-1}, \Phi^{n-1})\right]$$

2.2.5 TDMA Solver

The discretization process applied on the governing equations of the fluid flow results in a linearized algebraic equations which need to be solved. Mainly there are two families of solution techniques : direct methods and indirect or

ISBN:978-84-692-9056-9/DL:T-2069-2009

iterative methods. One of the most interesting features of the iterative methods is that only the non-zero coefficients of the equations need to be stored in core memory.

The TDMA is a direct method for one dimensional cases, but at the same time it can be applied iteratively in a line-by-line way to solve multi dimensional problems. It is computationally inexpensive and requires a minimum amount of storage.

3DINAMICS uses the TDMA as a matrix solver which is described below (for 2D case for simplicity).

The 2D discretized equation for the variable ϕ reads

$$a_P\phi_P = a_E\phi_E + a_W\phi_W + a_N\phi_N + a_S\phi_S + S_U \tag{2.13}$$

Equation (2.13) can be written in the form

$$a_i\phi_i = b_i\phi_{i+1} + c_i\phi_{i-1} + d_i \tag{2.14}$$

where

$$a_i = a_P, b_i = a_E, c_i = a_W$$

$$d_i = a_N\phi_N + a_S\phi_S + S_U$$

Again we can rewrite Equation (2.14) as

$$\phi_i = P_i\phi_{i+1} + Q_i \tag{2.15}$$

In order to put Equation (2.14) in the form of Equation (2.15) we need to write Equation (2.14) in a matrix form and apply elimination techniques. Equation (2.14) in matrix form reads

$$\begin{bmatrix} a_2 & -b_2 & 0 & \dots & & \\ -c_3 & a_3 & -b_3 & 0 & \dots & \\ 0 & -c_4 & a_4 & -b_4 & 0 & \dots \\ \vdots & \vdots & \vdots & \vdots & \vdots & \vdots \end{bmatrix} \begin{bmatrix} \phi_2 \\ \phi_3 \\ \phi_4 \\ \vdots \end{bmatrix} = \begin{bmatrix} d_2 + c_2\phi_1 \\ d_3 \\ d_4 \\ \vdots \end{bmatrix} \tag{2.16}$$

ISBN:978-84-692-9056-9/DL:T-2069-2009

Divide the first row by a_2

$$\begin{bmatrix} 1 & -P_2 & 0 & \dots & & \\ -c_3 & a_3 & -b_3 & 0 & \dots & \\ 0 & -c_4 & a_4 & -b_4 & 0 & \dots \\ \vdots & \vdots & \vdots & \vdots & \vdots & \vdots \end{bmatrix} \begin{bmatrix} \phi_2 \\ \phi_3 \\ \phi_4 \\ \vdots \end{bmatrix} = \begin{bmatrix} Q_2 \\ d_3 \\ d_4 \\ \vdots \end{bmatrix} \tag{2.17}$$

where

$$P_2 = \frac{b_2}{a_2}, Q_2 = \frac{d_2 + c_2\phi_1}{a_2}$$

In order to eliminate the $c's$ multiply the first row by c_3, add it to the second row and then divide the second row by $a_3 - c_3P_2$.

$$\begin{bmatrix} 1 & -P_2 & 0 & \dots & & \\ 0 & 1 & -P_3 & 0 & \dots & \\ 0 & -c_4 & a_4 & -b_4 & 0 & \dots \\ \vdots & \vdots & \vdots & \vdots & \vdots & \vdots \end{bmatrix} \begin{bmatrix} \phi_2 \\ \phi_3 \\ \phi_4 \\ \vdots \end{bmatrix} = \begin{bmatrix} Q_2 \\ Q_3 \\ d_4 \\ \vdots \end{bmatrix} \tag{2.18}$$

where

$$P_3 = \frac{b_3}{a_3 - c_3P_2}, Q_3 = \frac{d_3 + c_3Q_2}{a_3 - c_3P_2}$$

Now Equation (2.18) becomes an recursive equation for P_i and Q_i on the form

$$P_i = \frac{b_i}{a_i - c_iP_{i-1}}, Q_i = \frac{d_i + c_iQ_{i-1}}{a_i - c_iP_{i-1}}$$

2.2.6 Fractional step method

A pressure term appears in the system of the governing equations, and it does not have an explicit equation. The correct pressure field results in the correct velocity field which satisfies the continuity equation. The fractional step method, which is described below, is used in 3DINAMICS to handle the linkage between velocity and pressure field.

The discretized momentum equation using the guessed velocity field, indicated with a star, reads:

$$\frac{u_i^\star - u_i^n}{\delta t} = \frac{1}{2}\left[H_i^\star + H_i^n\right] - \frac{\delta p^n}{\delta x_i} + \delta_{i1}B \tag{2.19}$$

UNIVERSITAT ROVIRA I VIRGILI
NUMERICAL AND EXPERIMENTAL STUDY OF TRANSIENT LAMINAR NATURAL CONVECTION OF HIGH PRANDTL NUMBER FLUIDS IN A CUBICAL CAVITY
Obai Younis Taha Elamin
ISBN:978-84-692-9056-9/DL:T-2069-2009

where H is the convective and conductive fluxes and B is the buoyancy term. After solving the pressure equation, the corrected velocity field satisfies the continuity equation and the momentum equation reads:

$$\frac{u_i^{n+1} - u_i^n}{\delta t} = \frac{1}{2}\left[H_i^{n+1} + H_i^n\right] - \frac{\delta p^{n+1}}{\delta x_i} + \delta_{i1} B \tag{2.20}$$

By subtracting 2.20 from 2.19 and taking the derivative:

$$\frac{\delta}{\delta x_i}\left[\frac{u_i^{n+1} - u_i^\star}{\Delta t}\right] = \frac{1}{2}\frac{\delta}{\delta x_i}\left[H_i^{n+1} - H_i^\star\right] - \frac{\delta}{\delta x_i}\left[\frac{p^{n+1}}{\delta x_i} + \frac{p^n}{\delta x_i}\right] \tag{2.21}$$

According to Ferziger [30] the term $H_i^{n+1} - H_i^\star$ can be neglected since it will introduce an error of second order in time. Equation (2.21) can be written as:

$$-\frac{1}{\Delta t}\frac{\delta u_i^\star}{\delta x_i} = \frac{\delta}{\delta x_i}\left[-\frac{p^{n+1}}{\delta x_i} + \frac{p^n}{\delta x_i}\right] \tag{2.22}$$

Let $\phi = p^{n+1} - p^n$. The final resulting Poisson equation reads:

$$\frac{1}{\Delta t}\frac{\delta u_i^\star}{\delta x_i} = \frac{\delta^2 \phi}{\delta x_i^2} \tag{2.23}$$

The corrected velocity field can be computed as:

$$u_i^{n+1} = u_i^\star - \Delta t \frac{\delta \phi}{\delta x_i} \tag{2.24}$$

UNIVERSITAT ROVIRA I VIRGILI
NUMERICAL AND EXPERIMENTAL STUDY OF TRANSIENT LAMINAR NATURAL CONVECTION OF HIGH PRANDTL NUMBER FLUIDS IN A CUBICAL CAVITY
Obai Younis Taha Elamin
ISBN:978-84-692-9056-9/DL:T-2069-2009

UNIVERSITAT ROVIRA I VIRGILI
NUMERICAL AND EXPERIMENTAL STUDY OF TRANSIENT LAMINAR NATURAL CONVECTION OF HIGH PRANDTL NUMBER FLUIDS IN A CUBICAL CAVITY
Obai Younis Taha Elamin
ISBN:978-84-692-9056-9/DL:T-2069-2009

Chapter 3

Experimental approaches

3.1 Experimental setup

We consider transient natural convection in a side-cooled cavity, as sketched in Figure 3.1. The dimensions of the cubical cavity are $0.1*0.1*0.1m^3$. All walls are made of Perspex except the two gold-coated copper sidewalls of 1.13 mm thickness used to cool the fluid in the cavity. The Perspex is poor conductor in comparison with the gold-coated copper, and therefore it can be regarded as adiabatic. Moreover, the Perspex is transparent, and the flow can be visualised through the Perspex walls. The model cavity is separated from the water bath by the gold-coated copper sidewalls. The cavity is filled with preheated fluid, and the fluid temperature is kept constant using two constant temperature water baths attached to the gold-coated copper sidewalls. This process lasts for a relatively long time to ensure that the fluid in the cavity is isothermal and motionless before the experiment starts. Two circulator systems are used to provide hot and cold water for the water baths, respectively. The circulators maintain the temperature of the water in the water bath within a range of $\pm 0.01^oC$ at the specified temperature. At the start of the experiment, the hot water valve is turned off and the cold water valve is turned on. As a consequence, the cold water replaces the hot water in the water baths in order to cool the two sidewalls adjacent to the water baths. Due to the presence of temperature difference between the hot fluid in the cavity and the cold sidewalls, transient natural convection is initiated in the cavity.

UNIVERSITAT ROVIRA I VIRGILI
NUMERICAL AND EXPERIMENTAL STUDY OF TRANSIENT LAMINAR NATURAL CONVECTION OF HIGH PRANDTL NUMBER FLUIDS IN A CUBICAL CAVITY
Obai Younis Taha Elamin
ISBN:978-84-692-9056-9/DL:T-2069-2009

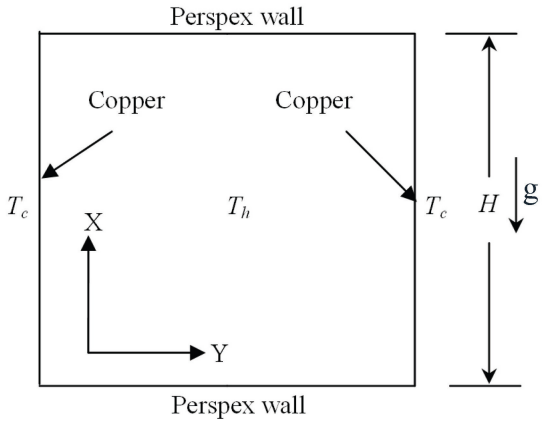

Figure 3.1: Sketch of the experimental model

3.2 Shadowgraph

Through out the experimental work, the flow field is visualized using the shadowgraph technique due to it is simplicity. The shadowgraph is an optical method to reveal non-uniformities in transparent media. A temperature variation within a flow field results in a density variation and in turn a variation in the refractive index. When light passes through such a flow field, initially parallel light rays are refracted so that patterns, which may identified with the temperature field, are formed on a screen and registered by a camera. The utilization of the shadow effects for scientific testing and flow visualization has been analyzed first by Dvorak in 1880 (see Mirzkirch [32]). Since then the shadowgraph techniques has been used to study the natural convection problems. Recently, Xu et. al. [31] utilized the shadowgraph techniques to study the unsteady thermal flow around a thin fin on a sidewall of a differentially heated cavity. Depending on the shadowgraph images, they were able to describe the transition of the unsteady thermal flow and to provide unsteady velocity scale of the lower intrusion and starting plume. The same shadowgraph technique was employed in this Thesis to study the transient natural

UNIVERSITAT ROVIRA I VIRGILI
NUMERICAL AND EXPERIMENTAL STUDY OF TRANSIENT LAMINAR NATURAL CONVECTION OF HIGH PRANDTL
NUMBER FLUIDS IN A CUBICAL CAVITY
Obai Younis Taha Elamin
ISBN:978-84-692-9056-9/DL:T-2069-2009

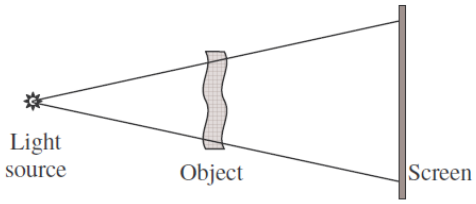

(a) Divergent beam

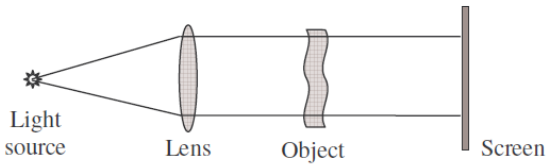

(b) parallel beam

Figure 3.2: Direct shadowgraph

convection in a side-cooled cavity.

3.2.1 Principle

Mainly there are two categories of shadowgraph, direct shadowgraph and focused shadowgraph. Figure 3.2(a) shows the simplest form of the direct shadowgraph that does not need any optical components. It consists of a point light source, a test object and a screen. The light diverging from the light source is transmitted through the test and the shadow picture produced by the inhomogeneous density field is recorded on the screen. A parallel light beam for the direct shadowgraph can be achieved by placing a lens between the point light source and the test object as shown in Figure 3.2(b). The

UNIVERSITAT ROVIRA I VIRGILI
NUMERICAL AND EXPERIMENTAL STUDY OF TRANSIENT LAMINAR NATURAL CONVECTION OF HIGH PRANDTL NUMBER FLUIDS IN A CUBICAL CAVITY
Obai Younis Taha Elamin
ISBN:978-84-692-9056-9/DL:T-2069-2009

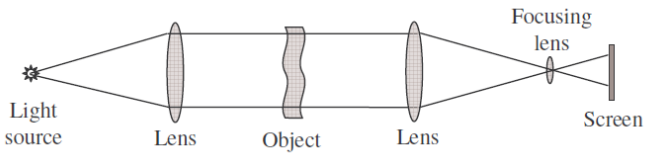

Figure 3.3: Focused shadowgraph

focused shadowgraph is shown in Figure 3.3. The parallel light results from the first lens passes the test object, recollected by the second lens, passes the focusing lens and projected on the screen. The two lenses can be replaced by spherical mirrors, while the focusing lens and the screen can be replaced by a camera. Although the focused shadowgraph is more complex than a direct one, the focused shadowgraph can more easily adjust the imaging position by utilizing the camera focusing. In this Thesis the focused shadowgraph was utilized. As explained before, the concept of the shadowgraph depends on the grey scales images resulting from non-uniform refraction index due to the inhomogeneous density field. The correlation between the varying refraction index and the light intensity of a shadowgraph image is discussed below as found in Mirzkirch [32]. When passing through the test object, the light rays are refracted and bent out of their original path. The distribution of the light intensity on the screen is altered with respect to the undistributed case (Mirzkirch [32]). Let $I(x, y)$ the light intensity distribution on the screen for the undistributed case, and $I^\star(x^\star, y^\star)$ is the intensity for the distributed case. The intensity $I^\star$ at point $(x^\star, y^\star)$ results from all intensities I_i at points (x_i, y_i). To determine the resulting intensity $I^\star$, we have to take into account that the illuminated area by a particular light beam is deformed due to the mapping of the (x, y) plane into the $(x^\star, y^\star)$ plane. Each intensity value I_i contributing to the summation has to be divided by a value which accounts for this mapping, and the denominator of this expression is the Jacobian of the mapping function of the system (x, y) into $(x^\star, y^\star)$. The resulting intensity in $(x^\star, y^\star)$ is given by:

ISBN:978-84-692-9056-9/DL:T-2069-2009

$$I^{\star}(x^{\star}, y^{\star}) = \sum_{i} \frac{I_i(x_i, y_i)}{\partial(x^*, y^*)/\partial(x,y)} \tag{3.1}$$

Assume that the new mapping coordinates are given by:

$$\begin{aligned} x^{\star} &= x + \Delta x(x, y) \\ y^{\star} &= y + \Delta y(x + y) \end{aligned}$$

If the test object is thin, the light deviation with the test object may be neglected and the displacement Δx and Δy may be given as (Mirzkirch [32]):

$$\Delta x = l\frac{dx(z_{ex})}{dz} = l\int \frac{1}{n}\frac{\partial n}{\partial x}dz \tag{3.2}$$

$$\Delta y = l\frac{dy(z_{ex})}{dz} = l\int \frac{1}{n}\frac{\partial n}{\partial y}dz \tag{3.3}$$

By assuming that delta x and delta y are small quantities and that their power products and higher powers could be neglected, the Jacobian is then:

$$|\frac{\partial(x^{\star}, y^{\star})}{\partial(x, y)}| \approxeq 1 + {}^{\partial\Delta x}/_{\partial x} + {}^{\partial\Delta y}/_{\partial y} \tag{3.4}$$

By substituting Equations (3.4, 3.2) and (3.3) into Equation (3.1), one can get:

$$\frac{\Delta I}{I} = l\int (\frac{\partial^2}{\partial x^2} + \frac{\partial^2}{\partial y^2})(\ln n)dz \tag{3.5}$$

Equation (3.5) demonstrates that the light intensity is sensitive to the second derivative of the refraction index. This equation is only valid for thin objects. However, for non-thin objects, Xu [33] showed that the shadowgraph images can be recorded on the wall of the object and therefore Equation (3.5) can be written as:

$$\frac{\Delta I}{I} = \int\int \frac{\partial^2}{\partial x^2}(\ln n)dzdz \tag{3.6}$$

Since the variation in z direction is very small, Equation (3.6) can be

UNIVERSITAT ROVIRA I VIRGILI
NUMERICAL AND EXPERIMENTAL STUDY OF TRANSIENT LAMINAR NATURAL CONVECTION OF HIGH PRANDTL NUMBER FLUIDS IN A CUBICAL CAVITY
Obai Younis Taha Elamin
ISBN:978-84-692-9056-9/DL:T-2069-2009

simplified to:

$$\frac{\Delta I}{I} = D^2 \frac{\partial^2}{\partial x^2}(\ln n) \tag{3.7}$$

Where D is the object thickness. Based on the weakly line dependence of the refractive index on temperature, the relation between the light intensity and temperature field can be given by:

$$\frac{\Delta I}{I} \propto D^2 \frac{\partial T^2}{\partial x^2} \tag{3.8}$$

Equation (3.8) demonstrates that the light intensity of the shadowgraph images is proportional to the square depth of the cavity and the second derivatives of the temperature of the thermal boundary layer.

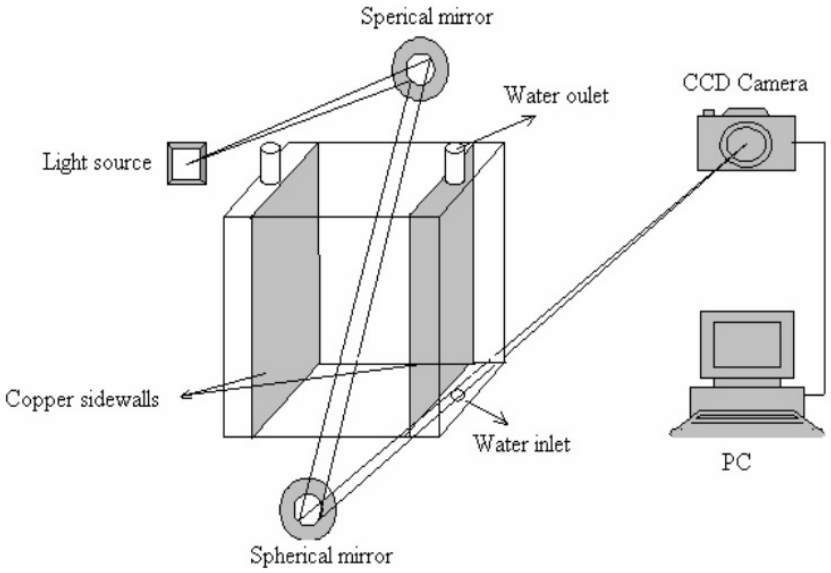

Figure 3.4: Schematic of the optic setup of the focused shadowgraph

UNIVERSITAT ROVIRA I VIRGILI
NUMERICAL AND EXPERIMENTAL STUDY OF TRANSIENT LAMINAR NATURAL CONVECTION OF HIGH PRANDTL NUMBER FLUIDS IN A CUBICAL CAVITY
Obai Younis Taha Elamin
ISBN:978-84-692-9056-9/DL:T-2069-2009

3.2.2 Optical setup

The used shadowgraph system is shown in Figure 3.4; it consists of two spherical mirrors with a diameter of $0.3m$ and focal length of $2.4m$, and a point light source. The light source is placed on the focal length of one of the spherical mirrors. The resulting parallel light beam passes through the cavity producing the shadowgraph. The shadowgraph is refocused by the other spherical mirror and it is recorded by a CCD camera. The CCD camera is connected to a frame-grabber board (Streampix), which is implemented in a computer. The board digitizes the shadowgraph images received by the CCD camera into an array of $576X768$ pixels with 256-bit grey-scale values. The shadowgraph images are stored on the hard disk of the computer at an adjustable sample rate of up to 4 frames per second. The same shadowgraph system was previously used successfully to visualize natural convection flows (e.g . Jeevaraj and Patterson [8] and Xu et.al. [9]).

UNIVERSITAT ROVIRA I VIRGILI
NUMERICAL AND EXPERIMENTAL STUDY OF TRANSIENT LAMINAR NATURAL CONVECTION OF HIGH PRANDTL NUMBER FLUIDS IN A CUBICAL CAVITY
Obai Younis Taha Elamin
ISBN:978-84-692-9056-9/DL:T-2069-2009

UNIVERSITAT ROVIRA I VIRGILI
NUMERICAL AND EXPERIMENTAL STUDY OF TRANSIENT LAMINAR NATURAL CONVECTION OF HIGH PRANDTL NUMBER FLUIDS IN A CUBICAL CAVITY
Obai Younis Taha Elamin
ISBN:978-84-692-9056-9/DL:T-2069-2009

Chapter 4

Results and discussions

In this chapter the numerical and experimental results of transient laminar natural convection in a cubical cavity is presented and discussed. The chapter is mainly divided into two sections. Section (4.1) examines the separate and combined effects of the fluid variable viscosity, wall conduction and thermal boundary conditions on the transient laminar natural convection of high Prandtl number fluid in a cubical cavity. The contents of this section have been submitted for journal publication. Section (4.2) describes the experimental observations and the numerical simulations of transient natural convection in a side-cooled cavity. In this section, the flow development processes are identified. New scalings for variable viscosity fluids are introduced, the effect of variable viscosity and effect of the Prandtl number are discussed. This part of the thesis is being rewritten as two papers for journal publication. The experimental part presented in this chapter was conducted during the author's short stay at the Natural Convection laboratory of James cook University, Townsville, Australia, under the supervision of Dr. Feng Xu and Prof. John C. Patterson.

UNIVERSITAT ROVIRA I VIRGILI
NUMERICAL AND EXPERIMENTAL STUDY OF TRANSIENT LAMINAR NATURAL CONVECTION OF HIGH PRANDTL NUMBER FLUIDS IN A CUBICAL CAVITY
Obai Younis Taha Elamin
ISBN:978-84-692-9056-9/DL:T-2069-2009

4.1 Numerical simulation of transient laminar natural convection in a cubical cavity at $Ra = 10^6$ and $Pr = 4.10^4$: Effect of the variable viscosity and thermal boundary conditions

The case under consideration is the three dimensional unsteady natural convection of high Prandtl number fluid (Golden Syrup), with viscosity highly dependent on temperature, in a cubical cavity (see Figure 4.1). The cavity is made of Plexiglas with dimension $H = 20cm$. Initially, the fluid in the cavity is considered to be at rest, at constant temperature ($T_h = 45^oC$) and the temperature of the six walls is set to constant value ($T_c = 25^oC$) through the cooling process. We have also studied the effect of insulating the bottom wall of the cavity. The physical properties of the golden syrup according to Davaille and Jaupart [10] are:

$$\begin{aligned} \rho &= 1.438 \cdot 10^3 \ \frac{kg}{m^3} \\ \beta &= 4.33 \cdot 10^{-4} \ K^{-1} \\ \alpha &= 1.21 \cdot 10^{-7} \ \frac{m^2}{s} \end{aligned}$$

The viscosity-temperature relation is given by:

$$\mu = \mu_0 \ exp\left(\frac{1}{AT^2 + BT + C}\right) \tag{4.1}$$

Where: $\mu_0 = 4.485 \cdot 10^{-8} \ Pa \ s$,$A = -7.5907 \cdot 10^{-7}$,$B = 3.8968 \cdot 10^{-4}$, $C = 4.0130 \cdot 10^{-2}$, and T is in celsius.
These fluid properties give $Ra_o = 10^6$ and $Pr_o = 4 \cdot 10^4$. Figure 4.2 shows the dependence of viscosity with temperature. It can be seen that for the temperatures considered, the initial viscosity contrast ($\frac{\nu_c}{\nu_h}$) is 12.

According to Kays and Crawford [34], the transition to the turbulent regime in a vertical boundary layer occurs at $Gr = 10^9$, with a tendency toward a higher Gr for higher Pr. The studied case has a fairly low Gr ($Gr = \frac{Ra}{Pr} = 25$), hence it can be classified as laminar natural convection. The Prandtl

UNIVERSITAT ROVIRA I VIRGILI
NUMERICAL AND EXPERIMENTAL STUDY OF TRANSIENT LAMINAR NATURAL CONVECTION OF HIGH PRANDTL NUMBER FLUIDS IN A CUBICAL CAVITY
Obai Younis Taha Elamin
ISBN:978-84-692-9056-9/DL:T-2069-2009

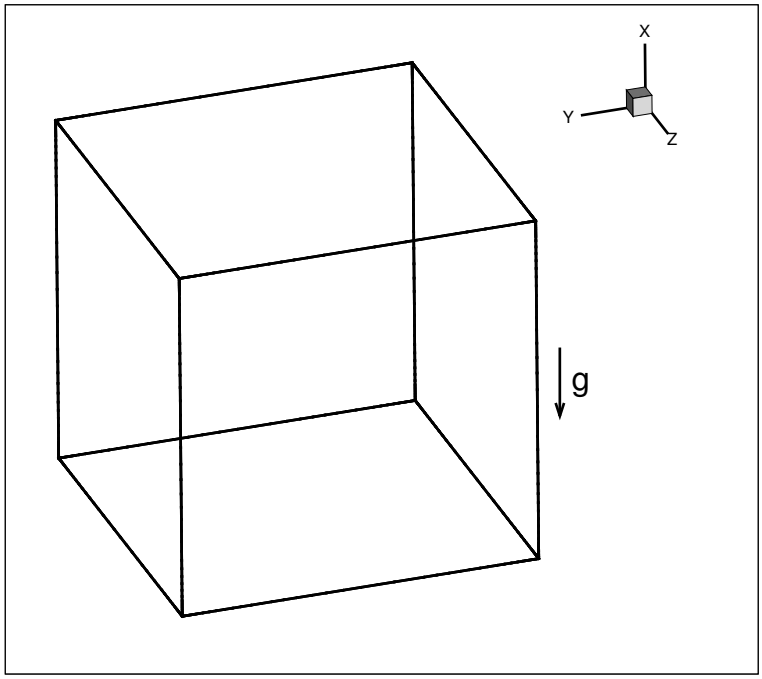

Figure 4.1: The computational domain

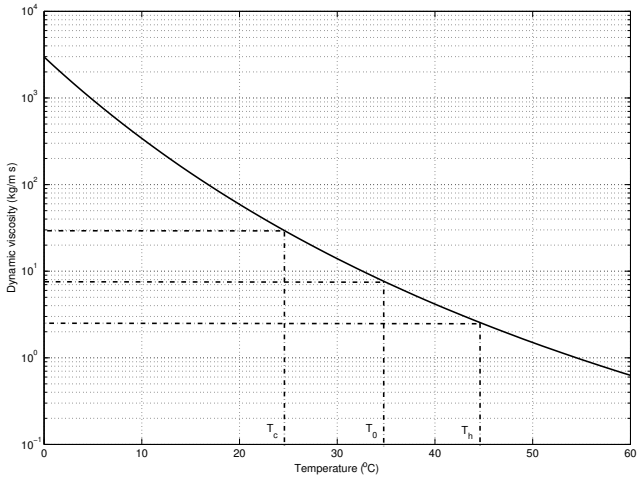

Figure 4.2: Variation of Corn Syrup viscosity with temperature

UNIVERSITAT ROVIRA I VIRGILI
NUMERICAL AND EXPERIMENTAL STUDY OF TRANSIENT LAMINAR NATURAL CONVECTION OF HIGH PRANDTL NUMBER FLUIDS IN A CUBICAL CAVITY
Obai Younis Taha Elamin
ISBN:978-84-692-9056-9/DL:T-2069-2009

Case	Viscosity	Thermal boundary conditions	Wall conduction	Case tag
1	Constant	TBC1	No	CV1
2	Constant	TBC2	No	CV2
3	Variable	TBC1	No	VV1
4	Variable	TBC2	No	VV2
5	Constant	TBC1	Yes	CVWC1
6	Constant	TBC2	Yes	CVWC2
7	Variable	TBC1	Yes	VVWC1
8	Variable	TBC2	Yes	VVWC2

Table 4.1: Studied cases

number that appears in the diffusion term in Equation (2.2) is calculated using Equation (4.1). The Prandtl and Rayleigh numbers (Pr_0 and Ra_0) in the buoyancy term are based on kinematic viscosity evaluated at the reference temperature $T_0 = (T_c + T_h)/2$.
The initial conditions are:
$u^* = v^* = w^* = T_h^* = 0$ when $t^* = 0$
And the boundary conditions for the velocity are :
$u^* = v^* = w^* = 0$ when $t^* > 0$
The different thermal boundary conditions used and the cases considered are summarised in Table (4.1) (TBC1 stands for ($T^*_{allwalls} = -1$) and TBC2 stands for ($T^*_{walls} = -1$, at bottom wall$\frac{\partial T^*}{\partial x^*} = 0$)).

Case (5), (6), (7) and (8) consider the heat conduction through the $1cm$ thick Plexiglass walls, $\frac{k_{wall}}{k_{fluid}} = 0.47$.

In order to have reliable results, the thermal and velocity boundary layers should be well resolved in terms of space and time. The flow contains different length scales ranging from the small scales of the thermal boundary layer to the big scales of the large rolling motions in the interior of the cavity. To be able to capture the whole range of scales it is necessary to use a fine mesh in the boundary layer. Taking this consideration into account, a mesh of 40^3 control volumes is employed. At the Ra and Pr numbers considered, the results obtained with 50^3 control volumes do not show a significant difference in comparison with the present results. The mesh is symmetrically distributed with respect to the symmetry elements of the cavity. The mesh size expands at a rate of 7%from the wall to a distance of 0.05. The mesh size is non-uniform

UNIVERSITAT ROVIRA I VIRGILI
NUMERICAL AND EXPERIMENTAL STUDY OF TRANSIENT LAMINAR NATURAL CONVECTION OF HIGH PRANDTL NUMBER FLUIDS IN A CUBICAL CAVITY
Obai Younis Taha Elamin
ISBN:978-84-692-9056-9/DL:T-2069-2009

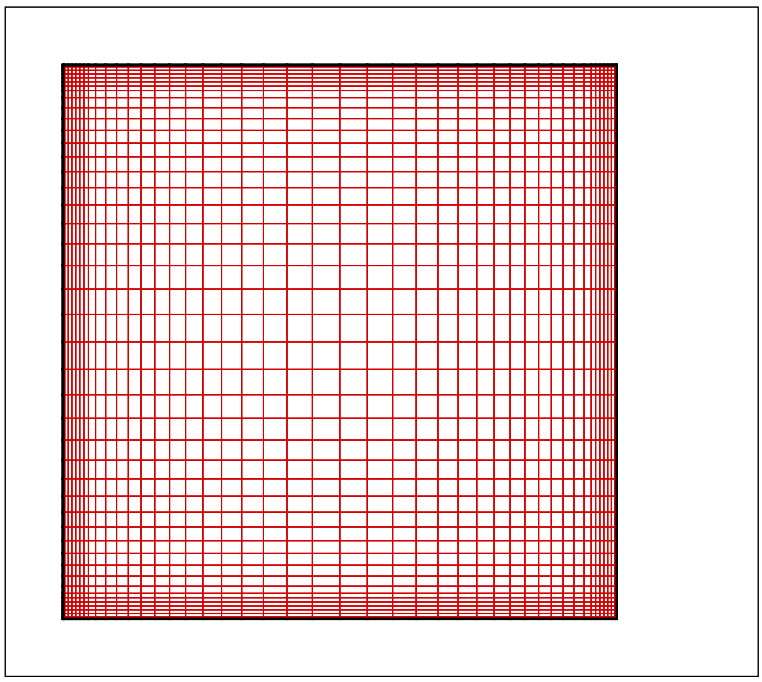

Figure 4.3: The mesh

in the interior of the cavity as shown in Figure 4.3. When the wall conduction is considered, the same mesh distribution employed in the fluid. The mesh in the solid walls, which are 1 cm thick, contains 4 control volumes in the direction perpendicular to the wall, resulting in a mesh of 48^3 control volumes. The time-step dependence study carried out shows that results are time-step independent if $\Delta t^* = 10^{-7}$ is used for the time marching scheme.

4.1.1 Method validation

The 3DINAMICS code, used to perform the computations, has been validated and tested in numerical simulation of turbulent and laminar natural convection flows by Pallares et al [26]. and Valencia et al [27]. However, here we provide a qualitative validation of the code by reproducing the results of Lin and Armfield [22]. They considered the transient natural convection cooling of rectangular and cylindrical containers for a range of Rayleigh numbers($10^6 \leq Ra \leq 10^9$). The selected case for validation is the rectangular container at $Ra = 10^6$. The results are presented in terms of temperature contours and stream lines in Figure 4.4. It is clear that our results are in a

UNIVERSITAT ROVIRA I VIRGILI
NUMERICAL AND EXPERIMENTAL STUDY OF TRANSIENT LAMINAR NATURAL CONVECTION OF HIGH PRANDTL NUMBER FLUIDS IN A CUBICAL CAVITY
Obai Younis Taha Elamin
ISBN:978-84-692-9056-9/DL:T-2069-2009

good agreement with the results of Lin and Armfield [22]. This only validates the code for constant viscosity fluids; the validation for variable viscosity fluids is presented in Section 4.2.

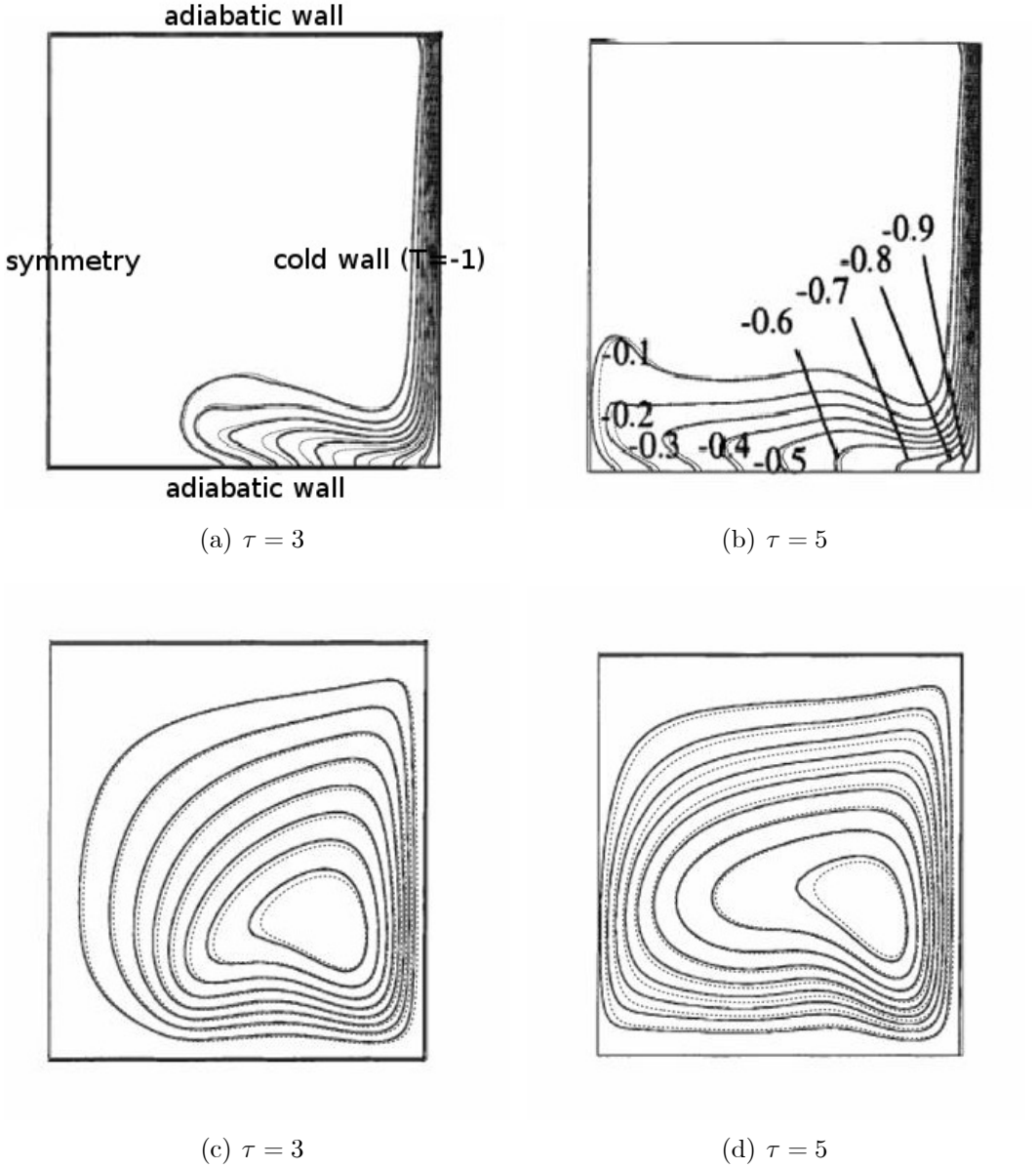

(a) $\tau = 3$ (b) $\tau = 5$

(c) $\tau = 3$ (d) $\tau = 5$

Figure 4.4: Temperature and stream function contours (continuous line: Lin and Armfield, dashed line: present study),(a)temperature contours at $\tau = 3$,(b)temperature contours at $\tau = 5$,(c)stream function contours at $\tau = 3$,(d)stream function contours at $\tau = 5$, (τ is the nondimensional time).

UNIVERSITAT ROVIRA I VIRGILI
NUMERICAL AND EXPERIMENTAL STUDY OF TRANSIENT LAMINAR NATURAL CONVECTION OF HIGH PRANDTL NUMBER FLUIDS IN A CUBICAL CAVITY
Obai Younis Taha Elamin
ISBN:978-84-692-9056-9/DL:T-2069-2009

4.1.2 Instantaneous fields

The flow has four planes of symmetry, $X-Y$ plane at $z^* = 0.5$, $X-Z$ plane at $y^* = 0.5$ and the diagonal planes. The presented flow fields are plotted in the $X-Y$ plane at $z^* = 0.5$. Figure 4.5 shows the velocity vector and the temperature isotherms at the very beginning stage of cooling at $t = 90s$. Due to the cooling mechanism, the flow near the lateral walls is descending while it is ascending in the center because of continuity (Figure 4.5). As a result, two counter rotating vortex are formed. It should be noticed according to the symmetry elements of the flow the 3D topology of these counter rotating vortices correspond to a toroidal rolling motion with its axis aligned with the vertical symmetry axis of the cubical cavity. The thermal boundary layer is confined near the walls due to the high Pr number. In this early stage, the flow patterns of the first four cases are almost the same. Very slight difference is noticed in the velocity magnitude near the lateral walls and in the center of the cube (see Figures 4.5(a), 4.5(b)) and (4.5(c) and 4.5(d)). For example, the non dimensional vertical velocity component at $x^* = 0.5, y^* = 0.5, z^* = 0.5$ and at $t = 90$ s is 632 and 752 for CV1 and VV1, respectively. This difference arise from the fact that cases (VV1 and VV2), see Table (4.1), considers variable viscosity in which the viscosity near the wall is much larger than its value in cases (CV1 and CV2) - for CV1 and CV2 the fluid viscosity is calculated using the reference temperature -, thus the flow retardation near the walls (wall shear stress) is higher and the flow in the center accelerates to satisfy the continuity.

It is clear that the wall conductivity inhibits the heat transfer from the fluid as shown in Figure 4.6. As a result the fluid is essentially stagnant and the hot core occupies the cube.

UNIVERSITAT ROVIRA I VIRGILI
NUMERICAL AND EXPERIMENTAL STUDY OF TRANSIENT LAMINAR NATURAL CONVECTION OF HIGH PRANDTL NUMBER FLUIDS IN A CUBICAL CAVITY
Obai Younis Taha Elamin
ISBN:978-84-692-9056-9/DL:T-2069-2009

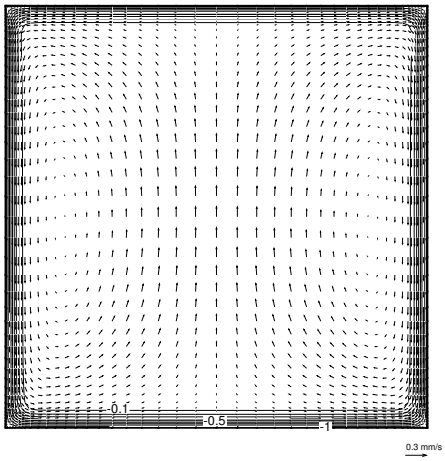

(a) CV1

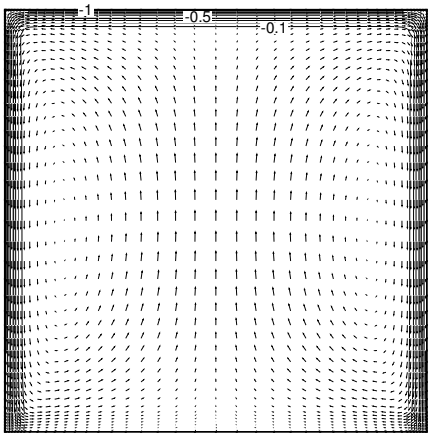

(b) CV2

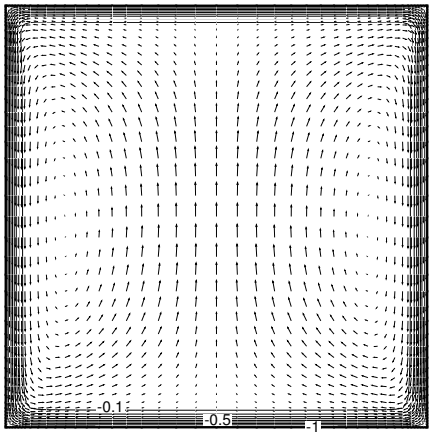

(c) VV1

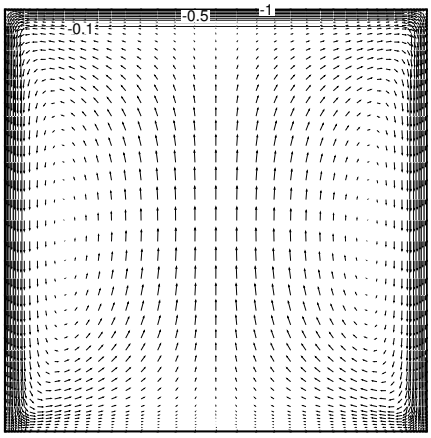

(d) VV2

Figure 4.5: Velocity vectors and temperature contours at $t = 90$ s, cases 1-4 (see Table (4.1)).

UNIVERSITAT ROVIRA I VIRGILI
NUMERICAL AND EXPERIMENTAL STUDY OF TRANSIENT LAMINAR NATURAL CONVECTION OF HIGH PRANDTL NUMBER FLUIDS IN A CUBICAL CAVITY
Obai Younis Taha Elamin
ISBN:978-84-692-9056-9/DL:T-2069-2009

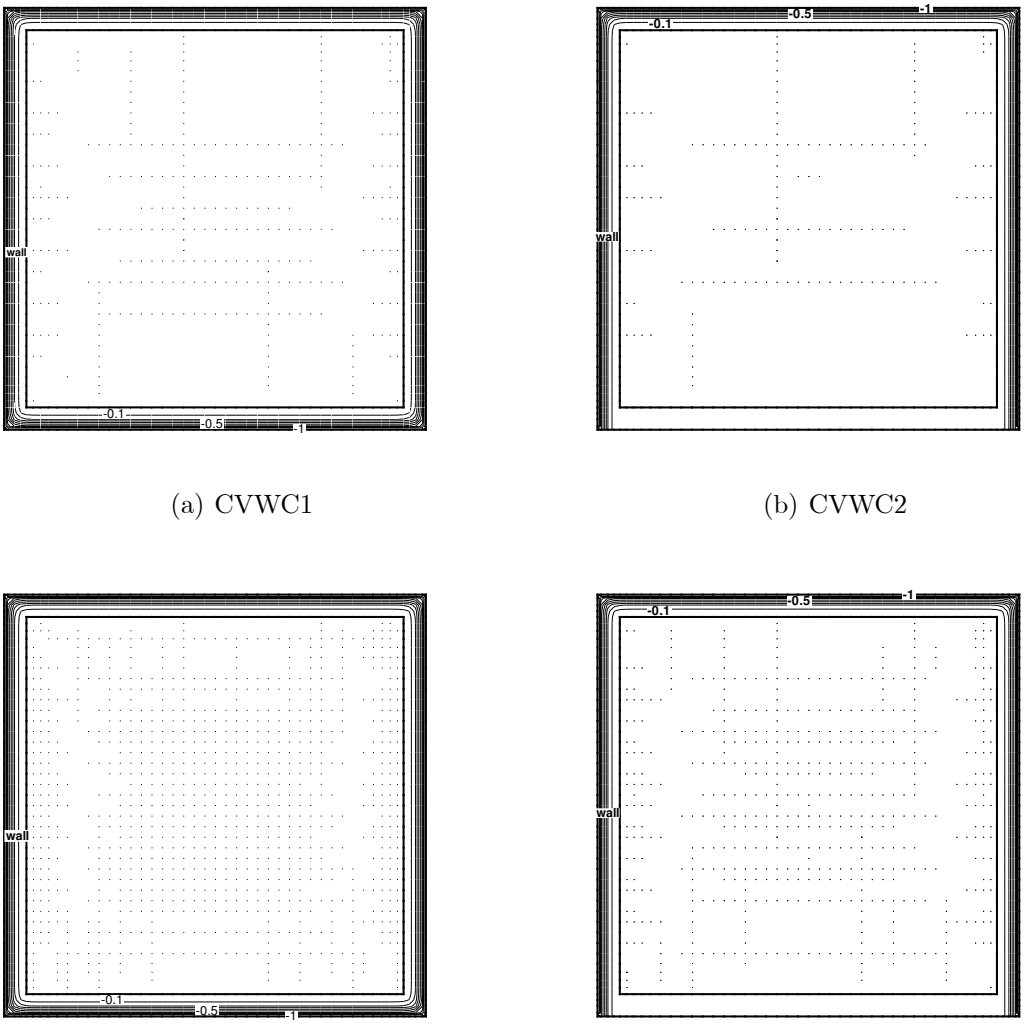

(a) CVWC1

(b) CVWC2

(c) VVWC1

(d) VVWC2

Figure 4.6: Velocity vectors and temperature contours at $t = 90$ s, cases 5-8 (see Table (4.1)).

ISBN:978-84-692-9056-9/DL:T-2069-2009

As time evolves the flow patterns start to present differences. The velocity vector fields and the temperature isotherms at $t = 1200$ s are presented in Figure 4.7. The heat transfer thorough the bottom wall has a small contribution to the flow since it produces a stable stratified region. This region forces the location of vortex center to move towards the top wall in comparison with the cases in which the bottom wall is insulated. The heat transfer through the top wall produces an unstable stratified region, forcing the fluid at the top to descend. The contribution of the top and bottom wall produces a secondary flow region near the center of the top wall. The size of this region is not the same in the all studied cases. A possible explanation for this difference could be obtained by studying the instability on the top wall in terms of the Rayleigh number. According to Koschmieder [35] the critical Rayleigh number (Ra_c) for the onset of convection in an infinite shear-free layer of fluid heated from below is 700. The calculation of Ra number of the top wall based on the maximum temperature difference between the wall and the hot core and the thermal boundary layer thickness near the top wall revealed that instability was evident in CV1, VV1 and VV2 having Ra of 700, 5000 and 1700 respectively. For CV2 no instability was detected as the Ra number was well below the critical value ($Ra = 50$). In general, the instability near the top wall was stronger in VV1 than CV1 due to the effect of variable viscosity.

UNIVERSITAT ROVIRA I VIRGILI
NUMERICAL AND EXPERIMENTAL STUDY OF TRANSIENT LAMINAR NATURAL CONVECTION OF HIGH PRANDTL NUMBER FLUIDS IN A CUBICAL CAVITY
Obai Younis Taha Elamin
ISBN:978-84-692-9056-9/DL:T-2069-2009

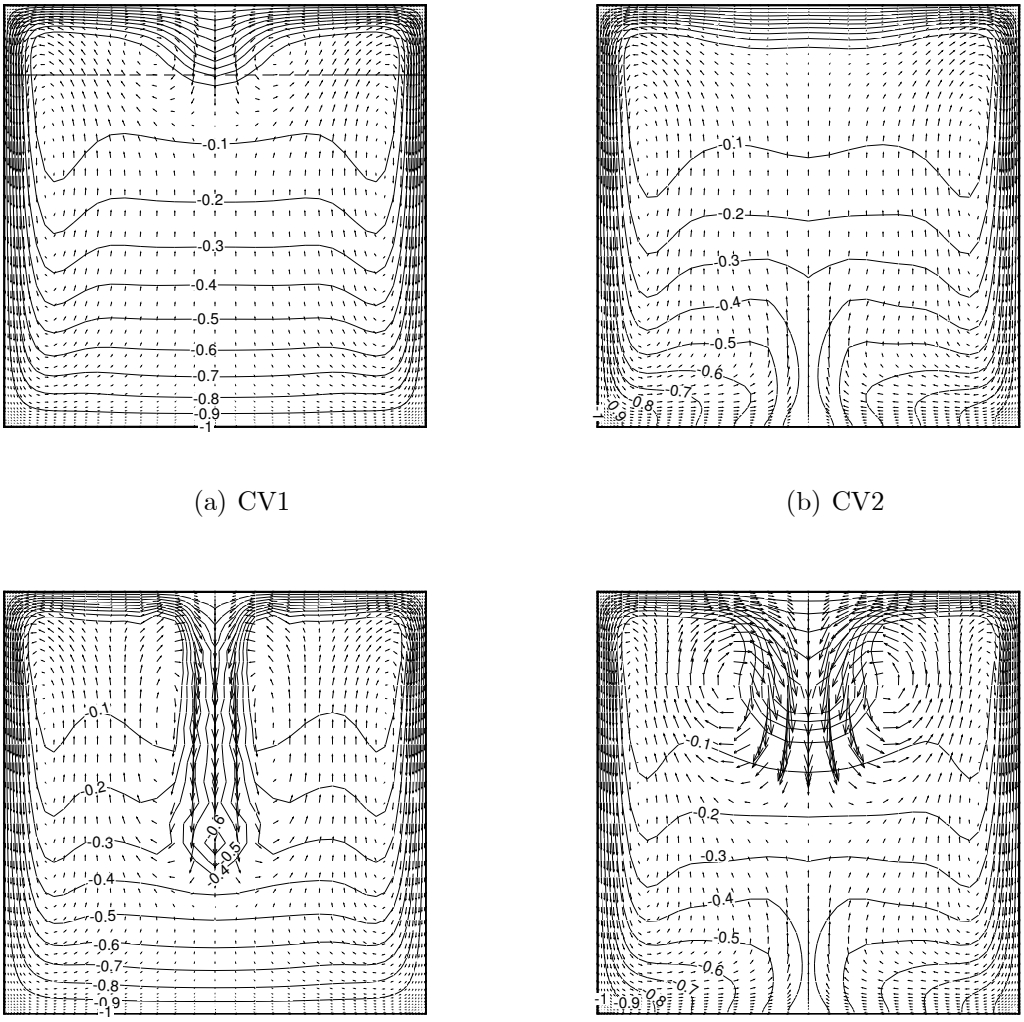

(a) CV1

(b) CV2

(c) VV1

(d) VV2

Figure 4.7: Velocity vectors and temperature contours at $t = 1200$ s, cases 1-4 (see Table (4.1)).

UNIVERSITAT ROVIRA I VIRGILI
NUMERICAL AND EXPERIMENTAL STUDY OF TRANSIENT LAMINAR NATURAL CONVECTION OF HIGH PRANDTL NUMBER FLUIDS IN A CUBICAL CAVITY
Obai Younis Taha Elamin
ISBN:978-84-692-9056-9/DL:T-2069-2009

Figure 4.8 presents the cases that account for wall conduction at $t = 1200$ s. The flow consists in two main counter rotating vortex, which are very similar to cases CV1, CV2, VV1 and VV2 at $t = 90$ s. The temperature contours near the bottom wall for VVWC1 and VVWC2 (Figures 4.8(c) and 4.8(d)) advance faster towards the core than in cases CVWC1 and CVWC2 (Figures 4.8(a) and 4.8(b)), as mentioned before. This is a direct result of the variable viscosity. The flow is not strong enough to generate secondary flow. The hot core was occupies the 70% of the cube.

UNIVERSITAT ROVIRA I VIRGILI
NUMERICAL AND EXPERIMENTAL STUDY OF TRANSIENT LAMINAR NATURAL CONVECTION OF HIGH PRANDTL NUMBER FLUIDS IN A CUBICAL CAVITY
Obai Younis Taha Elamin
ISBN:978-84-692-9056-9/DL:T-2069-2009

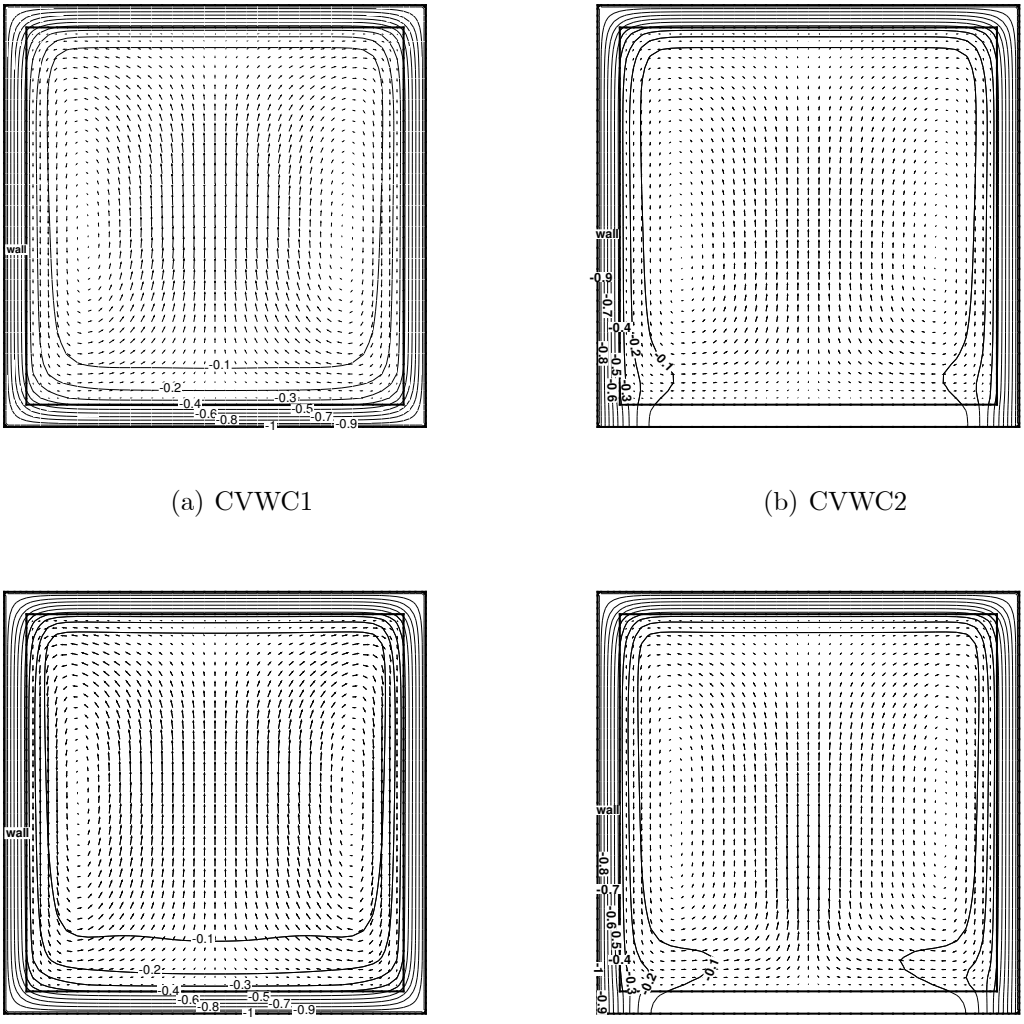

(a) CVWC1

(b) CVWC2

(c) VVWC1

(d) VVWC2

Figure 4.8: Velocity vectors and temperature contours at $t = 1200$ s, cases 5-8 (see Table (4.1)).

ISBN:978-84-692-9056-9/DL:T-2069-2009

In order to analyze the differences between the mechanism of the rolling motion and the effect of the variable viscosity, the budget of the X-momentum along the line $z^* = 0.5$ and $x^* = 0.83$ (indicated by the dashed line in Figure 4.7(a)) at $t = 1200$ s for cases CV2 and VV2 is presented in Figures 4.9(a) and 4.9(b). The different terms of the X-momentum equation (Equation 2.2) have been divided by $(Ra \cdot Pr)$ and moved to the right hand side of the equation. Due to the high Prandtl number of the Golden syrup and the relatively low Rayleigh number, the convective and the unsteady terms have no significant contribution to the balance and have been omitted in Figures 4.9(a) and 4.9(b) for clarity. The vertical velocity component (u^*) is also plotted in Figure 4.9(a) and 4.9(b) to indicate the sense of rotation of the rolling motion. The values of (u^*) have been divided by 1000 to fit into the scale of the figure. It is clear that the vertical velocity profile follows the buoyancy profile as it is the driving force. Inside the thermal boundary layer $(0.9 < y^* < 0.1)$, the fluid is descending near the cavity walls due to the negative buoyancy force. For case VV2 (Figure 4.9(b)), due to the flow instability near the top wall, the cold fluid descends in the center of the cavity. The large viscosity of this descending plume results in increasing the contribution of the diffusion term and consequently the contribution of the buoyancy force is also increased for balance requirements. However, the flow instability near the top wall is not obserevd in case CV2 at $t = 1200$ s because the fluid is not cold enough to develop such behavior near the top wall at $t = 1200$ s, instead the fluid is almost stagnant near the cavity center.

UNIVERSITAT ROVIRA I VIRGILI
NUMERICAL AND EXPERIMENTAL STUDY OF TRANSIENT LAMINAR NATURAL CONVECTION OF HIGH PRANDTL NUMBER FLUIDS IN A CUBICAL CAVITY
Obai Younis Taha Elamin
ISBN:978-84-692-9056-9/DL:T-2069-2009

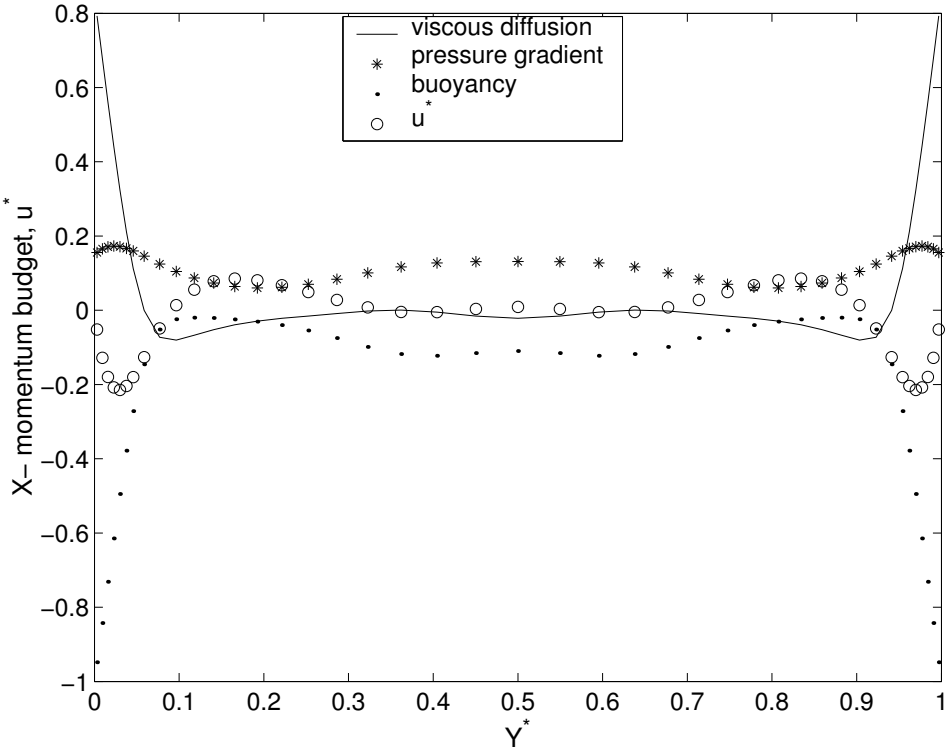

(a) CV2

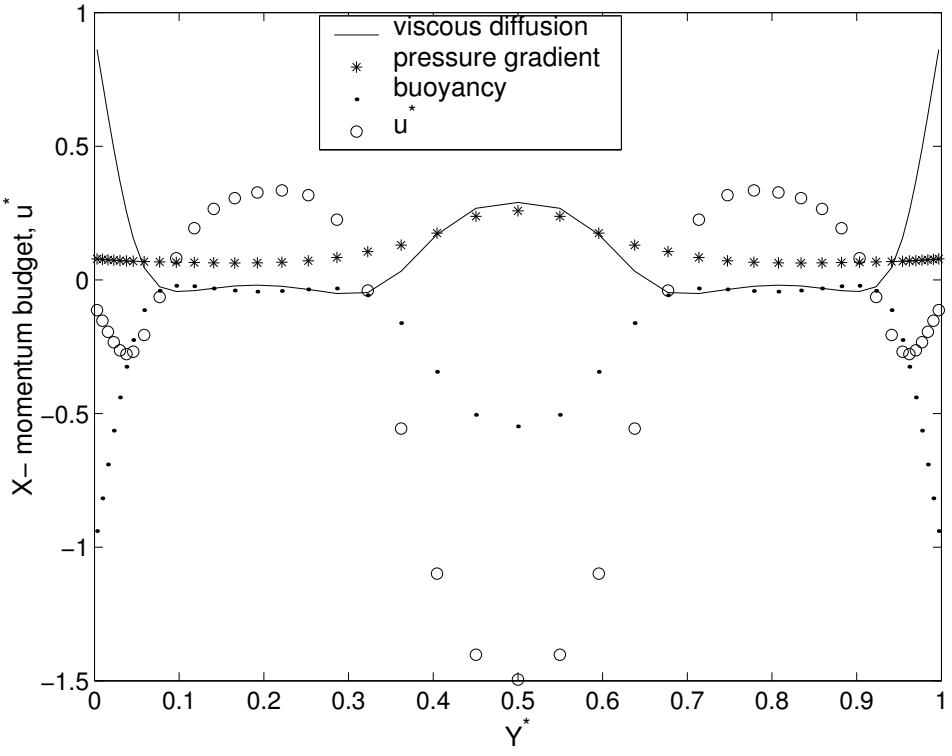

(b) VV2

Figure 4.9: Budget of X momentum along Y -axis at $z^* = 0.5, x^* = 0.75$ and $t = 1200$ s.

UNIVERSITAT ROVIRA I VIRGILI
NUMERICAL AND EXPERIMENTAL STUDY OF TRANSIENT LAMINAR NATURAL CONVECTION OF HIGH PRANDTL NUMBER FLUIDS IN A CUBICAL CAVITY
Obai Younis Taha Elamin
ISBN:978-84-692-9056-9/DL:T-2069-2009

According to Jeong and Hussain [36], the location of the vortex cores can be detected by calculating the eigenvalues of the velocity gradient tensor, and plotting the isosurfaces of the second largest eigenvalue. Figure 4.10 presents the vortex cores for cases CV1, CV2, VV1 and VV2 at $t = 1200$ s. It can be seen that the instantaneous flow at this stage consists of two vortex rings, the bigger one is located near the cavity walls, while the cavity center is occupied by the smaller vortex ring.

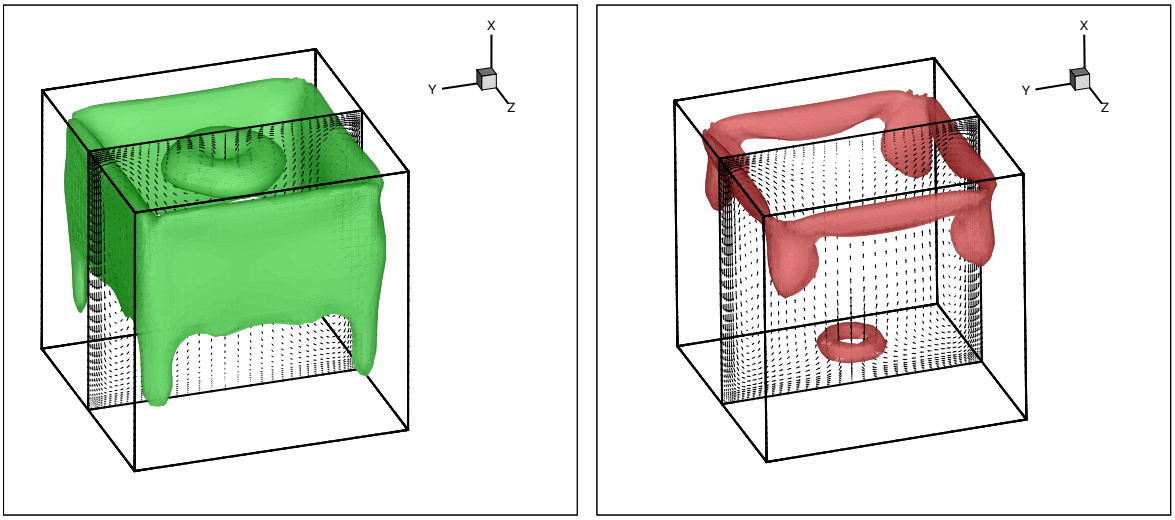

(a) CV1

(b) CV2

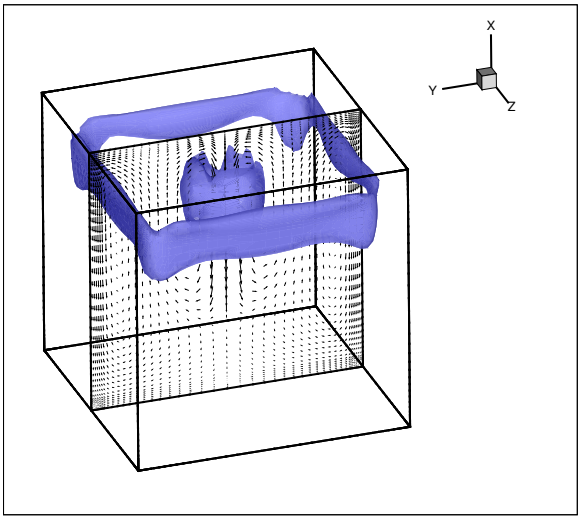

(c) VV1

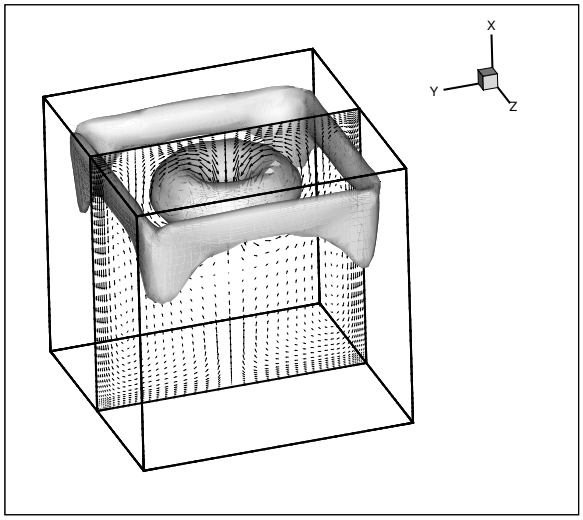

(d) VV2

Figure 4.10: The isosurfaces of the second largest eigenvalue of the velocity tensor $t = 1200$ s, , cases 1-4 (see Table (4.1)).

UNIVERSITAT ROVIRA I VIRGILI
NUMERICAL AND EXPERIMENTAL STUDY OF TRANSIENT LAMINAR NATURAL CONVECTION OF HIGH PRANDTL NUMBER FLUIDS IN A CUBICAL CAVITY
Obai Younis Taha Elamin
ISBN:978-84-692-9056-9/DL:T-2069-2009

Figure 4.11 shows the velocity vector and the temperature isotherms at $t = 1800$ s. It can be seen that for CV1 and VV1, the flow velocities in the lower half of the cube are considerably reduced where a stagnant layer forms. The convection is confined in the upper half of the cube (Figures 4.11(a), and 4.11(c)). Instability effects starts to become evident in CV2 as indicated by the descending plume in Figure 4.11(b). The delay of the instability is associated with the thermal boundary condition (insulation of bottom wall). The flow velocities in the upper half of the cavity for case VV2 (Figure 4.11(d)) are considerably reduced, pushing the secondary flow towards the center of the cavity. No big changes in the lower half are observed due to the combined effects of thermal boundary condition and variable viscosity. No new features observed for cases CVWC1, CVWC2,VVWC1 and CVWC2. The presented flow field and temperature contours for these cases (Figure 4.12) exactly follow the trend of CV1, CV2, VV1 and VV2 with a certain time lag. This is a clear evidence that the only effect of wall conduction is to delay the onset of the convection.

UNIVERSITAT ROVIRA I VIRGILI
NUMERICAL AND EXPERIMENTAL STUDY OF TRANSIENT LAMINAR NATURAL CONVECTION OF HIGH PRANDTL NUMBER FLUIDS IN A CUBICAL CAVITY
Obai Younis Taha Elamin
ISBN:978-84-692-9056-9/DL:T-2069-2009

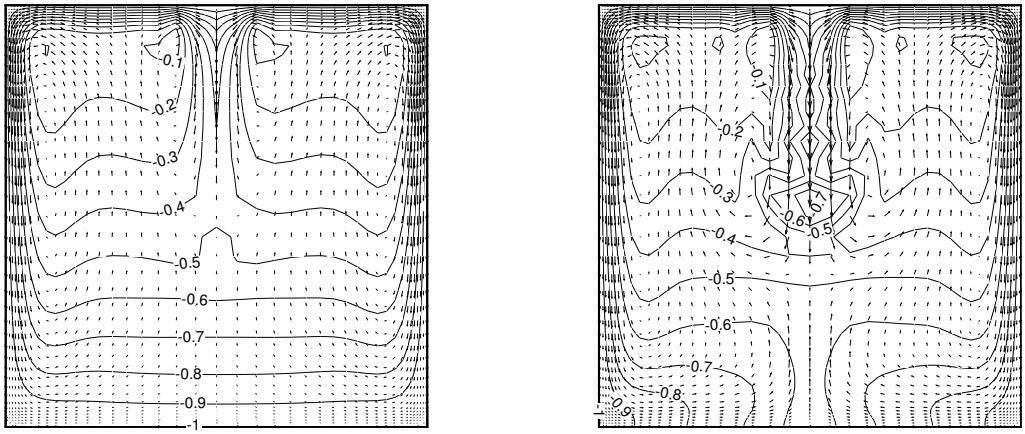

(a) CV1

(b) CV2

(c) VV1

(d) VV2

Figure 4.11: Velocity vectors and temperature contours at $t = 1800$ s, cases 1-4 (see Table (4.1)).

UNIVERSITAT ROVIRA I VIRGILI
NUMERICAL AND EXPERIMENTAL STUDY OF TRANSIENT LAMINAR NATURAL CONVECTION OF HIGH PRANDTL NUMBER FLUIDS IN A CUBICAL CAVITY
Obai Younis Taha Elamin
ISBN:978-84-692-9056-9/DL:T-2069-2009

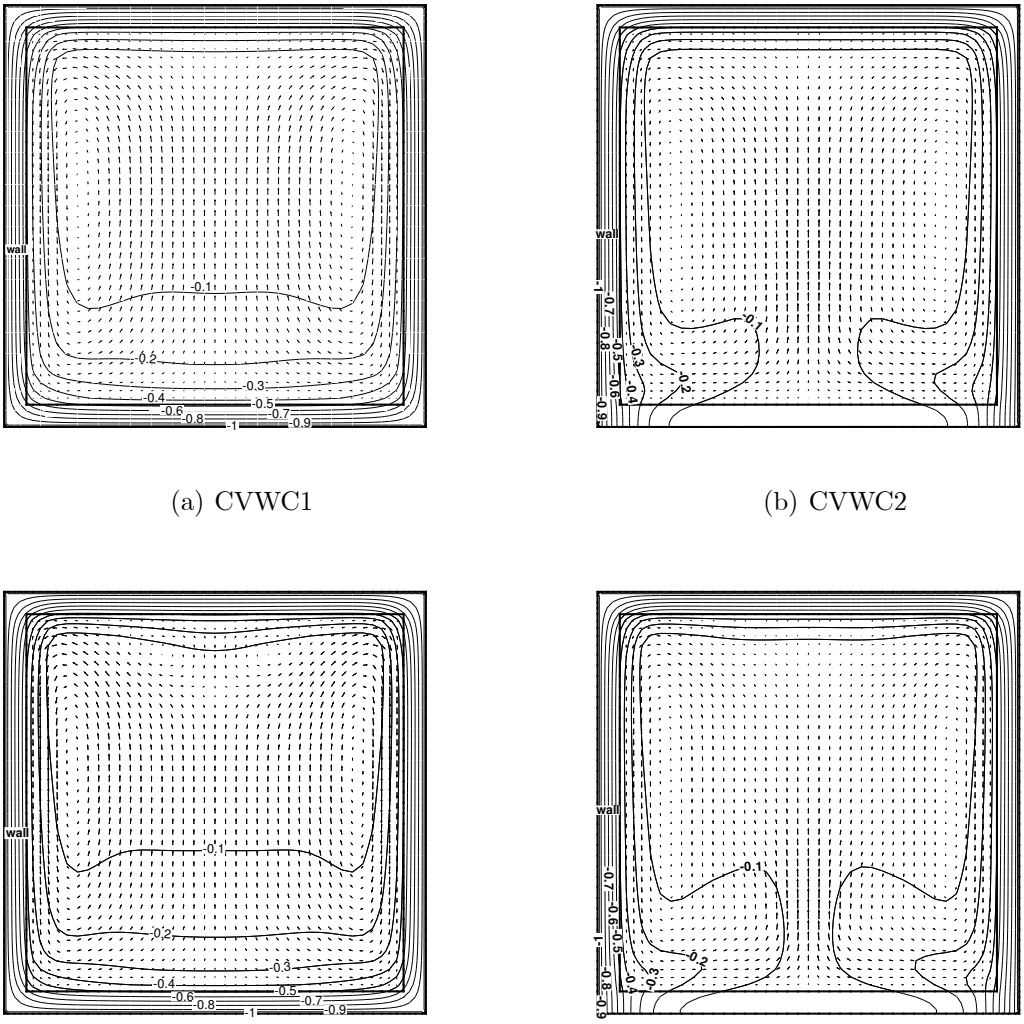

(a) CVWC1

(b) CVWC2

(c) VVWC1

(d) VVWC2

Figure 4.12: Velocity vectors and temperature contours at $t = 1800$ s, cases 5-8 (see Table (4.1)).

UNIVERSITAT ROVIRA I VIRGILI
NUMERICAL AND EXPERIMENTAL STUDY OF TRANSIENT LAMINAR NATURAL CONVECTION OF HIGH PRANDTL NUMBER FLUIDS IN A CUBICAL CAVITY
Obai Younis Taha Elamin
ISBN:978-84-692-9056-9/DL:T-2069-2009

4.1.3 Time Averaged quantities

The time evolution of the volume averaged temperature of the fluid is plotted in Figure 4.13. As expected, CV1 and VV1 achieved the minimum temperature due to the thermal boundary condition (all the walls are active). In the early beginning of cooling ($t > 600s$ s), viscosity variation has no effects of the volume averaged temperature. However after $t = 600$ s, viscosity variation slightly affects the averaged temperature because of the presence of the temperature, and viscosity, gradients within the fluid as shown in Figures 4.7(c) and 4.7(d). For cases of constant viscosity (CV1 and CV2) and variable viscosity (VV1 and VV2), the difference of the averaged temperature is negligible (at $t = 1800$ s the difference is only 1%). The difference of the averaged temperature of CV1 and CV2 (or VV1 and VV2) is mainly attributed to the thermal boundary conditions. Regarding the wall conduction cases, the low value of the thermal conductivity of the walls has a great impact on to the cooling process, as can be deduced from the low value of the slope of the time evolution of the averaged temperature of CVWC1, CVWC2, VVWC1 and VVWC2 as shown in Figure 4.13. The fluid cools down very slowly due to the convection delay.

The averaged non-dimensional heat transfer rate (Nu) on the walls of the cavity is shown in Figures 4.14 and 4.15. For CV1 and VV1, the variable viscosity has no effect on the heat transfer rate. At $t > 600s$, the heat transfer rates of CV1 and VV2 are not significantly different. Nu of VV2 is clearly deviated from Nu of CV2. The deviation is caused by the combined effect of the thermal boundary condition and the variable viscosity. Moreover, Nu of CV1,CV2 and VV1 has the same trend, it drops linearly between (0 s $< t >$ 800 s) and (1400 s $< t >$ 1800 s). The non-linear drop between (800 s $< t >$ 1400 s) is a associated with the top wall instability (Figures 4.7(a),4.7(c) and 4.7(d)). For CV2, Nu approximately has a linear drop for $t > 1500$ s when the top wall instability takes place (Figure 4.11(b)).

For the wall conduction cases (Figure 4.15), the heat transfer rate starts from 0 (due to the wall conductivity) and starts to grow as time evolves. It reaches the maximum at $t = 800$ s, at this stage the convection starts to be dominant and the Nu starts to decrease. In contrast to other cases (Figure 4.14), where Nu starts form its maximum (due to the step change in the

UNIVERSITAT ROVIRA I VIRGILI
NUMERICAL AND EXPERIMENTAL STUDY OF TRANSIENT LAMINAR NATURAL CONVECTION OF HIGH PRANDTL NUMBER FLUIDS IN A CUBICAL CAVITY
Obai Younis Taha Elamin
ISBN:978-84-692-9056-9/DL:T-2069-2009

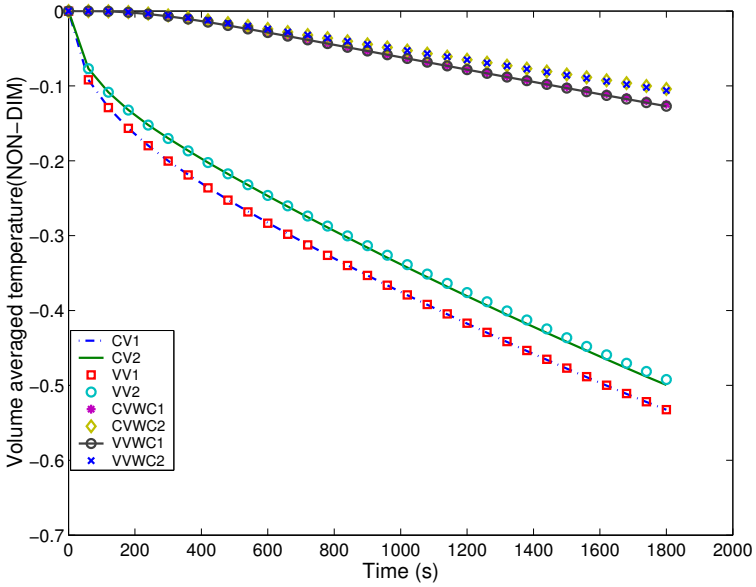

Figure 4.13: Time evolution of the non-dimensional volume averaged temperature

temperature between the fluid and the cavity walls) and then decreases.

To explain the contribution of top and bottom wall to the heat transfer process, the averaged heat transfer rate of the top (Nu_t) and bottom (Nu_b) wall of CV1 are plotted in Figure 4.16. Both heat transfer rates are similar in the early stage of cooling when the convection is dominant (at $t < 100$ s). Nu_b is reduced faster than Nu_t. At $t > 400$ s, Nu_t is approximately constant while Nu_b is still decreasing. At $t > 800$ s Nu_b is almost constant and very close to 1 (the conduction limit). This supports the assumption that the convection is confined in the upper half of the cavity. A slight oscillation appears in the time evolution of Nu_t at ($1200s < t < 1800s$) due to the flow instability near the top wall that generates the secondary flows shown in Figure 4.7(a).

UNIVERSITAT ROVIRA I VIRGILI
NUMERICAL AND EXPERIMENTAL STUDY OF TRANSIENT LAMINAR NATURAL CONVECTION OF HIGH PRANDTL NUMBER FLUIDS IN A CUBICAL CAVITY
Obai Younis Taha Elamin
ISBN:978-84-692-9056-9/DL:T-2069-2009

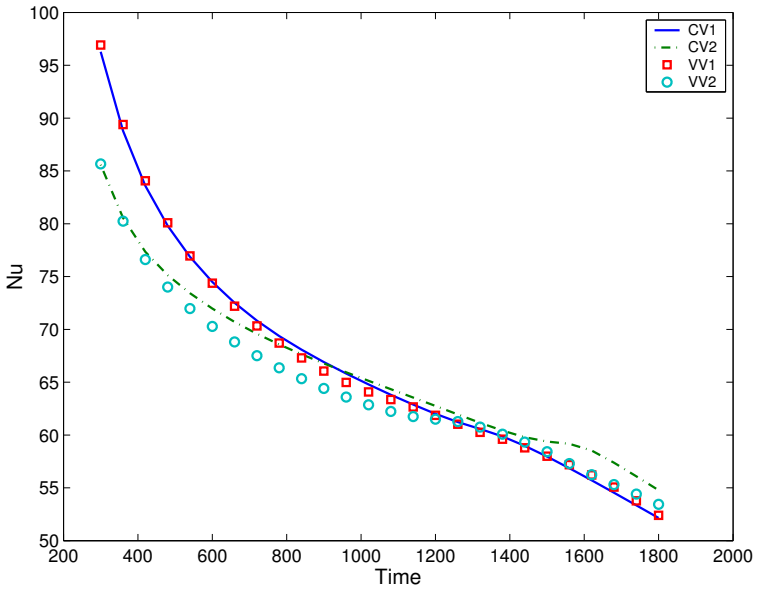

Figure 4.14: Time evolution of the overall Nusselt number

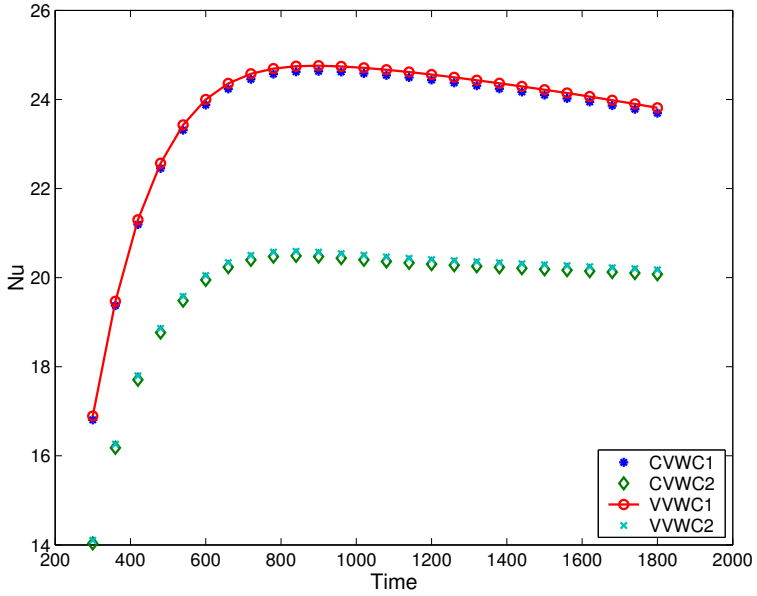

Figure 4.15: Time evolution of the overall Nusselt number

UNIVERSITAT ROVIRA I VIRGILI
NUMERICAL AND EXPERIMENTAL STUDY OF TRANSIENT LAMINAR NATURAL CONVECTION OF HIGH PRANDTL NUMBER FLUIDS IN A CUBICAL CAVITY
Obai Younis Taha Elamin
ISBN:978-84-692-9056-9/DL:T-2069-2009

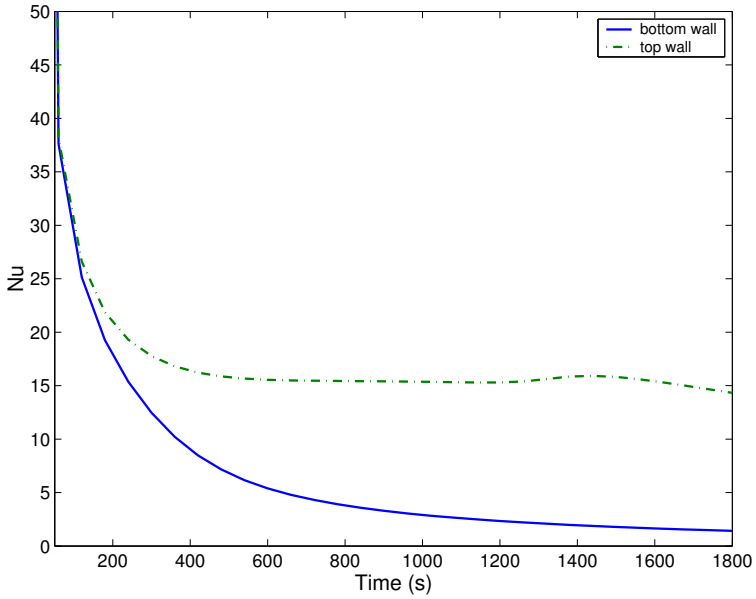

Figure 4.16: Time evolution of the local Nusselt numbers at the top and bottom walls for CV1

UNIVERSITAT ROVIRA I VIRGILI
NUMERICAL AND EXPERIMENTAL STUDY OF TRANSIENT LAMINAR NATURAL CONVECTION OF HIGH PRANDTL NUMBER FLUIDS IN A CUBICAL CAVITY
Obai Younis Taha Elamin
ISBN:978-84-692-9056-9/DL:T-2069-2009

4.2 Experiments and numerical simulation of transient natural convection in a side-cooled cubical cavity: Scaling for variable viscosity fluids

The transient natural convection undergoes a number of stages in the side-cooled cubical cavity. It starts from the step change of the temperature of the side walls and it ends with the isothermal conditions. In the following subsections, these stages are discussed and identified by presenting the shadowgraph images corresponding to each stage. New scaling relations based on the shadowgraph images are developed. In addition, a comparison between the shadowgraph images of these stages and the corresponding numerical results is carried out to validate the numerical tool. The effect of variable viscosity and high Prandtl number is also discussed. For the experiments as well as the numerical simulation, two kinds of working fluids are employed, water for the constant viscosity cases, and different concentrations of Glycerin-water solutions for the variable viscosity cases. The initial temperature (T_h) of the working fluid set to 10^oC, while the temperature of the cold vertical side-walls (T_c) ranges from 15^oC to 50^oC. This results in temperature differences ranging from 5^oC to 40^oC. The corresponding ranges of the Rayleigh number, Prandtl number and viscosity contrast are $2.9.10^7$ to $1.4.10^8$, 6.2 to 190.0 and 1.00 to 5.87, respectively. The experimentally and numerically studied cases are shown in Table (4.2).

UNIVERSITAT ROVIRA I VIRGILI
NUMERICAL AND EXPERIMENTAL STUDY OF TRANSIENT LAMINAR NATURAL CONVECTION OF HIGH PRANDTL NUMBER FLUIDS IN A CUBICAL CAVITY
Obai Younis Taha Elamin
ISBN:978-84-692-9056-9/DL:T-2069-2009

Case	Fluid	Ra	Pr	T_c^oC	T_h^oC	ν_c/ν_h
1	Water	$9.0.10^7$	8.24	10	20	1.00
2	Water	$2.6.10^8$	7.00	10	30	1.00
3	Water	$4.2.10^8$	6.60	10	35	1.00
4	Water	$5.9.10^8$	6.20	10	40	1.00
5	Water70%-Glycerin30%	$2.9.10^7$	23.00	10	15	1.14
6	Water70%-Glycerin30%	$6.7.10^7$	21.00	10	20	1.39
7	Water50%-Glycerin50%	$3.1.10^7$	55.00	10	18	1.50
8	Water50%-Glycerin50%	$1.0.10^8$	44.00	10	30	2.14
9	Water30%-Glycerin70%	$4.1.10^7$	190.00	10	30	2.77
10	Water30%-Glycerin70%	$1.4.10^8$	120.00	10	50	5.87

Table 4.2: The experimentally and numerically studied cases

4.2.1 Experiments of transient natural convection in a side-cooled cubical cavity

In the following subsection, the shadowgraph images are presented to show transient features of the convective flow in a side-cooled cavity. Measurements based on the shadowgraph images are used to validate the new scaling relations introduced in this subsection.

4.2.1.1 The initial growth stage

The main characteristics of this stage are the growth of the vertical thermal boundary layers and the formation of the horizontal intrusions. At the very beginning, the dominating heat transfer mode is conduction which occurs due to the contact of the hot fluid in the cavity with the cold vertical copper walls. This results in the progressive growth of the thermal boundary layer adjacent to the vertical walls. Figure 4.17 shows a time series of shadowgraph images representing the boundary layer growth near the right vertical wall of the cavity. These images were processed by subtracting a background image recorded immediately before the start of the experiment so that the thermal boundary layers can be clearly identified in the images. The boundary layer thickness is approximately represented by the vertical dark strips. At $t < 9$ s (Figure 4.17 *a-c*) these strips are parallel to the vertical wall and the horizontal intrusions are not evident, which indicates that convection has not started yet

UNIVERSITAT ROVIRA I VIRGILI
NUMERICAL AND EXPERIMENTAL STUDY OF TRANSIENT LAMINAR NATURAL CONVECTION OF HIGH PRANDTL NUMBER FLUIDS IN A CUBICAL CAVITY
Obai Younis Taha Elamin
ISBN:978-84-692-9056-9/DL:T-2069-2009

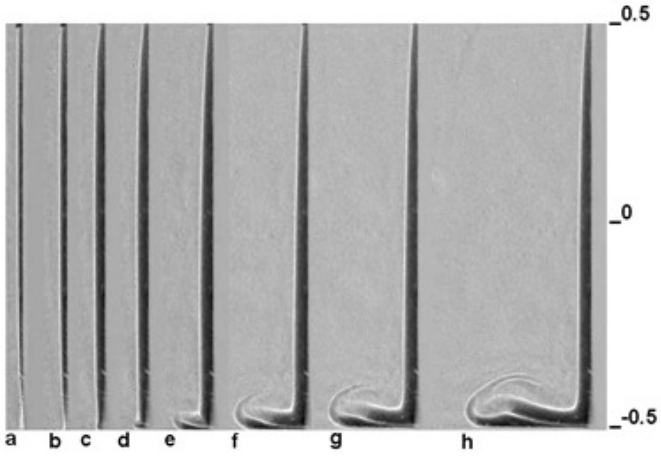

Figure 4.17: Growth of the boundary layer and horizontal intrusions for case 2 ($Ra = 2.6.10^8$, $Pr = 7$, $\frac{\nu_c}{\nu_h} = 1$) (see Table (4.2)), $(a)t = 3$ s, $(b)t = 5$ s, $(c)t = 8$ s, $(d)t = 9$ s, $(e)t = 11$ s, $(f)t = 13$ s, $(g)t = 14$ s, $(h)t = 15s$.

and thus the main heat transfer mode is conduction. However conduction heat transfer only dominates over very short time. As time evolves more fluid is cooled near the vertical walls and it is progressively discharged at the bottom of the cavity. At $t \geq 9$ s (Figures 4.17d to 4.17h) convection becomes important resulting in the generation of the horizontal intrusions, which travel towards the bottom wall bisector. The time evolution of the vertical boundary layer thickness at $x^* = 0$, for selected cases (with different Ra and Pr) is plotted in Figure 4.18 to show that different growth behaviour results from different flow conditions. The boundary layer thickness was estimated by the thickness of the dark strips adjacent to the vertical wall. The same method was successfully employed in previous studies (Xu et. al. [9] and Lei and Patterson [37]). However, the measured boundary layer growth is not smooth; it experiences step changes of 0.02 cm which corresponds to the resolution of the imaging system.

Generally, the boundary layer grows as $\tau^{0.5}$ through a short period of time

UNIVERSITAT ROVIRA I VIRGILI
NUMERICAL AND EXPERIMENTAL STUDY OF TRANSIENT LAMINAR NATURAL CONVECTION OF HIGH PRANDTL NUMBER FLUIDS IN A CUBICAL CAVITY
Obai Younis Taha Elamin
ISBN:978-84-692-9056-9/DL:T-2069-2009

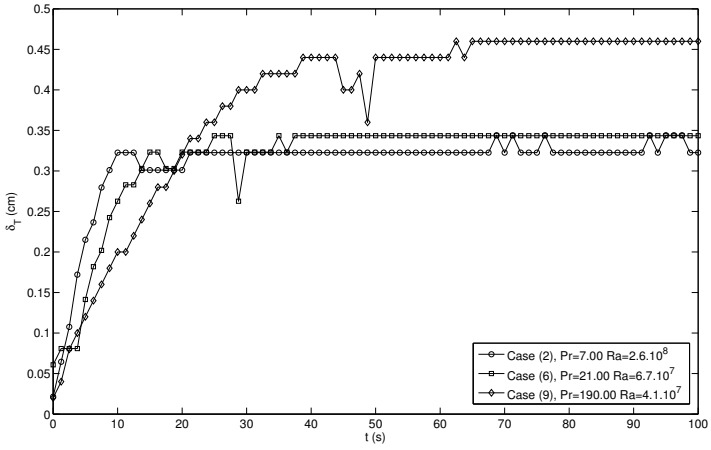

Figure 4.18: Time evolution of boundary layer thickness

(when conduction is the dominant mechanism as discussed earlier) until the maximum thickness is reached. During this period of time the boundary layer thickness only depends on α as suggested by Patterson and Imberger [15]. Then the thickness drops slightly to achieve steady state. The thickness at the steady state only depends on the Ra (see Patterson and Imberger [15]), while the time on which the onset of the convection starts (the time at which the boundary layer deviates from the conduction trend) shows sensitivity for Pr. In Figure 4.18, the onset of convection starts at 9 s, 23.5 s and 37.75 s for the cases of $Pr = 7, 21$ and 190 respectively.

Lin & Armfield [23] suggested the following scaling relationship to describe the boundary layer growth during this stage:

$$\delta_T^* \approx Ra^{-1/4}\tau^{1/2} \tag{4.2}$$

In Figure 4.19, the non-dimensional boundary layer thickness at the middle of the vertical wall ($x^* = 0$) is plotted against the suggested scaling. In consideration of the experimental error, the data fits reasonably well with the scaling for $\tau \leq 1$ in which the conduction is dominating. As time increases, the measured boundary layer thickness deviates from the scaling indicating the onset of convection and shows dependence on Ra and Pr.

Patterson and Imberger [15] showed that the steady state thermal boundary

UNIVERSITAT ROVIRA I VIRGILI
NUMERICAL AND EXPERIMENTAL STUDY OF TRANSIENT LAMINAR NATURAL CONVECTION OF HIGH PRANDTL NUMBER FLUIDS IN A CUBICAL CAVITY
Obai Younis Taha Elamin
ISBN:978-84-692-9056-9/DL:T-2069-2009

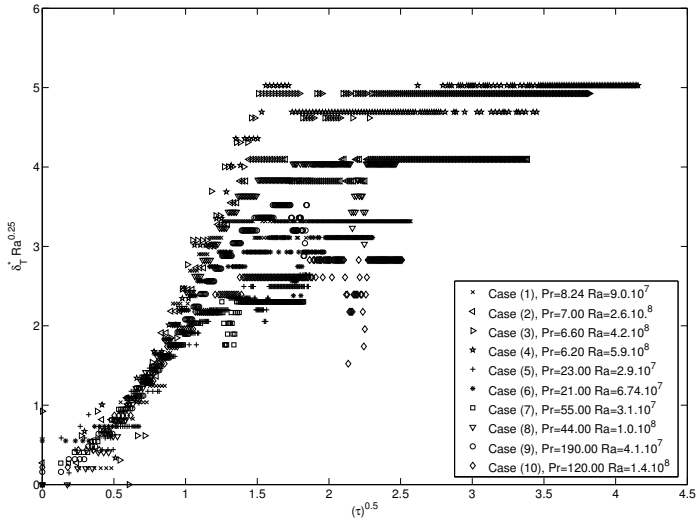

Figure 4.19: $\delta Ra^{1/4}$ against $\tau^{1/2}$

layer thickness scale δ_T was given by:

$$\delta_T = HRa^{-1/4} \tag{4.3}$$

Occurring after time scale t_s:

$$t_s = \frac{H^2}{\alpha Ra^{1/2}} \tag{4.4}$$

Jeevaraj and Patterson [8] modified the time scale (Equation (4.4)) to give a time scaling depending on the height x due to the non-uniformity of the thermal boundary layer thickness (see Figure 4.17). The scaling was given by:

$$t_s(x) = \frac{H^{3/2}x^{1/2}}{\alpha Ra^{1/2}} \tag{4.5}$$

Due to the viscosity dependence on temperature and therefore on time, this time scale should be modified to account for the effect of the variable viscosity. The only modification should be on the momentum equation in which the motion is driven by the buoyancy and viscous force:

$$\frac{\partial}{\partial y}(\nu\frac{\partial u}{\partial y}) \approx g\beta\Delta T \tag{4.6}$$

UNIVERSITAT ROVIRA I VIRGILI
NUMERICAL AND EXPERIMENTAL STUDY OF TRANSIENT LAMINAR NATURAL CONVECTION OF HIGH PRANDTL NUMBER FLUIDS IN A CUBICAL CAVITY
Obai Younis Taha Elamin
ISBN:978-84-692-9056-9/DL:T-2069-2009

Equation (4.6) can be expressed as:

$$\frac{\partial \nu}{\partial y}\frac{\partial u}{\partial y} + \nu\frac{\partial^2 u}{\partial y^2} \approx g\beta\Delta T \tag{4.7}$$

And thus

$$\frac{\Delta \nu}{\delta_T}\frac{u}{\delta_T} + \nu_0\frac{u}{\delta_T^2} \approx g\beta\Delta T \tag{4.8}$$

The growth of the thermal boundary layer continues until the balance between the convection along the vertical x direction and conduction is satisfied

$$u\frac{\Delta T}{x} \approx \alpha\frac{\Delta T}{\delta_T^2} \tag{4.9}$$

Equations (4.8 and 4.9) give a new time scale as follows:

$$t_s(x) = \frac{H^{3/2}x^{1/2}(1 + {}^{\Delta\nu}/_{\nu_0})^{1/2}}{\alpha Ra^{1/2}} \tag{4.10}$$

Using the same arguments, Equation (4.4) is modified to give:

$$t_s = \frac{H^2(1 + {}^{\Delta\nu}/_{\nu_0})^{1/2}}{\alpha Ra^{1/2}} \tag{4.11}$$

The new obtained time scale (Equation (4.11)) is plotted against the observed time in Figure 4.20. With consideration of the experimental and the imaging system error, Figure 4.20 shows a linear correlation between the time scale and the observed time, which confirms the scaling. The time scale of Jeevaraj and Patterson [8] (Equation (4.5)) is also included in Figure 4.20 to show the effect of the variable viscosity. It is clear that the inclusion of the variable viscosity in the time scale improves the correlation by pushing the data points towards the fitting line. The standard deviation of the modified time scale is 1.7 while the time scale of Jeevaraj and Patterson [8] has a standard deviation of 5.8.

As time increases further beyond the time needed for the boundary layer to reach steady state, the horizontal intrusions travel towards the cavity center through the bottom boundary and the flow enters a new stage.

UNIVERSITAT ROVIRA I VIRGILI
NUMERICAL AND EXPERIMENTAL STUDY OF TRANSIENT LAMINAR NATURAL CONVECTION OF HIGH PRANDTL NUMBER FLUIDS IN A CUBICAL CAVITY
Obai Younis Taha Elamin
ISBN:978-84-692-9056-9/DL:T-2069-2009

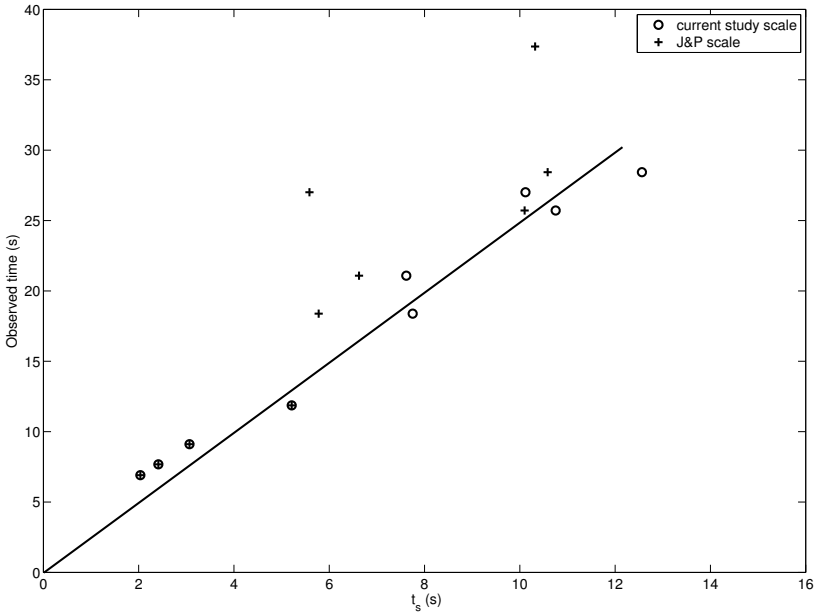

Figure 4.20: The observed time for the thermal boundary layer to reach the maximum thickness plotted against the time scale. J&P stands for Jeevaraj and Patterson [8].

UNIVERSITAT ROVIRA I VIRGILI
NUMERICAL AND EXPERIMENTAL STUDY OF TRANSIENT LAMINAR NATURAL CONVECTION OF HIGH PRANDTL NUMBER FLUIDS IN A CUBICAL CAVITY
Obai Younis Taha Elamin
ISBN:978-84-692-9056-9/DL:T-2069-2009

4.2.1.2 The interaction of the horizontal viscous intrusions

The onset of heat convection results in cold horizontal intrusions travelling form the cold side walls towards the bottom wall bisector. The development of the horizontal intrusions is shown in Figure 4.21 for case 2 ($Ra = 2.6.10^8$, $Pr = 7$, $\frac{\nu_c}{\nu_h} = 1$) (see Table (4.2)). Clearly, separation of the two horizontal intrusions arises near the bottom corners (see Figure 4.21 a and b). Xu et. al. [9] experienced similar separation and reported that separation from the bottom wall was caused by an adverse pressure gradient. However in their case, the intrusion reattached after leaving the corner, while in Figure 4.21 there is no evidence of reattachment. A possible explanation for this difference can be the different thermal boundary conditions and/or the cavity dimensions. Xu et. al. [9] cooled one side wall and heated the opposing one while in current study both side walls are cooled. As time increases, more cold flow driven by the intrusion is accumulated on the bottom wall. This accumulation of the cold fluid results in drawing the intrusions closer to the sidewalls forming an upright flow structure near the bottom corners (see Figure 4.21 c and d).

The effect of Rayleigh number on the horizontal intrusion is shown in Figure 4.22. It can be seen that, as the Rayleigh number increases, the intrusions thickness and nose size increase, and the intrusions travel at larger distances towards the bottom wall bisector.

Xu et. al. [31] introduced intrusion velocity scale by considering the variable flux of intrusion. The variable flux of intrusion is given by:

$$Q = u\delta_T \tag{4.12}$$

According to Patterson and Imberger [15], for a fluid with constant viscosity the variable flux of intrusion can be expressed as:

$$Q = {}^{\alpha^{5/2} Ra t^{3/2}}/_{H^3} \tag{4.13}$$

Xu et. al. [31] used also the balance between the buoyancy induced pressure gradient and inertia which reads:

$$-\frac{1}{\rho}\frac{\Delta P}{\Delta y} \approx \frac{v}{t} \tag{4.14}$$

UNIVERSITAT ROVIRA I VIRGILI
NUMERICAL AND EXPERIMENTAL STUDY OF TRANSIENT LAMINAR NATURAL CONVECTION OF HIGH PRANDTL NUMBER FLUIDS IN A CUBICAL CAVITY
Obai Younis Taha Elamin
ISBN:978-84-692-9056-9/DL:T-2069-2009

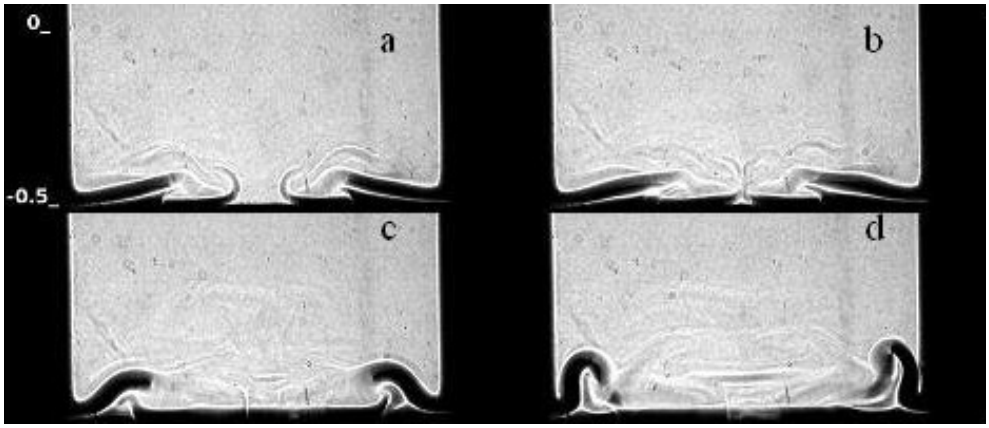

Figure 4.21: Development of the horizontal intrusions for case 2 ($Ra = 2.6.10^8$, $Pr = 7$, $\frac{\nu_c}{\nu_h} = 1$)(see Table (4.2)), $(a)t = 18$ s, $(b)t = 20$ s, $(c)t = 28$ s and $(d)t = 33$ s.

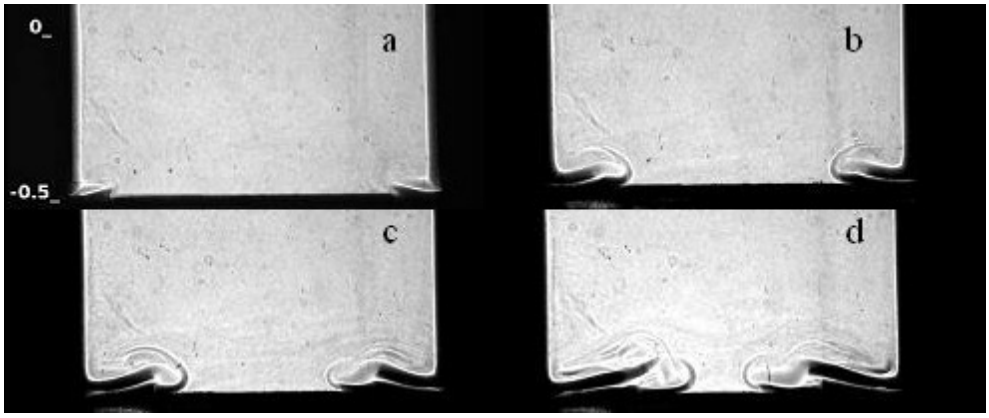

Figure 4.22: Development of the horizontal intrusions at different Rayleigh numbers at $t = 14$ s and $Pr = 7$, $(a)Ra = 0.9.10^8$ case (1), $(b)Ra = 2.6.10^8$ case (2), $(c)Ra = 4.2.10^8$ case (3), $(d)Ra = 5.9.10^8$ case (4).

The balance in the vertical direction reads:

$$-\frac{1}{\rho}\frac{\Delta P}{\Delta x} + g\beta\Delta T \approx 0 \tag{4.15}$$

Δy and Δx can be estimated as vt and δ_I respectively, where δ_I is the intrusion thickness. Equation (4.15) gives:

$$\Delta P = \rho g \beta \Delta T \delta_I \tag{4.16}$$

Hence Equation (4.14) can be rewritten as:

$$\frac{g\beta\Delta T\delta_I}{vt} = \frac{v}{t} \tag{4.17}$$

The same methodology of Xu et. al. [31] is followed here to obtain new intrusion velocity scale taking into account the fluid variable viscosity. To be able to include the variable viscosity effect, the boundary layer velocity scale used to drive the variable heat flux of intrusion (Equation (4.13)) should be further developed since the viscous term is involved. Equation (4.6) gives directly the new boundary layer velocity scale as follows:

$$u = \frac{g\beta\Delta T t}{Pr(1 + {}^{\Delta\nu}/_{\nu_0})} \tag{4.18}$$

Equation (4.18) along with the boundary layer thickness of Patterson and Imberger [15] ($\delta_T = \alpha^{1/2}t^{1/2}$), give the new variable flux of intrusion:

$$Q = \frac{Ra\alpha^{5/2}t^{3/2}}{H^3(1 + {}^{\Delta\nu}/_{\nu_0})} \tag{4.19}$$

The intrusion velocity scale is obtained by balancing the buoyancy induced pressure gradient and inertia (Equation (4.17)). This balance along with Equation (4.19) give:

$$v_I = \frac{Ra^{3/2}\alpha^{3/2}t^{1/2}Pr^{1/3}}{H^2(1 + {}^{\Delta\nu}/_{\nu_0})} \tag{4.20}$$

According to Huppert [38], the initial balance in the intrusion is between the buoyancy-induced pressure gradient and the viscous term but quickly becomes between the buoyancy-induced pressure gradient and inertia (see also Patterson and Imberger [15]). However, for high Pr numbers the viscous forces are still

dominating and the initial balance between the buoyancy-induced pressure gradient and the viscous term ($g\beta\Delta T\delta_I/vt \approx v(\Delta\nu+\nu_0)/\delta_I^2$) continues for larger time. Considering this balance and Equation (4.19), another intrusion velocity scale for high Pr ($Pr \geq 30$) is obtained:

$$v_I = \frac{Ra^{4/5}\alpha^{5/2}t^{7/10}Pr^{4/5}}{H^{12/5}(1+\Delta\nu/\nu_0)^{4/5}} \tag{4.21}$$

The intrusion velocity were extracted from the shadowgraph images and plotted against the intrusion velocity scale in Figures 4.23(a) and 4.23(b). In Figure 4.23(a), the observed velocity is plotted against the velocity scale of Xu et. al. [9]. It is clear that the data is highly scattered and a good fitting of the data can not be obtained without modification due to the presence of the variable viscosity and the high Pr numbers. The modified scale (Equations (4.20) and (4.21)) is shown in Figure 4.23(b). It can be seen that the fitting is improved by including the variable viscosity effect, which acted to force the scattered data points to move closer towards the fitting line.

As suggested by Figures 4.17 and 4.22, the intrusion thickness increases with time and the Rayleigh number. A scale for the intrusion thickness can be directly extracted from Equations (4.12)-(4.21): For $Pr < 30$:

$$\delta_I = \frac{Ra^{1/3}\alpha t}{H(1+\Delta\nu/\nu_0)^{2/3}Pr^{1/3}} \tag{4.22}$$

For $Pr \geq 30$:

$$\delta_I = \frac{Ra^{1/5}\alpha t^{8/10}Pr^{1/5}}{H^{3/5}(\Delta\nu+\nu_0)^{1/5}} \tag{4.23}$$

In Figure 4.24, the intrusions thickness scale is plotted against the observed intrusion thickness. The linear correlation between the observed thickness and the scale confirmed the scaling relationship. To show the effect of the high Pr number (when $Pr \geq 30$) on the scaling argument, the intrusion thickness scale for $Pr < 30$ (Equation (4.22) is used for the cases of $Pr > 30$(cases 7-10) and plotted against the observed thickness (the square symbols) in Figure 4.24. Clearly, the consideration of the high Pr number improves the scaling (the arrow in Figure 4.24 shows the displacement applied to the data point when using the proper scale).

The effect of the Pr number on the growth of the horizontal intrusions

UNIVERSITAT ROVIRA I VIRGILI
NUMERICAL AND EXPERIMENTAL STUDY OF TRANSIENT LAMINAR NATURAL CONVECTION OF HIGH PRANDTL NUMBER FLUIDS IN A CUBICAL CAVITY
Obai Younis Taha Elamin
ISBN:978-84-692-9056-9/DL:T-2069-2009

can be directly extracted from Figure 4.25, which shows the shadowgraph images of the horizontal intrusion registered at the same time at different Prandtl numbers. The images show that at a given time the intrusion velocity and intrusion thickness are reduced when Pr number increased. At the same time, the scaling relation for the intrusion velocity and intrusion thickness suggested in Equations (4.20)-(4.23) indicates that the intrusion velocity and the thickness are increased with Pr number. To prove the validity of these scales, the measured distance travelled by the intrusion and the measured intrusion thickness of different Pr numbers are plotted along with the proper scales against the time in Figures 4.26 and 4.27 respectively. It is clearly shown in Figures 4.26 and 4.27, that at a given time the distance travelled by the intrusion and the intrusion thickness decrease as the Pr number increases. It can be seen that the scaling given in Equation (4.23) for $Pr \geq 30$ suggests the opposite trend. However as Equation (4.23) indicates there is influence of other parameters such as $\alpha, \Delta\nu$ and ν_0 on the intrusion thickness.

UNIVERSITAT ROVIRA I VIRGILI
NUMERICAL AND EXPERIMENTAL STUDY OF TRANSIENT LAMINAR NATURAL CONVECTION OF HIGH PRANDTL NUMBER FLUIDS IN A CUBICAL CAVITY
Obai Younis Taha Elamin
ISBN:978-84-692-9056-9/DL:T-2069-2009

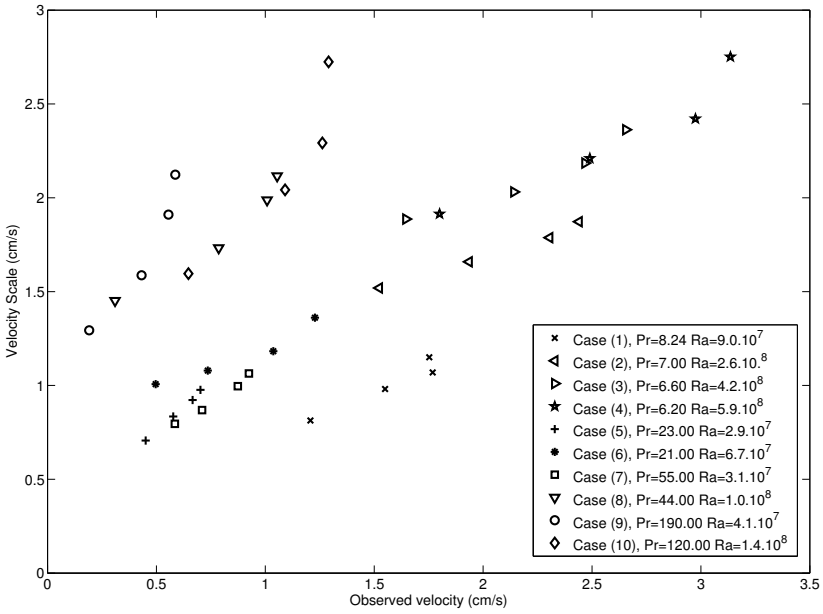

(a) Xu et. al. [9] scale

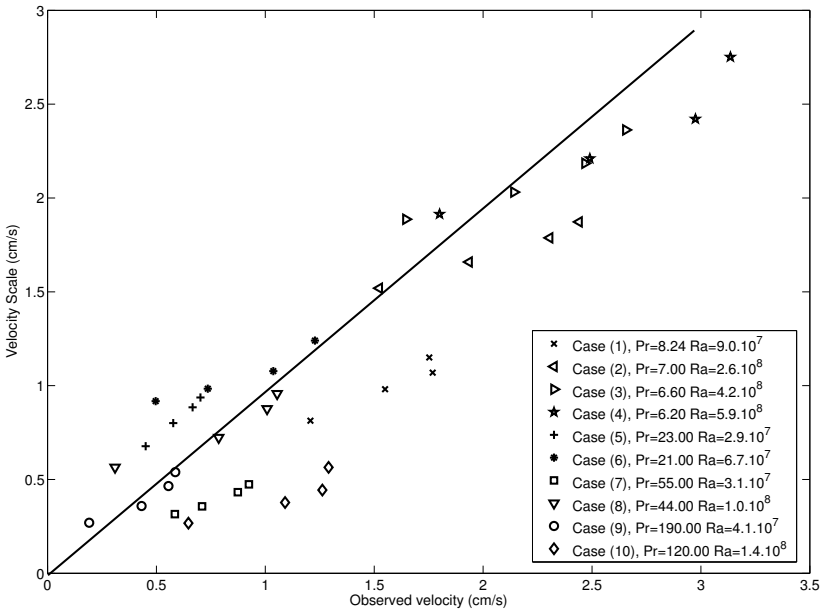

(b) present study scale

Figure 4.23: Observed intrusion velocity plotted against the intrusion velocity scale given in Equation (4.20) and Equation (4.21)

UNIVERSITAT ROVIRA I VIRGILI
NUMERICAL AND EXPERIMENTAL STUDY OF TRANSIENT LAMINAR NATURAL CONVECTION OF HIGH PRANDTL NUMBER FLUIDS IN A CUBICAL CAVITY
Obai Younis Taha Elamin
ISBN:978-84-692-9056-9/DL:T-2069-2009

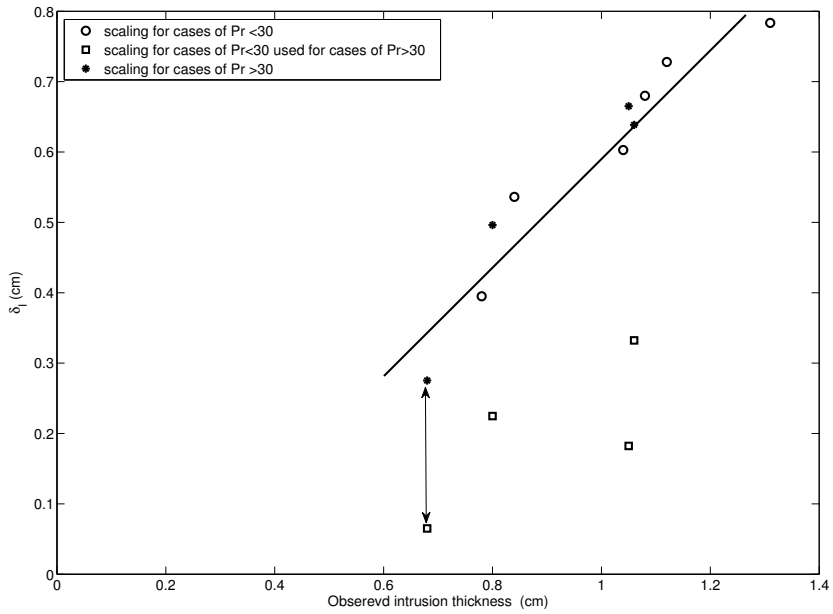

Figure 4.24: Observed intrusion thickness for cases 1-10 plotted against the intrusion thickness scale given in Equation (4.22) and Equation (4.23).

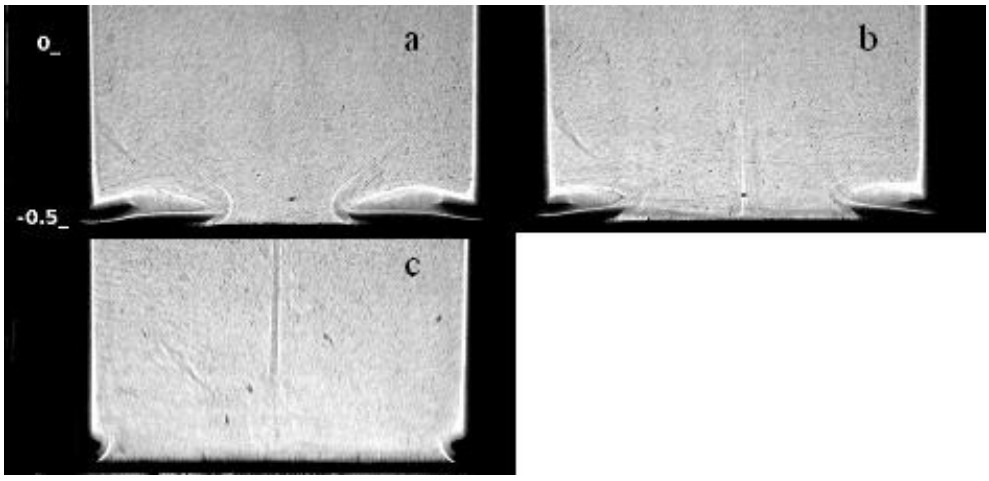

Figure 4.25: Development of the horizontal intrusions at different Prandtl numbers at $t = 33$ s and $Ra \approx 5.10^7$ for, $(a)Pr = 21$, $Ra = 6.74.10^7$ case 6, $(b)Pr = 55$, $Ra = 3.1.10^7$ case 7 and $(c)Pr = 190$, $Ra = 4.1.10^7$ case 9.

UNIVERSITAT ROVIRA I VIRGILI
NUMERICAL AND EXPERIMENTAL STUDY OF TRANSIENT LAMINAR NATURAL CONVECTION OF HIGH PRANDTL NUMBER FLUIDS IN A CUBICAL CAVITY
Obai Younis Taha Elamin
ISBN:978-84-692-9056-9/DL:T-2069-2009

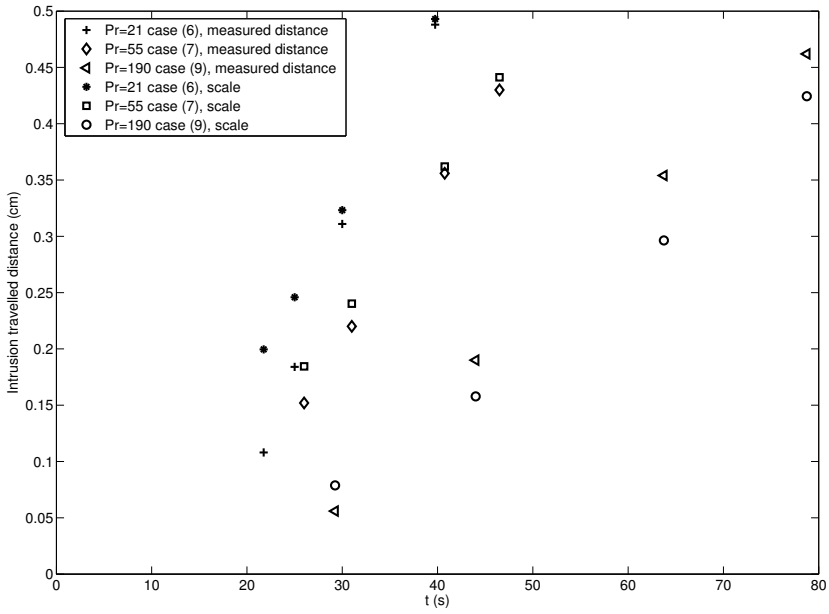

Figure 4.26: The observed distance travelled by the intrusion and the scale (Equation (4.20)and Equation (4.21)) plotted against time, $Ra \approx 5.10^7$

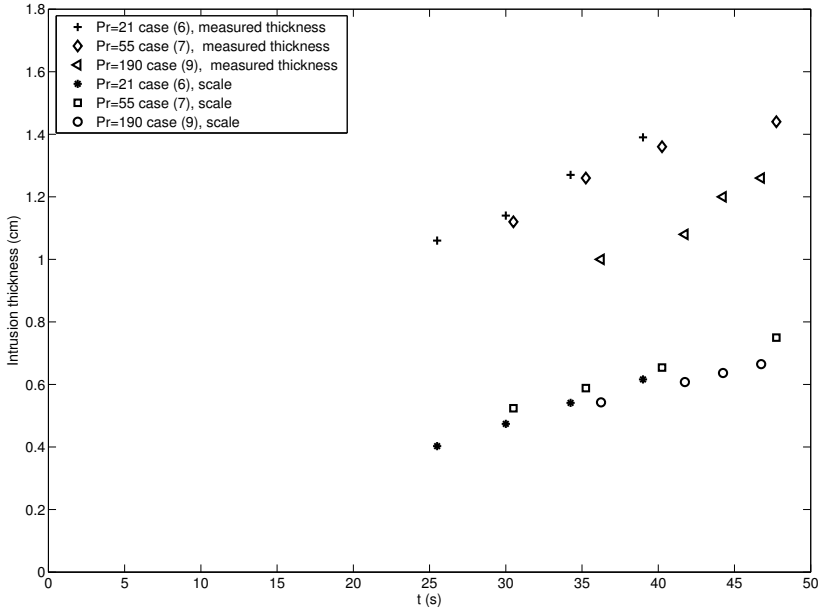

Figure 4.27: The observed intrusion thickness and the scale (Equation (4.22)and Equation (4.23)) plotted against time, $Ra \approx 5.10^7$

UNIVERSITAT ROVIRA I VIRGILI
NUMERICAL AND EXPERIMENTAL STUDY OF TRANSIENT LAMINAR NATURAL CONVECTION OF HIGH PRANDTL NUMBER FLUIDS IN A CUBICAL CAVITY
Obai Younis Taha Elamin
ISBN:978-84-692-9056-9/DL:T-2069-2009

4.2.1.3 Stratification of the core

After the merge of the horizontal intrusions (Figure 4.21 c and d), the cavity begins to fill with cold fluid discharged from the vertical thermal boundary layer. In this stage, the cavity core is composed of two regions, stratified fluid at the bottom and isothermal fluid at the top. The filling up process starts from the bottom upwards until the whole cavity is filled with stratified fluid. Due to the presence of the stratification, double-layer structures of the vertical boundary layers, represented by the two bright strips in the shadowgraph images in Figure 4.28 are formed. Three features can bee seen immediately from these shadowgraph images. The first feature is that the height of the double layer structure is increasing with time indicating the upward extension of the stratification. The other two features are that as time increases the double-layer structure becomes unclear in the shadowgraph images, because of the progressive reduction of the temperature gradients, and that its thickness is reduced.

The effect of Rayleigh number on the double layer structure is presented in Figure 4.29. As the Rayleigh number increases the double layer structure becomes clearer in the shadowgraph images and it increases in height indicating a faster rate of stratification.

Figure 4.30 shows the double-layer structure at different Prandtl numbers. The double-layer structure can hardly be seen as the Rayleigh number is low. The height of the double-layer structure (showed by the white arrow) is reduced as the Pr number increased and the layer became more distinct.

As stated earlier, the double-layer structure is formed when the core starts to be filled with cold fluid. The height of the double-layer structure can be interpreted as the height of the stratified region. Lin and Armfield [22] introduced a scaling for the rate of stratification. At any non dimensional time the stratification height is given by:

$$x^*_{st}(\tau) = 1 - (1 - ({}^{C_s A\tau}/_{Ra^{1/4}}))^4 \tag{4.24}$$

Where C_s is a constant of proportionality and A is the aspect ratio of the cavity. The height of the double-layer structure has been obtained from the shadowgraph images for all experiments. The obtained heights are non dimensionalized and plotted against ${}^{\tau}/_{Ra^{1/4}}$ in Figure 4.31(a). The experimental

UNIVERSITAT ROVIRA I VIRGILI
NUMERICAL AND EXPERIMENTAL STUDY OF TRANSIENT LAMINAR NATURAL CONVECTION OF HIGH PRANDTL NUMBER FLUIDS IN A CUBICAL CAVITY
Obai Younis Taha Elamin
ISBN:978-84-692-9056-9/DL:T-2069-2009

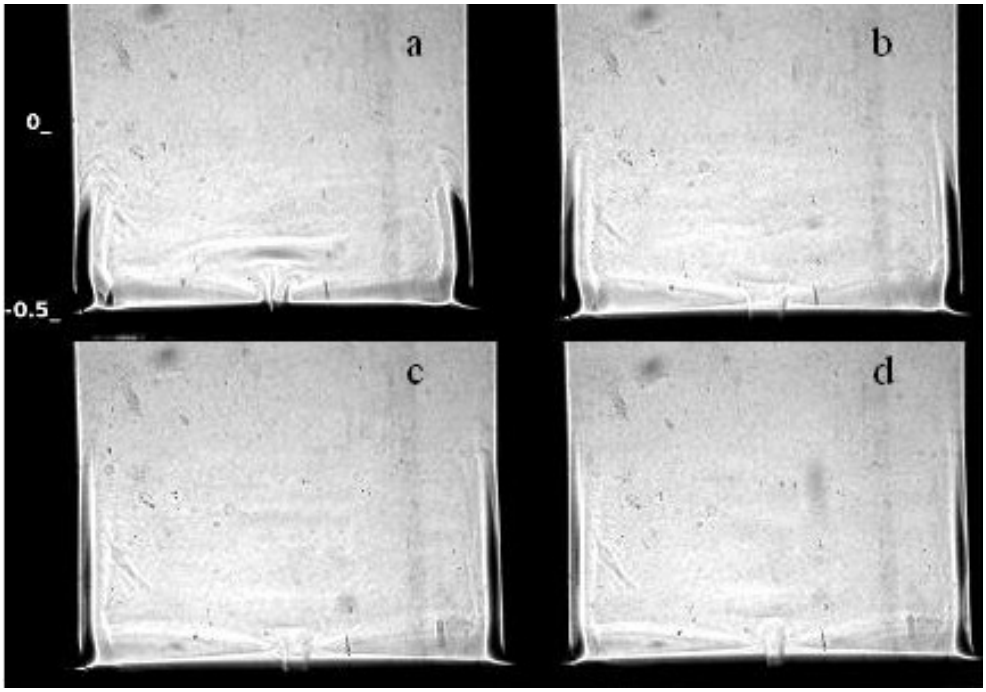

Figure 4.28: The development of double-layer structure for case 2, ($Ra = 2.6.10^8$, $Pr = 7$, $\frac{\nu_c}{\nu_h} = 1$) (see Table (4.2)), $(a)t = 58$ s, $(b)t = 68$ s, $(c)t = 96$ s and $(d) = 133$ s.

UNIVERSITAT ROVIRA I VIRGILI
NUMERICAL AND EXPERIMENTAL STUDY OF TRANSIENT LAMINAR NATURAL CONVECTION OF HIGH PRANDTL NUMBER FLUIDS IN A CUBICAL CAVITY
Obai Younis Taha Elamin
ISBN:978-84-692-9056-9/DL:T-2069-2009

results shown in this figure confirm the scaling. However more data points at earlier or later times could not be obtained from the shadowgraph images due to the unclearness of the double-layer structure. Due to lack of the measurement and the fact that the boundary layer velocity could not be obtained from the shadowgraph images, the validity of the boundary layer velocity scale Equation (4.18) can not be tested. However, the stratification height scaling (Equation (4.24)) can serve as an indirect indicator of the validation of the velocity scale. The time in Equation (4.24) is non dimensionalized by using Equation (4.18) ($\tau = \frac{t}{H/v}$), hence the collapse of the data in Figure 4.31(a) does not only confirms the scaling of Equation (4.24) but also Equation (4.18). However, Figure 4.31(b) re-plots the non dimensional stratification height against $\tau/Ra^{1/4}$, where the time is non dimesionalized by using the conventional velocity scale (see Patterson and Imberger [15]). The figure clearly shows that the data is scattered widely when neglecting the effect of the variable velocity, in which confirms the validity of the velocity scale of Equation (4.18). The scale of the stratification rate (Equation (4.24)) can be further supported by the shadowgraph images shown in Figures 4.29 and 4.30. To be able to compare these figures with the stratification rate scale, Equation (4.24) has to be written in dimensional form. By using Equations (4.11) and (4.18), the dimensional form of Equation (4.24) is presented in two different forms in terms of Rayleigh and Prandtl numbers:

$$x_{st} \propto \left(\frac{t\alpha}{H}\right) \frac{Ra^{1/4}}{(1 + \Delta\nu/\nu_0)} \tag{4.25}$$

$$x_{st} \propto \left(\frac{t^2 g}{Ra^{1/4}}\right) \frac{\beta\Delta T}{Pr(1 + \Delta\nu/\nu_0)} \tag{4.26}$$

Equation (4.25) indicates that for the same time, fluid and cavity size, the height of the double layer-structure only depends on $Ra^{1/4}/(1+\Delta\nu/\nu_0)$. However, for the cases presented in Figure 4.29 the viscosity was constant and therefore the height of the double layer-structure is directly proportional to the Rayleigh number. Equation (4.26) reveals that for the same time and Rayleigh number, some fluid properties as well as the temperature difference are involved. The value of the parameter $(\beta\Delta T/Pr(1+\Delta\nu/\nu_0))$ was found to be $9.10^{-5}, 4.10^{-5}$ and 2.10^{-5} for shadowgraph images of Figures 4.28a, b and c respectively, which support the inverse proportionality of the Prandtl number.

UNIVERSITAT ROVIRA I VIRGILI
NUMERICAL AND EXPERIMENTAL STUDY OF TRANSIENT LAMINAR NATURAL CONVECTION OF HIGH PRANDTL NUMBER FLUIDS IN A CUBICAL CAVITY
Obai Younis Taha Elamin
ISBN:978-84-692-9056-9/DL:T-2069-2009

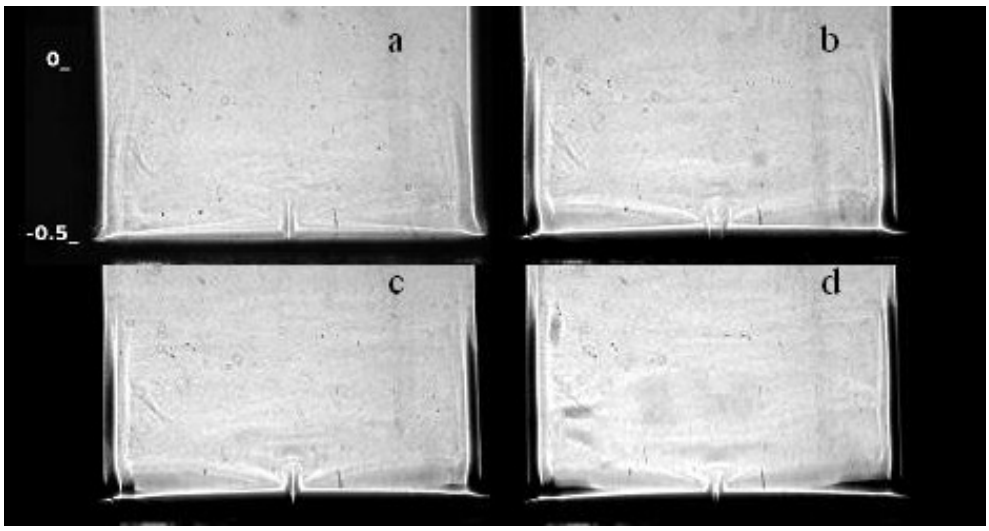

Figure 4.29: Double-layer structure at different Rayleigh number at $t = 89$ s and $Pr \approx 7$, $(a)Ra = 9.10^7$ case 1, $(b)Ra = 2.6.10^8$ case 2, $(c)Ra = 4.2.10^8$ case 3 and $(d)Ra = 5.9.10^8$ case 4.

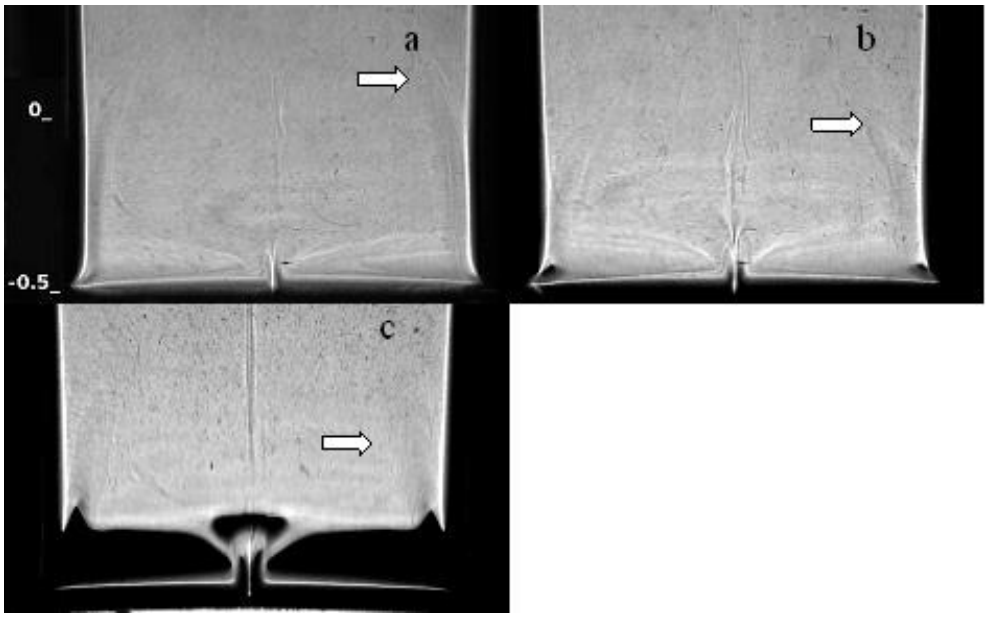

Figure 4.30: Double-layer structure at different Prandtl number at $t = 143$ s, and $Ra \approx 5.10^7$, $(a)Pr = 21$, $Ra = 6.74.10^7$ case 6, $(b)Pr = 55$, $Ra = 3.1.10^7$ case 7 and $(c)Pr = 190$, $Ra = 4.1.10^7$ case 9, the white arrow indicates the height of the double-layer structure.

UNIVERSITAT ROVIRA I VIRGILI
NUMERICAL AND EXPERIMENTAL STUDY OF TRANSIENT LAMINAR NATURAL CONVECTION OF HIGH PRANDTL NUMBER FLUIDS IN A CUBICAL CAVITY
Obai Younis Taha Elamin
ISBN:978-84-692-9056-9/DL:T-2069-2009

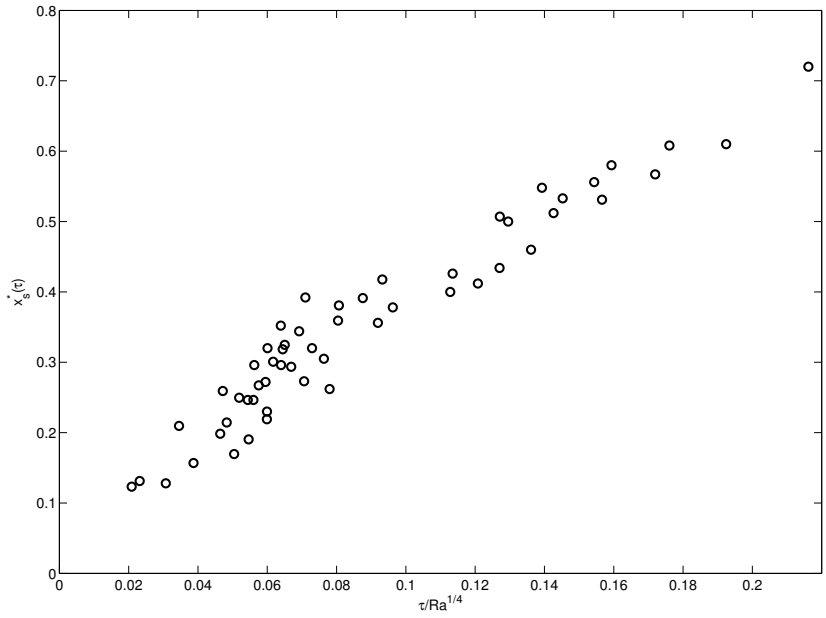

(a) Using present study velocity scale, Equation (4.18)

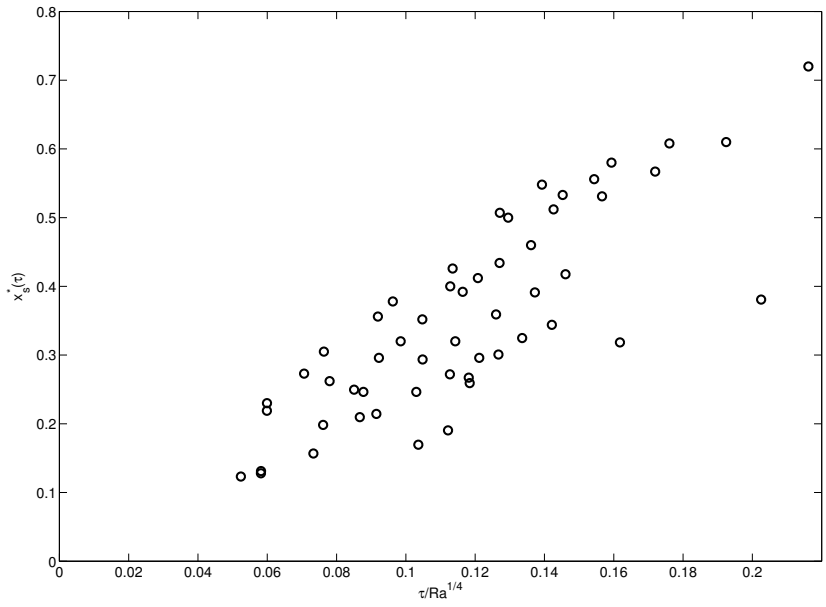

(b) Using Patterson and Imberger [15] velocity scale,$(u = \frac{g\beta\Delta Tt}{Pr})$

Figure 4.31: x_s^* against $\tau/Ra^{1/4}$

UNIVERSITAT ROVIRA I VIRGILI
NUMERICAL AND EXPERIMENTAL STUDY OF TRANSIENT LAMINAR NATURAL CONVECTION OF HIGH PRANDTL NUMBER FLUIDS IN A CUBICAL CAVITY
Obai Younis Taha Elamin
ISBN:978-84-692-9056-9/DL:T-2069-2009

4.2.2 Numerical simulation of transient natural convection in a side-cooled cubical cavity

In the simulations, the experimental set-up is modelled by a square two-dimensional cavity. The simulations use the same mesh introduced in Section (4.1) (see Figure 4.3). The results of the two-dimensional numerical simulations of the transient natural convection in a side-cooled cavity are presented and discussed in the following subsection.

4.2.2.1 Constant viscosity (case 1)

Figure 4.32 shows the shadowgraph images (experimental) and the isotherms (numerical) of the development of the thermal boundary layer and the horizontal intrusions at different time during the initial stage of growth for case 1 ($Ra = 9.10^7$, $Pr = 8.24$ and $\frac{\nu_c}{\nu_h} = 1$) (see Table (4.2)). The shadowgraph images were processed by subtracting a background image recorded immediately before the start of the experiment so that the thermal boundary layers can be clearly identified. It is clear that the numerical results agree with the experimental observations, although there is a time lag between the experiments and the simulations as revealed by the corresponding times (see Figure 4.32). This lag originates from a smaller actual Rayleigh number in the experiments than that in the numerical simulations, due to the initial conditions. In the experiments, the achieved temperature difference between the fluid and the sidewalls is smaller than the specified temperature difference in the numerical simulations due to the nature of the adopted heating and cooling methods in the experiments (see Patterson and Armfield [7]). As discussed earlier in chapter (3), The cavity is filled with preheated fluid, and the fluid temperature is kept constant using two constant temperature water baths attached to the gold-coated copper sidewalls. This process lasts for a relatively long time to ensure that the fluid in the cavity is isothermal and motionless before the experiment starts. Two circulator systems are used to provide hot and cold water for the water baths, respectively. At the start of the experiment, the hot water valve is turned off and the cold water valve is turned on. As a consequence, the cold water replaces the hot water in the water baths in order to cool the two sidewalls adjacent to the water baths. The switch of the valves might result in initial stratification of the water in the water baths. This initial stratification

ISBN:978-84-692-9056-9/DL:T-2069-2009

and minor heat losses through the cavity walls may account for the lagged experimental results. Figures 4.32(b), 4.32(d) and 4.32(f) show that, as time increases the thermal boundary layer thickness increases. The boundary layer thickness is defined as the horizontal distance between the vertical wall and the location of the contour $T^* = -.01$. It can be seen that the horizontal intrusions travel towards the bottom wall bisector and that the thickness of the intrusion nose is increasing with time. This is consistent with the scale of the intrusion thickness (Equation (4.22)) discussed in Section (3).

The initial growth stage can be divided into three distinct sub stages, which are: the start-up, the transition and the steady state. Figure 4.33 shows these three distinct substages in terms of the numerically predicted time series of the local temperature at $x^* = 0.5$ and $y^* = 0.05$, the boundary layer thickness and the local Nusselt number at $y^* = 0.5$. The initial growth stage is characterized by rapid development of the quantities plotted in Figure 4.33. During this substage heat conduction is the dominant heat transfer mode. As shown in Figure 4.33 δ_T^* reachs a local maximum. At this point the one dimensional heat conduction transits to two-dimensional heat convection and the boundary layer growth enters the transition substage for short time and finally the steady state substage as indicated in Figure 4.33.

ISBN:978-84-692-9056-9/DL:T-2069-2009

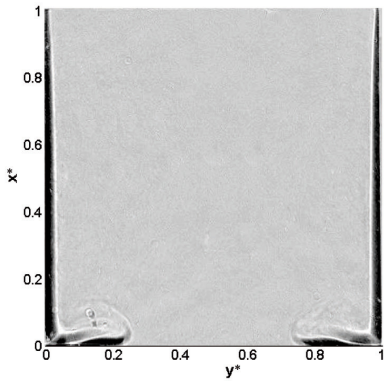

(a) 18 s

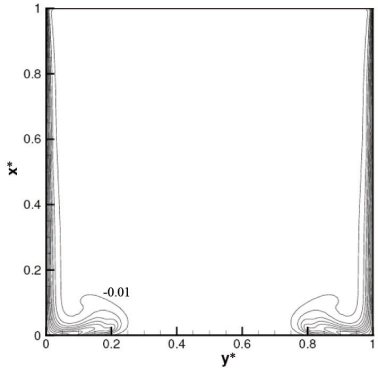

(b) 12 s

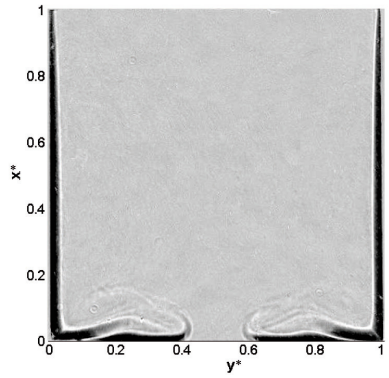

(c) 24 s

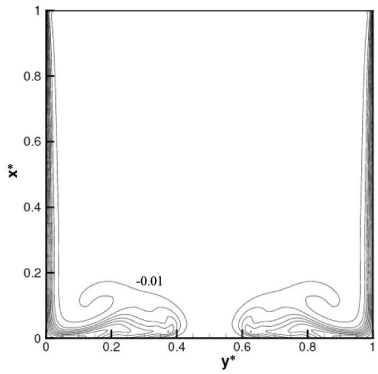

(d) 18 s

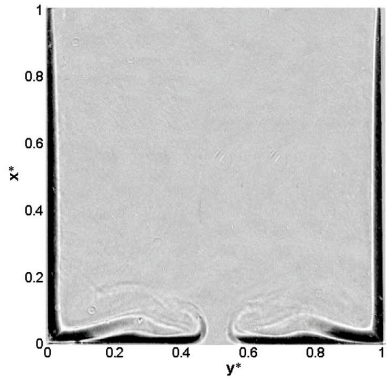

(e) 26 s

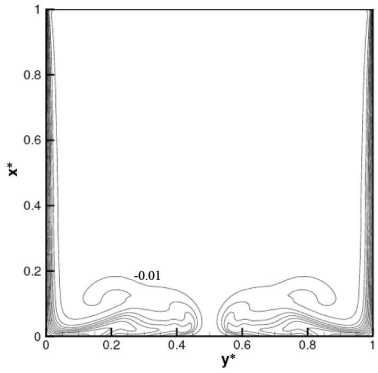

(f) 20 s

Figure 4.32: Shadowgraph images (experimental) and nondimensional temperature contours (numerical) for case 1 ($Ra = 9.10^7$, $Pr = 8.24$, $\frac{\nu_c}{\nu_h} = 1$) (contours between -1 to -0.1 with an interval of 0.1, and the contour $T^* = -0.01$).

UNIVERSITAT ROVIRA I VIRGILI
NUMERICAL AND EXPERIMENTAL STUDY OF TRANSIENT LAMINAR NATURAL CONVECTION OF HIGH PRANDTL NUMBER FLUIDS IN A CUBICAL CAVITY
Obai Younis Taha Elamin
ISBN:978-84-692-9056-9/DL:T-2069-2009

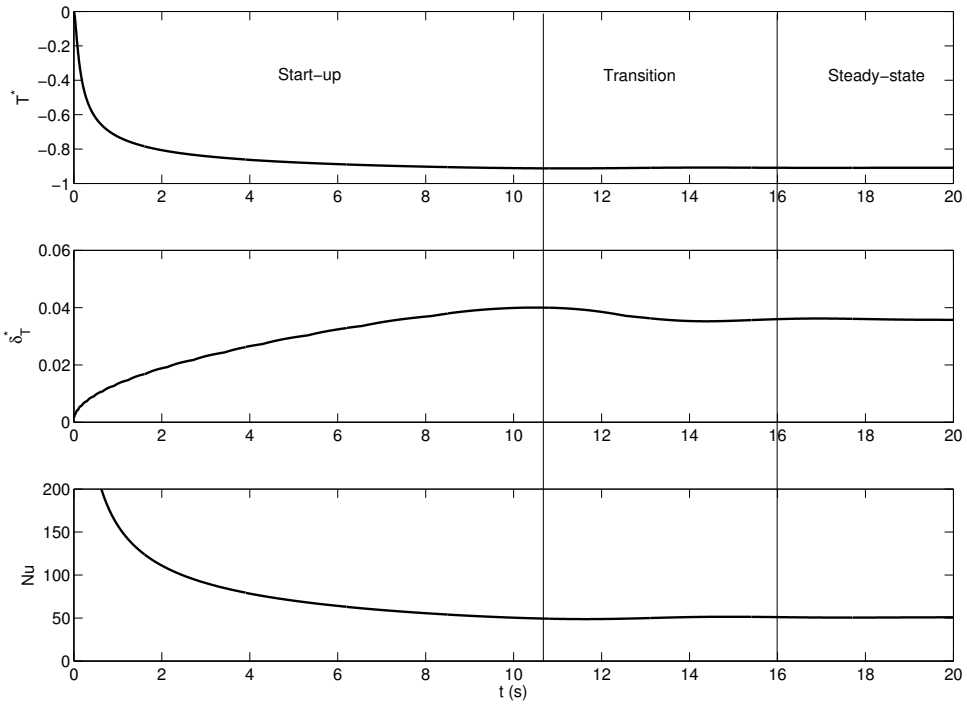

Figure 4.33: Substages of the initial growth stage, (a) the local temperature at $x^* = 0.05$ and $y^* = 0.5$, (b) local thermal boundary layer thickness at $x^* = 0.5$ and (c) the local Nusselt number at $x^* = 0.5$ for case 1 ($Ra = 9.10^7$, $Pr = 8.24$, $\frac{\nu_c}{\nu_h} = 1$) (see Table (4.2)).

UNIVERSITAT ROVIRA I VIRGILI
NUMERICAL AND EXPERIMENTAL STUDY OF TRANSIENT LAMINAR NATURAL CONVECTION OF HIGH PRANDTL NUMBER FLUIDS IN A CUBICAL CAVITY
Obai Younis Taha Elamin
ISBN:978-84-692-9056-9/DL:T-2069-2009

4.2.2.2 Variable viscosity (case 7)

A qualitative comparison between the shadowgraph images (experimental) and the isotherms (numerical) for the variable viscosity 7 ($Ra = 3.1.10^7$, $Pr = 55$, $\frac{\nu_c}{\nu_h} = 1.5$) (see Table (4.2)) is presented in Figure 4.34. A good agreement between the numerical and the experimental results is achieved (taking into account the time lag). Figure 4.34(b) shows the very early stage of cooling, at $t = 5$ s, the conduction is dominant as indicated by the uniform boundary layer thickness along the vertical walls. At this stage the horizontal intrusion starts to form. As time evolves, the boundary layer thickness experiences non-uniform growth due to the convection onset and the horizontal intrusion travels towards the bottom wall bisector (see Figure 4.34(d)). At $t = 45$ s, the horizontal intrusions are already merged and the cavity started to be filled by the cold fluid (see Figure 4.34(f)).

Although there is no experimental quantitative measurements, the time evolution of the velocity of the horizontal intrusion extracted from the shadowgraph images (as discussed in Chapter 3) can be compared with the velocity obtained from the numerical simulations. The time evolution of the velocity of the horizontal intrusion is obtained from the simulations by tracing the horizontal position of the temperature contour $T^* = -0.01$. Figure 4.35 shows the time evolution of velocity of the horizontal intrusion for the experimental and numerical simulation. The agreement between the experiment and the numerical simulation is clear. It should be noted that a time lag of 12 s has been added to the experimental data plotted in this figure. This time has been obtained by the comparison of the observed positions of the intrusion front with those predicted numerically.

UNIVERSITAT ROVIRA I VIRGILI
NUMERICAL AND EXPERIMENTAL STUDY OF TRANSIENT LAMINAR NATURAL CONVECTION OF HIGH PRANDTL NUMBER FLUIDS IN A CUBICAL CAVITY
Obai Younis Taha Elamin
ISBN:978-84-692-9056-9/DL:T-2069-2009

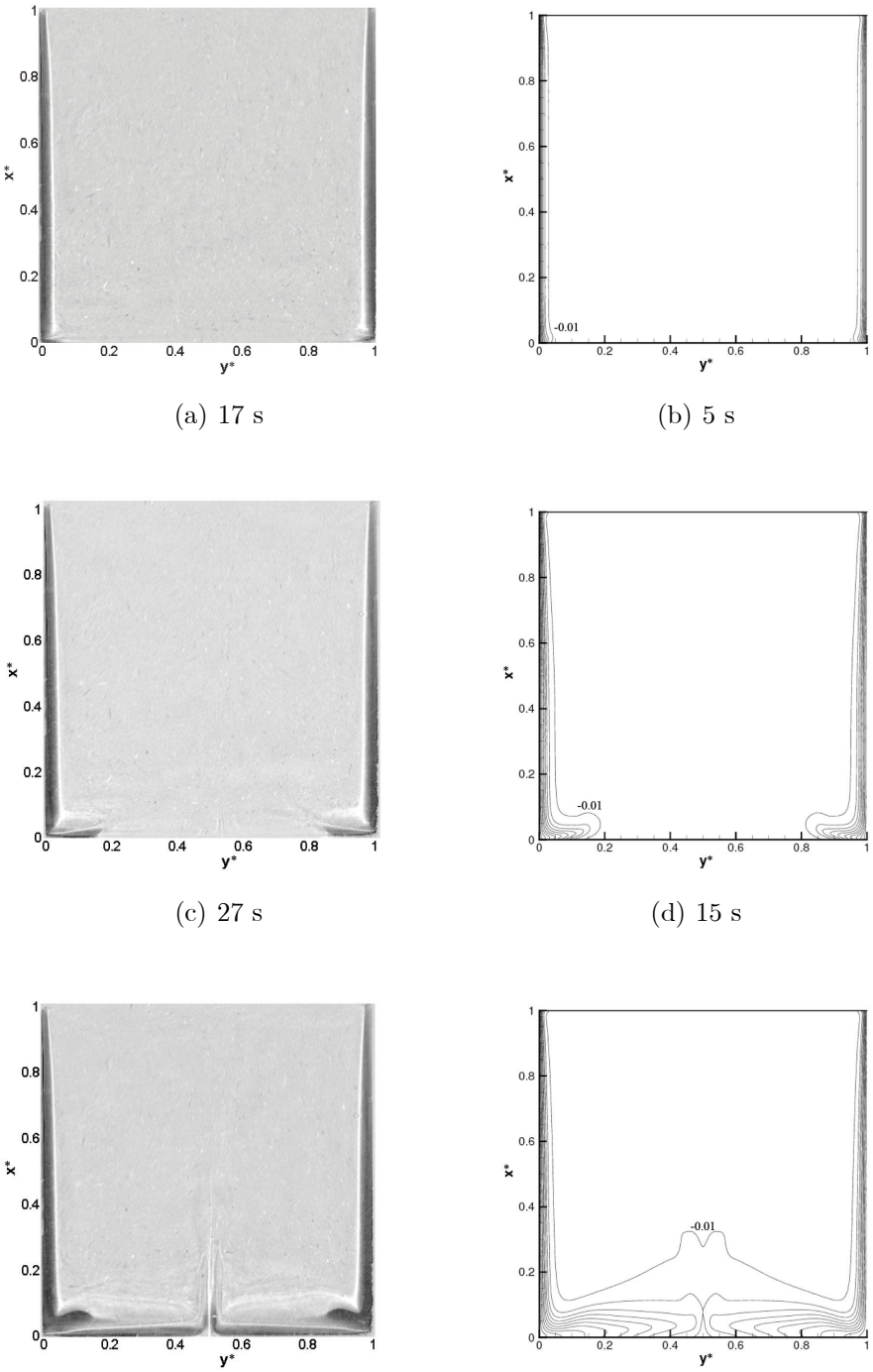

(a) 17 s (b) 5 s

(c) 27 s (d) 15 s

(e) 57 s (f) 45 s

Figure 4.34: Shadowgraph images (experimental) and nondimensional temperature contours (numerical) for the variable viscosity case 7 ($Ra = 3.1.10^7$, $Pr = 55$, $\frac{\nu_c}{\nu_h} = 1.5$) (see Table (4.2)), (contours between -1 to -0.1 with an interval of 0.1, and the contour $T^* = -0.01$).

UNIVERSITAT ROVIRA I VIRGILI
NUMERICAL AND EXPERIMENTAL STUDY OF TRANSIENT LAMINAR NATURAL CONVECTION OF HIGH PRANDTL NUMBER FLUIDS IN A CUBICAL CAVITY
Obai Younis Taha Elamin
ISBN:978-84-692-9056-9/DL:T-2069-2009

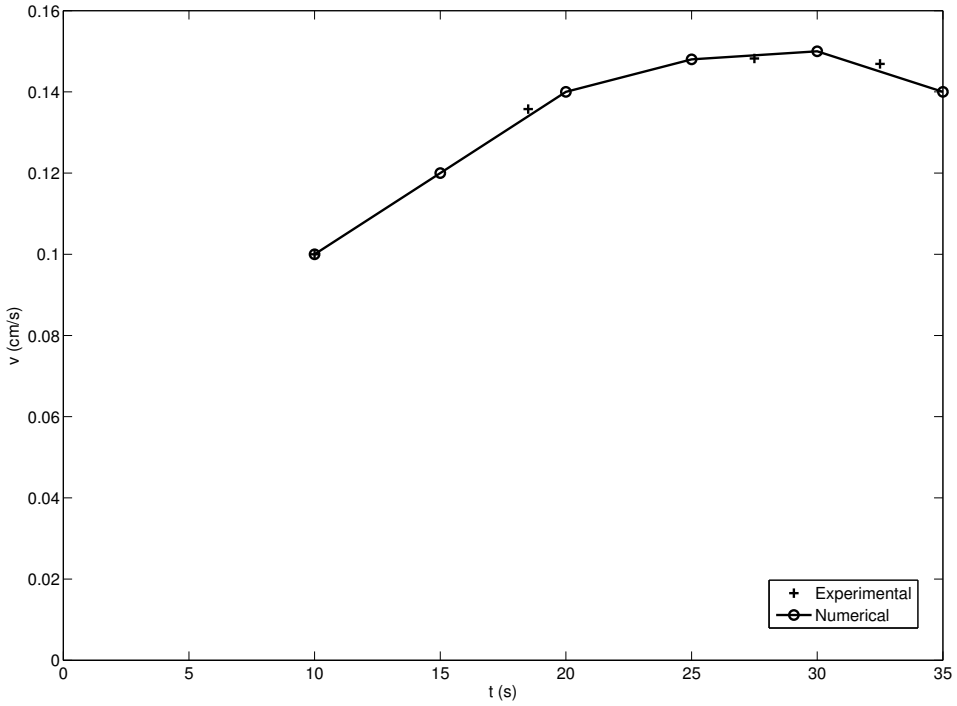

Figure 4.35: The time evolution of observed (experimental) and predicted (numerical) velocity of the horizontal intrusions for case 7 ($Ra = 3.1.10^7$, $Pr = 55$, $\frac{\nu_c}{\nu_h} = 1.5$) (see Table (4.2)).

UNIVERSITAT ROVIRA I VIRGILI
NUMERICAL AND EXPERIMENTAL STUDY OF TRANSIENT LAMINAR NATURAL CONVECTION OF HIGH PRANDTL NUMBER FLUIDS IN A CUBICAL CAVITY
Obai Younis Taha Elamin
ISBN:978-84-692-9056-9/DL:T-2069-2009

4.2.2.3 Effect of variable viscosity (case 7)

To show the effect of the variable viscosity on the simulations, the numerical simulation of case 7 ($Ra = 3.1.10^7$, $Pr = 55$, $\frac{\nu_c}{\nu_h} = 1.5$) (see Table (4.2)) was carried out by assuming constant viscosity ($\frac{\nu_c}{\nu_h} = 1.0$) and variable viscosity ($\frac{\nu_c}{\nu_h} = 1.5$). The development of the thermal vertical boundary layer and horizontal intrusions at two different times for the both cases are shown in Figure 4.36. It is clear that the boundary layer thickness and the intrusion thickness grow slightly faster for the constant viscosity case especially away from the cold side-walls (see Figure 4.36(a)). This is because of the temperature gradient close to the cold-side walls results in viscosity gradient for the variable viscosity case, and hence the viscosity value close to the walls are closer to the mean viscosity used for constant viscosity case. While in the core of the cavity the temperature gradient is very small and the viscosity difference is larger.

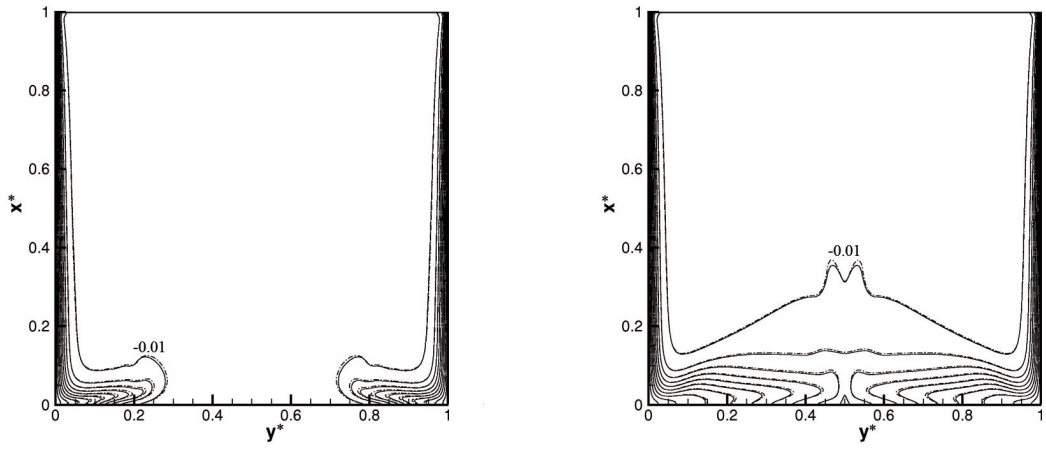

(a) 20 s (b) 50 s

Figure 4.36: Non-dimensional temperature contours for case 7 ($Ra = 3.1.10^7$, $Pr = 55$, $\frac{\nu_c}{\nu_h} = 1.5$) (see Table (4.2)), (contours between -1 to -0.1 with an interval of 0.1, and the contour $T^* = -0.01$), solid line: variable viscosity simulation, dashed line: constant viscosity simulation.

Figures 4.37 and 4.38 show the vertical and horizontal velocity components u^*, v^* at different times. It can be seen that the instantaneous velocity fields are more sensitive for the viscosity variation than the temperature field especially in the cavity core. The main driving force of the flow is the buoyancy force

UNIVERSITAT ROVIRA I VIRGILI
NUMERICAL AND EXPERIMENTAL STUDY OF TRANSIENT LAMINAR NATURAL CONVECTION OF HIGH PRANDTL NUMBER FLUIDS IN A CUBICAL CAVITY
Obai Younis Taha Elamin
ISBN:978-84-692-9056-9/DL:T-2069-2009

which is increased with Prandtl number (see Equation (2.2)). At the beginning, in the cavity core the constant viscosity case achieve higher Prandtl number than the variable viscosity case, and hence higher buoyancy force and higher velocities. However the Prandtl number of the variable viscosity case increases with time, and the difference in the velocities is reduced as time evolves as shown in Figures 4.37(b) and 4.38(b).

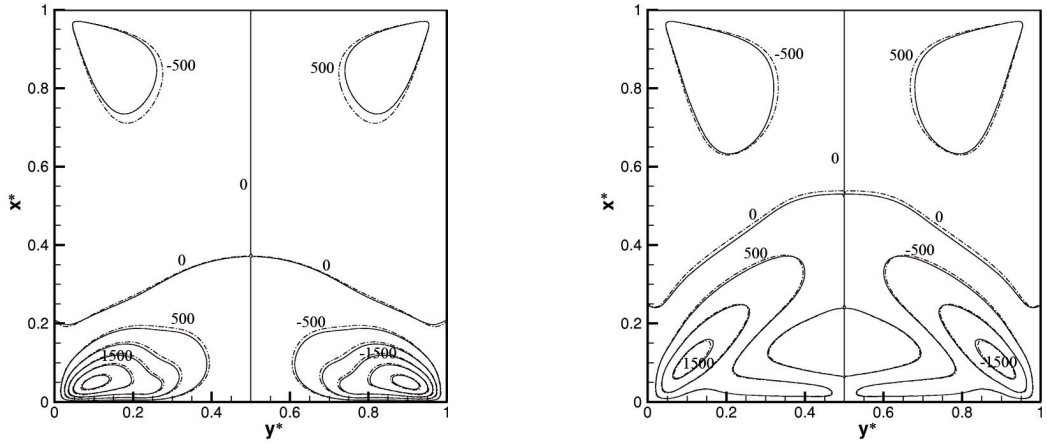

(a) 20 s (b) 50 s

Figure 4.37: Non-dimensional horizontal velocity contours for case 7 ($Ra = 3.1.10^7$, $Pr = 55$, $\frac{\nu_c}{\nu_h} = 1.5$) (see Table (4.2)), solid line: variable viscosity simulation, dashed line: constant viscosity simulation.

UNIVERSITAT ROVIRA I VIRGILI
NUMERICAL AND EXPERIMENTAL STUDY OF TRANSIENT LAMINAR NATURAL CONVECTION OF HIGH PRANDTL NUMBER FLUIDS IN A CUBICAL CAVITY
Obai Younis Taha Elamin
ISBN:978-84-692-9056-9/DL:T-2069-2009

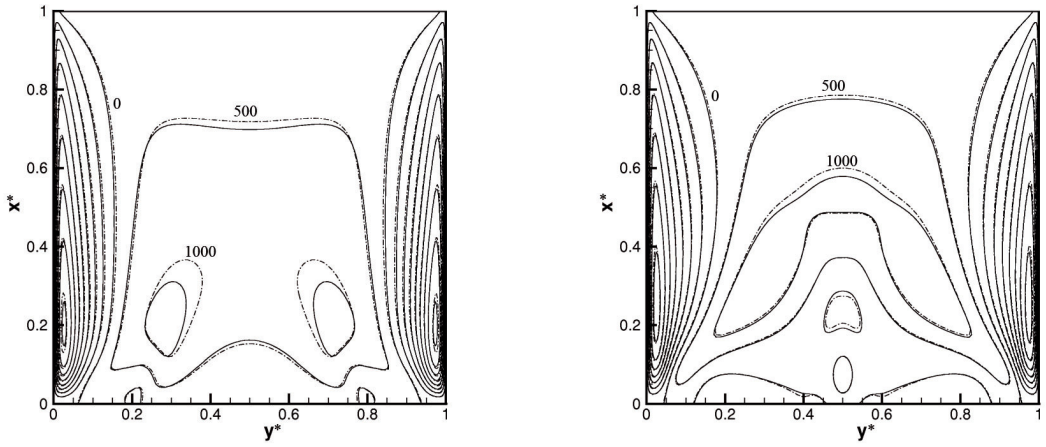

(a) 20 s (b) 50 s

Figure 4.38: Non-dimensional vertical velocity contours for case 7 ($Ra = 3.1.10^7$, $Pr = 55$, $\frac{\nu_c}{\nu_h} = 1.5$) (see Table (4.2)), solid line: variable viscosity simulation, dashed line: constant viscosity simulation.

4.2.2.4 Pr number effect (cases 1 and 10)

Figure 4.39 presents the time evolution of the thermal boundary layer thickness at $x^* = 0.5$, for case 1 ($Ra = 9.10^7$, $Pr = 8.24$, $\frac{\nu_c}{\nu_h} = 1$) and case 10 ($Ra = 1.4.10^8$, $Pr = 120$, $\frac{\nu_c}{\nu_h} = 5.87$) (see Table (4.2)) for the experiments and the numerical simulations. The simulations reasonably predicted the growth of the thermal boundary layer especially at earlier time ($t^* \leq 0.0001$). The boundary layer thickness grows after the initiation of cooling to achieve the maximum through the early period in which the conduction is dominant. For this early period of time the Prandtl number effect is not evident. As time evolves convection takes place and the boundary layer thickness drops slightly to achieve the steady state. The boundary layer steady state thickness is smaller for the high Prandtl number case. The discrepancy between the experiments and the numerical simulation is argued due to the resolution of the imaging system and values of the grey scale.

The time evolution of the intrusion position for cases 1 and 10 is presented in Figure 4.40. Clearly the intrusion of the higher Prandtl number (case 10) travels faster than the lower Prandtl number (case 1). As discussed earlier this is because of the magnitude of the buoyancy force as it is the main driving

UNIVERSITAT ROVIRA I VIRGILI
NUMERICAL AND EXPERIMENTAL STUDY OF TRANSIENT LAMINAR NATURAL CONVECTION OF HIGH PRANDTL NUMBER FLUIDS IN A CUBICAL CAVITY
Obai Younis Taha Elamin
ISBN:978-84-692-9056-9/DL:T-2069-2009

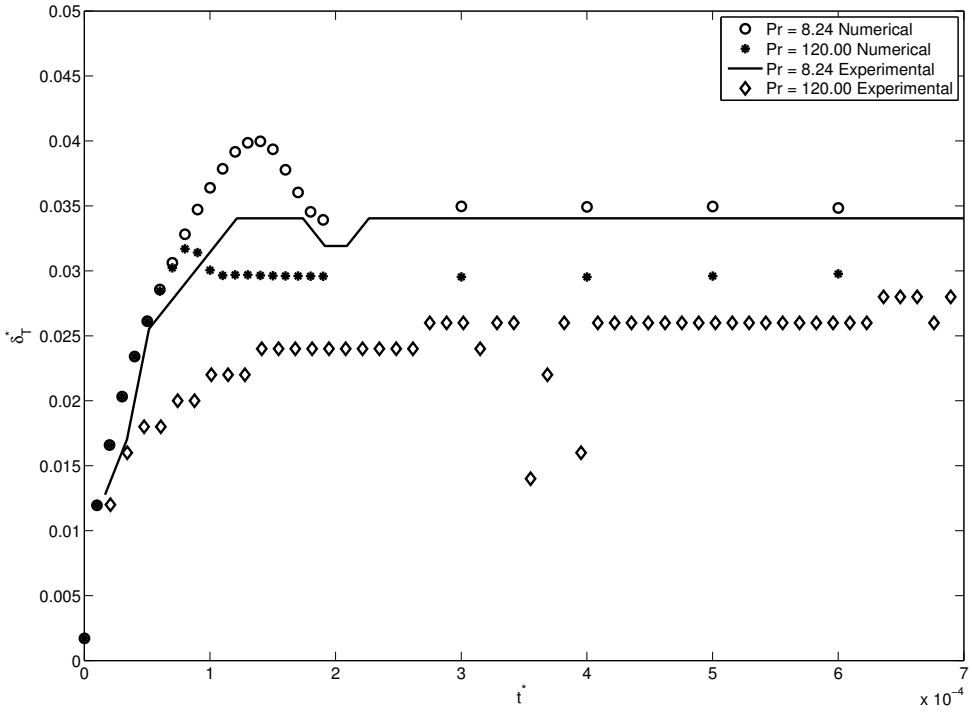

Figure 4.39: The time evolution of the observed (experimental) and the predicted (numerical) thermal boundary layer thickness for case 1 ($Ra = 9.10^7$, $Pr = 8.24$, $\frac{\nu_c}{\nu_h} = 1$) and case 10 ($Ra = 1.4.10^8$, $Pr = 120$, $\frac{\nu_c}{\nu_h} = 5.87$) (see Table (4.2)).

force. Moreover, for high Prandtl number the thermal boundary layer is thin (see Figure 4.39) resulting in a narrow passage through which the cold fluid descends to entertain the hot fluid of the cavity core. Hence velocity of the cold descending fluid is higher for higher Prandtl number. This implies that the intrusion thickness grows faster for high Prandtl number. This is confirmed in Figure 4.40, which shows the time evolution of the horizontal intrusion at $x^* = 0.25$.

In addition to the horizontal intrusion thickness, the horizontal averaged temperate is good representatives for the rate of cooling. The time evolution of the horizontal averaged temperature at $x^* = 0.25$ is presented in Figure 4.41 (the time evolution is only presented for a short period of time at the early stage for clarity). Both figures show faster cooling for higher Prandtl number case. The onset of the convection is defined as the time at which the temperature

UNIVERSITAT ROVIRA I VIRGILI
NUMERICAL AND EXPERIMENTAL STUDY OF TRANSIENT LAMINAR NATURAL CONVECTION OF HIGH PRANDTL NUMBER FLUIDS IN A CUBICAL CAVITY
Obai Younis Taha Elamin
ISBN:978-84-692-9056-9/DL:T-2069-2009

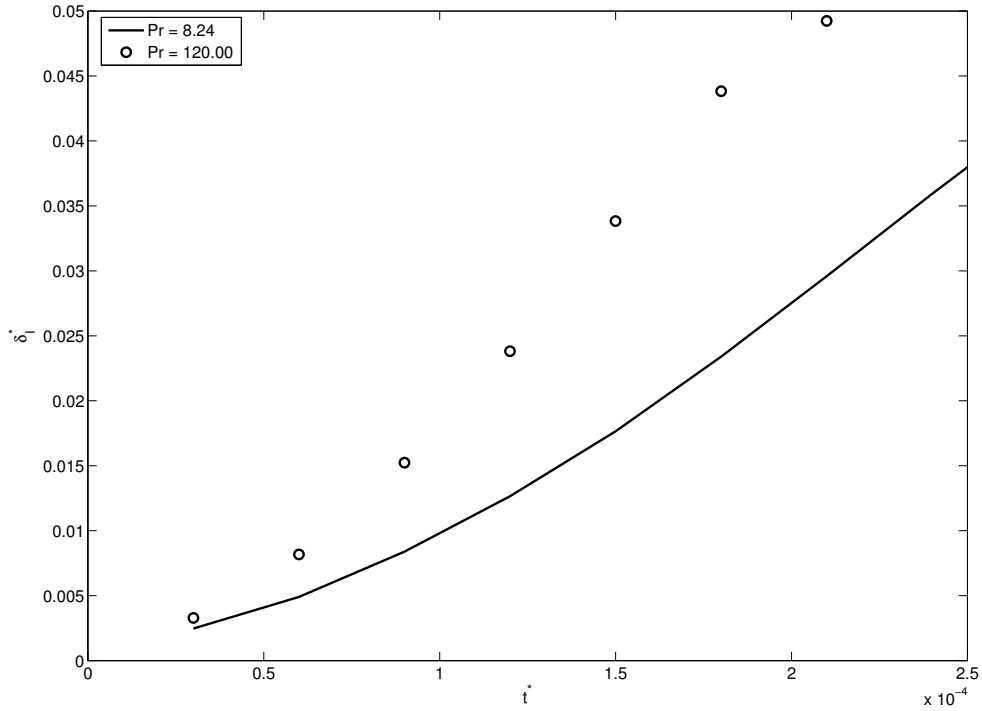

Figure 4.40: The time evolution of the predicted (numerical) horizontal intrusion thickness for case 1 ($Ra = 9.10^7$, $Pr = 8.24$, $\frac{\nu_c}{\nu_h} = 1$) and case 10 ($Ra = 1.4.10^8$, $Pr = 120$, $\frac{\nu_c}{\nu_h} = 5.87$) (see Table(4.2)).

deviates from the initial cooling trend (conduction), this deviation is showed by the dotted line in Figure 4.41. The onset of convection starts earlier for the lower Prandtl number case due to the thicker boundary layer. However at earlier time ($t^* = 0.00005$) the higher Prandtl number case experiences thermal perturbation earlier than the lower Prandtl number case. As at this early stage the horizontal intrusion thickness does not extend to the quarter of the cavity, the thermal boundary layer is only involved in such perturbation. Although the thermal boundary layer is thinner for the high Prandtl number case, but the steep temperature gradient results in faster perturbation. Unlike the horizontal averaged temperature for the high Prandtl number, the horizontal averged temperature for the lower Prandtl number case experiences oscillations after the convection onset. These oscillations are associated with the boundary layer thickness oscillations. Figure 4.42 shows the boundary layer thickness of the

UNIVERSITAT ROVIRA I VIRGILI
NUMERICAL AND EXPERIMENTAL STUDY OF TRANSIENT LAMINAR NATURAL CONVECTION OF HIGH PRANDTL NUMBER FLUIDS IN A CUBICAL CAVITY
Obai Younis Taha Elamin
ISBN:978-84-692-9056-9/DL:T-2069-2009

lower Prandtl number case at the time marked by the letters a and b in Figure 4.41. It can be seen that the thermal boundary layer reduced although the time increased (see also the transitional stage in Figure 4.33).

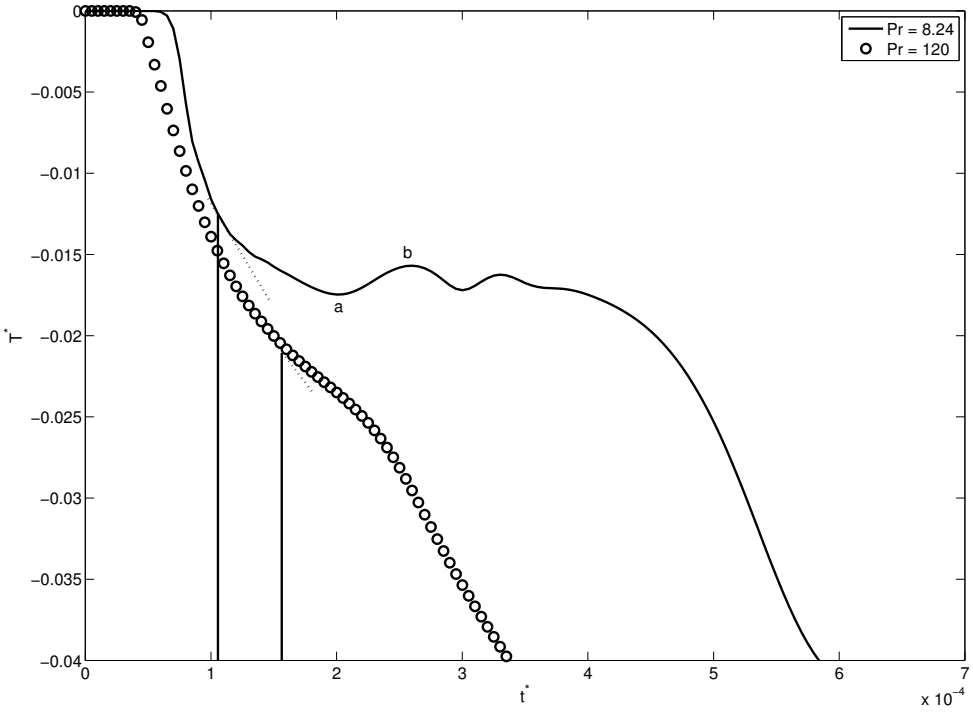

Figure 4.41: The time evolution of the predicted (numerical) horizontal averaged temperature at $x^* = 0.25$ for case 1 ($Ra = 9.10^7$, $Pr = 8.24$, $\frac{\nu_c}{\nu_h} = 1$) and case 10 ($Ra = 1.4.10^8$, $Pr = 120$, $\frac{\nu_c}{\nu_h} = 5.87$) (see Table(4.1)).

UNIVERSITAT ROVIRA I VIRGILI
NUMERICAL AND EXPERIMENTAL STUDY OF TRANSIENT LAMINAR NATURAL CONVECTION OF HIGH PRANDTL NUMBER FLUIDS IN A CUBICAL CAVITY
Obai Younis Taha Elamin
ISBN:978-84-692-9056-9/DL:T-2069-2009

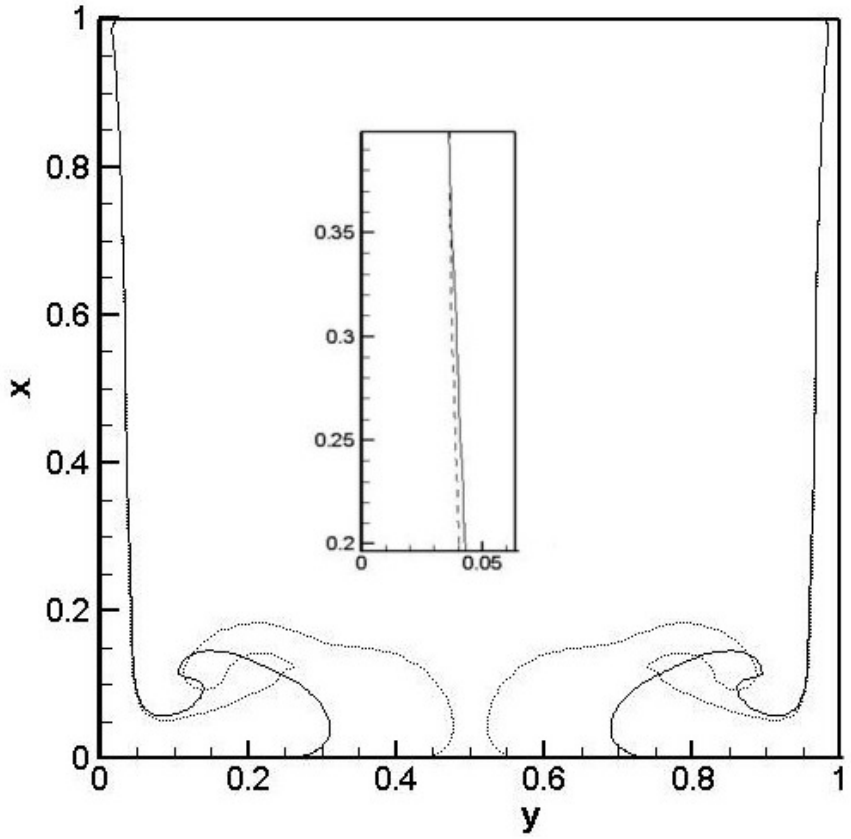

Figure 4.42: Temperature contours for case 1 ($Ra = 9.10^7$, $Pr = 8.24$, $\frac{\nu_c}{\nu_h} = 1$), solid line: thermal boundary layer at point a (see Figure 4.41), dashed line: thermal boundary layer at point b (see Figure 4.41), (only the contour $T^* = -0.01$ is presented to show the boundary layer thickness).

UNIVERSITAT ROVIRA I VIRGILI
NUMERICAL AND EXPERIMENTAL STUDY OF TRANSIENT LAMINAR NATURAL CONVECTION OF HIGH PRANDTL NUMBER FLUIDS IN A CUBICAL CAVITY
Obai Younis Taha Elamin
ISBN:978-84-692-9056-9/DL:T-2069-2009

UNIVERSITAT ROVIRA I VIRGILI
NUMERICAL AND EXPERIMENTAL STUDY OF TRANSIENT LAMINAR NATURAL CONVECTION OF HIGH PRANDTL NUMBER FLUIDS IN A CUBICAL CAVITY
Obai Younis Taha Elamin
ISBN:978-84-692-9056-9/DL:T-2069-2009

Chapter 5

Conclusions

The thesis presents numerical and experimental study of transient natural convection of high Prandtl number fluid with variable viscosity in a cubical cavity. Firstly, numerical simulations of high Prandtl number under different thermal boundary conditions and with consideration of wall conduction is studied. The transient flow features of fluids with variable viscosity in a side-cooled cavity is experimentally visualized and numerically studied. The results indicted good a agreement between the experimental and numerical results. Based on the results, new scaling relations are developed taking into account the variable viscosity of the fluid. In this chapter, the major findings of the thesis are summarized.

5.1 Numerical simulation of high Prandtl number fluid in a cavity

Transient natural convection of high Pr (4.10^4) number fluid (Golden syrup) in a cubical cavity has been studied numerically to determine the combined and separate effects of thermal boundary conditions, variable viscosity and wall conductivity. The simulation Rayleigh number is $Ra = 10^6$ and the viscosity contrast is $\frac{\nu_h}{\nu_c} = 12$. At the very beginning of the cooling process, the flow consists of a toroidal rolling motion that constitutes the main flow. Secondary flow starts to develop near the top wall as time evolves. The insulation of the bottom wall results in increasing the averaged temperature by 6% after 30 minutes of the initiation of the cooling process. The instantaneous flow field is

UNIVERSITAT ROVIRA I VIRGILI
NUMERICAL AND EXPERIMENTAL STUDY OF TRANSIENT LAMINAR NATURAL CONVECTION OF HIGH PRANDTL NUMBER FLUIDS IN A CUBICAL CAVITY
Obai Younis Taha Elamin
ISBN:978-84-692-9056-9/DL:T-2069-2009

significantly affected by the effect of the variable viscosity. However this effect is damped out in the averaged quantities (e.g. averaged temperature and heat transfer rate). The consideration of the wall conductivity adds an additional resistance to the heat transfer and delays the convection.

5.2 Shadowgraph observations of transient natural convection in a side-cooled cavity

A series of experiments are conducted to study the transient natural convection in a side-cooled cavity. To achieve different Prandtl number and different viscosity contrast, water and Glycerine-water solutions of different concentration are employed as working fluids. The experimental Rayleigh number is ranging from $2.9.10^7$ to $5.9.10^8$, Prandtl number 6.2 to 190 and viscosity contrast from 1 to 5.87. Shadowgraph technique is utilized to visualize the convective flow field in the cavity; the images acquired by the shadowgraph system are used to analyze the different stages of the flow. A new scaling analysis of the transient behaviour is conducted to include the effect of the variable viscosity. All the presented new scalings have been validated by measurements based on the shadowgraph images. The results indicate that the flow development is characterized by the following distinct processes: (a) the initial growth of the vertical thermal boundary layers and horizontal intrusions; (b) the interaction of the horizontal intrusions and filling up of the cavity with stratified cold fluid; and (c) the stratification and formation of double layer structures. For the first two stages, new scaling relations have been developed showing the dependence on the Rayleigh, the Prandtl numbers and the variable viscosity, while for the third stage the scaling of the rate of the stratification is previously obtained by Lin and Armfield [22]. Considering the experimental and imaging system errors, the measurements showed a good agreement with the scaling relations. It was found that the variable fluid viscosity has a significant influence even for small viscosity variation. Unlike the constant viscosity fluid, the scalings of the variable viscosity fluid are not only dependant on Rayleigh and Prandtl numbers, but also on the fluid properties (β, ν_0), and flow conditions (ΔT).

UNIVERSITAT ROVIRA I VIRGILI
NUMERICAL AND EXPERIMENTAL STUDY OF TRANSIENT LAMINAR NATURAL CONVECTION OF HIGH PRANDTL NUMBER FLUIDS IN A CUBICAL CAVITY
Obai Younis Taha Elamin
ISBN:978-84-692-9056-9/DL:T-2069-2009

5.3 Numerical simulation of transient natural convection in a side-cooled cavity

For the purpose of validating the 3DINAMICS code for variable viscosity simulation, the studied experimental cases are numerically simulated. The comparison between the numerical and experimental results showed good agreement with consideration of time lag due to the different initial conditions in the simulations and in the experiments. In addition to the three distinct processes that characterize the flow development; three substages in the initial growth stage are identified: (a) start-up stage, (b) transition stage and (c) steady state stage. The instantaneous flow field is slightly affected by the viscosity variation due to the relatively low Prandtl number and the viscosity contrasts considered. Although the magnitude of the convective velocity is larger for higher Prandtl numbers, the results showed that the onset of convection is delayed for high Prandtl numbers.

UNIVERSITAT ROVIRA I VIRGILI
NUMERICAL AND EXPERIMENTAL STUDY OF TRANSIENT LAMINAR NATURAL CONVECTION OF HIGH PRANDTL NUMBER FLUIDS IN A CUBICAL CAVITY
Obai Younis Taha Elamin
ISBN:978-84-692-9056-9/DL:T-2069-2009

UNIVERSITAT ROVIRA I VIRGILI
NUMERICAL AND EXPERIMENTAL STUDY OF TRANSIENT LAMINAR NATURAL CONVECTION OF HIGH PRANDTL NUMBER FLUIDS IN A CUBICAL CAVITY
Obai Younis Taha Elamin
ISBN:978-84-692-9056-9/DL:T-2069-2009

Chapter 6

Conclusiones

Esta tesis presenta el estudio experimental y numérico de la convección natural transitoria, en una cavidad cúbica, de un fluido con número de Prandtl elevado y viscosidad variable. En primer lugar se han llevado a cabo simulaciones numéricas a Prandtl elevado bajo diferentes condiciones de contorno térmicas y considerando conducción térmica en la pared. Estas simulaciones han permitido diseñar el trabajo experimental posterior. Así pues, se ha visualizado experimentalmente y estudiado numéricamente las características de flujo no estacionario de fluidos con viscosidad variable en una cavidad refrigerada lateralmente. Los resultados muestran un buen ajuste entre los resultados experimentales y numéricos. Basado en los resultados, se han desarrollado nuevas relaciones de escala que tienen en cuenta la viscosidad variable del fluido. En este capítulo se resumen los principales descubrimientos de la tesis.

6.1 Simulación numérica de un fluido con elevado número de Prandtl en una cavidad

Se ha estudiado numéricamente la convección natural transitoria de un fluido (Golden syrup) con número de Prandtl elevado (4.10^4). Ello ha permitido determinar los efectos simples y combinados de las condiciones de contorno térmicas, de viscosidad variable y de conducción en la pared. El número de Rayleigh en la simulación es $Ra = 10^6$ y el contraste de viscosidad es $\frac{\nu_c}{\nu_h} = 12$. Al principio del proceso de refrigeración el flujo consiste en un movimiento toroidal ondulante que constituye el flujo principal. A medida que el tiempo

UNIVERSITAT ROVIRA I VIRGILI
NUMERICAL AND EXPERIMENTAL STUDY OF TRANSIENT LAMINAR NATURAL CONVECTION OF HIGH PRANDTL NUMBER FLUIDS IN A CUBICAL CAVITY
Obai Younis Taha Elamin
ISBN:978-84-692-9056-9/DL:T-2069-2009

pasa, el flujo empieza a desarrollarse cerca de la pared superior. El aislamiento en la pared inferior resulta en un incremento de la temperatura promedio del 6% después de 30 minutos de proceso de refrigeración. El campo de flujo se ve afectado significativamente por efecto de la viscosidad variable. No obstante, este efecto se ve amortiguado en las cantidades promedio (e.g. temperatura y tasa de transferencia de calor). Al tener en cuenta la conducción en la pared se añade una resistencia adicional a la transferencia de calor y se retrasa la convección.

6.2 Observaciones shadowgraph de la convección natural transitoria en una cavidad refrigerada lateralmente

Se ha llevado a cabo una serie de experimentos para estudiar la convección natural transitoria en una cavidad refrigerada lateralmente. Se han empleado soluciones de agua y agua-glicerina a diferentes concentraciones, para obtener diferentes números de Prandtl y diferentes contrastes de viscosidad. El rango de número de Rayleigh experimental ha sido de $2.9.10^7$ a $5.9.10^8$, el número de Prandtl de 6.2 a 190 y el contraste de viscosidad de 1.00 a 5.87. La técnica shadowgraph se utiliza para analizar los diferentes estados del flujo. Se ha realizado un nuevo análisis de escala del comportamiento transitorio para incluir el efecto de viscosidad variable. Todas las escalas nuevas presentadas han sido validadas con mediciones basadas en imágenes shadowgraph. Los resultados indican que el desarrollo del flujo se caracteriza por los siguientes procesos: (a) El crecimiento inicial de la capa límite térmica y de las intrusiones horizontales; (b) la interacción de las intrusiones horizontales y la estratificación de la cavidad con fluido frío; y (c) la estratificación y formación de estructuras de capa doble. Para las primeras dos etapas se han desarrollado nuevas relaciones de escala en función de los números de Rayleigh y Prandtl y de la viscosidad variable, mientras que para la tercera etapa la escala de velocidad de estratificación se obtuvo previamente por Lin y Armfield [22]. Teniendo en cuenta los errores del sistema experimental y de imagen, las mediciones mostraron un buen ajuste con las relaciones de escala. Se ha observado que

UNIVERSITAT ROVIRA I VIRGILI
NUMERICAL AND EXPERIMENTAL STUDY OF TRANSIENT LAMINAR NATURAL CONVECTION OF HIGH PRANDTL NUMBER FLUIDS IN A CUBICAL CAVITY
Obai Younis Taha Elamin
ISBN:978-84-692-9056-9/DL:T-2069-2009

la viscosidad variable del fluido tiene una influencia significativa incluso para pequeñas variaciones de viscosidad. Al contrario que en el caso de viscosidad constante, las escalas de viscosidad variable no sólo dependen de los números de Rayleigh y Prandtl, sino también de las propiedades del fluido (β, ν_0), y de las condiciones del flujo (ΔT).

6.3 Simulación numérica de la convección natural transitoria en una cavidad refrigerada lateralmente

Con el propósito de validar el código de simulación 3DINAMICS con viscosidad variable, los casos estudiados experimentalmente se han simulado numéricamente. La comparación entre resultados numéricos y experimentales muestra un buen ajuste teniendo en cuenta el desfase temporal debido a las condiciones iniciales. Además de los tres procesos que caracterizan el desarrollo de flujo; se han identificado tres subetapas en la etapa inicial de crecimiento: (a) etapa de arranque, (b) etapa de transición y (c) etapa de estado estacionario. Los campos de flujo instantáneos se vieron ligeramente afectados por la variación de viscosidad debido al número relativamente bajo de Prandtl y al contraste de viscosidad. Aunque la magnitud de velocidad convectiva es mayor para números de Prandtl mayores, los resultados muestran que el inicio de la convección se retrasa para números de Prandtl grandes.

UNIVERSITAT ROVIRA I VIRGILI
NUMERICAL AND EXPERIMENTAL STUDY OF TRANSIENT LAMINAR NATURAL CONVECTION OF HIGH PRANDTL NUMBER FLUIDS IN A CUBICAL CAVITY
Obai Younis Taha Elamin
ISBN:978-84-692-9056-9/DL:T-2069-2009

UNIVERSITAT ROVIRA I VIRGILI
NUMERICAL AND EXPERIMENTAL STUDY OF TRANSIENT LAMINAR NATURAL CONVECTION OF HIGH PRANDTL NUMBER FLUIDS IN A CUBICAL CAVITY
Obai Younis Taha Elamin
ISBN:978-84-692-9056-9/DL:T-2069-2009

Chapter 7

Future work

The 3DINAMICS code is successfully employed to run numerical simulation of transient natural convection of high Prandtl number fluids, taking into account wall conduction and variation of viscosity with temperature. A set of experiments using the shadowgraph techniques are conducted to visualise the transient convective flow in a side-cooled cavity. The experimental rustles are used to validate the numerical code and a good agreement is found. However, the experimental and numerical work discussed in this thesis can be extended for better validation and documentation. The extension of this study can be summarized as:

- Due to the limitation of the experimental model and experimental initial and boundary conditions, only limited ranges of Rayleigh numbers, Prandtl numbers and viscosity contrast are studied. I t is of primary interest to make these ranges border. The temperature measurements in the thermal boundary layer as well as in the cavity core well asses the code validation.
- Numerical simulations for:
  - Comparison with the experiments.
  - Validation the new scaling relations.
  - Study the Prandtl number effect on the onset of convection.
  - Study the viscosity contrast effect on the onset of convection.

UNIVERSITAT ROVIRA I VIRGILI
NUMERICAL AND EXPERIMENTAL STUDY OF TRANSIENT LAMINAR NATURAL CONVECTION OF HIGH PRANDTL NUMBER FLUIDS IN A CUBICAL CAVITY
Obai Younis Taha Elamin
ISBN:978-84-692-9056-9/DL:T-2069-2009

UNIVERSITAT ROVIRA I VIRGILI
NUMERICAL AND EXPERIMENTAL STUDY OF TRANSIENT LAMINAR NATURAL CONVECTION OF HIGH PRANDTL NUMBER FLUIDS IN A CUBICAL CAVITY
Obai Younis Taha Elamin
ISBN:978-84-692-9056-9/DL:T-2069-2009

Nomenclature

A, B, C	Constants
Gr	Grashof number ($= \beta g(T_i - T_w)H^3/\nu^2$)
k	Thermal conductivity, W/m K
H	Cavity dimension, m
h	Convective heat transfer coefficient, W/m^2 K
Nu	Nusselt number ($= hH/k$)
P	Pressure, N/m^2
Pr	Prandtl number ($= \nu/\alpha$)
Q	Flux of intrusion ($= {}^{\alpha^{5/2}Rat^{3/2}}/_{H^3}$) m^2/s
Ra	Rayleigh number ($= \beta g(T_i - T_w)H^3/\nu\alpha$)
T	Temperature, ^oC
g	gravitational acceleration, m/s^2
t	time, s
u, v, w	velocity components, m/s
x, y, z	Cartesian coordinates, m

Greek letters

α	thermal diffusivity, m^2/s
β	thermal expansion coefficient K^{-1}
δ	boundary layer thickness, m
δ_{ij}	Kronecher delta
Δ	increment
μ	dynamic viscosity, kg/m s
ν	kinematic viscosity, m^2/s
ρ	density, kg/m^3
τ	non dimensional time ($= t\alpha Ra^{1/2}/H^2$)

ISBN:978-84-692-9056-9/DL:T-2069-2009

Subscripts

b	bottom
d	double-layer
I	intrusion
i	initial value
o	reference value
s	scale
st	stratification
T	thermal
t	top
w	wall value
$\star$	non-dimensional quantity

UNIVERSITAT ROVIRA I VIRGILI
NUMERICAL AND EXPERIMENTAL STUDY OF TRANSIENT LAMINAR NATURAL CONVECTION OF HIGH PRANDTL NUMBER FLUIDS IN A CUBICAL CAVITY
Obai Younis Taha Elamin
ISBN:978-84-692-9056-9/DL:T-2069-2009

Bibliography

[1] J. M. Fernàndez, C. S. Morros, K. M. Argüelles and P. L. Garcia, Numerical Simulation of the Fuel Oil Cooling Process in a Wrecked Ship, J Fluids Eng, 128 (2006) 1390-1394.

[2] J. Pallarès, I. Cuesta, A. Fabregat and F. X. Grau, Numerical simulation of fuel-oil cooling in the sunken prestige tanker, Proceedings of The ASME-ZSIS Int Thermal Sci Seminar II (2004) 439-445.

[3] G. K. Batchelor,Heat transfer by free convection across a closed cavity between vertical boundaries at different temperatures, Q J Appl Maths 12 (1954) 209-233.

[4] S. Ostrach, An analysis of laminar free-convection flow and heat transfer about a plate parallel to the direction of the generating body force, Report 1111. NACA(1952).

[5] V. P. Carey and J. C. Mollendrof,Variable viscosity effects in several natural convection flows, Int J Heat Mass Transfer 23 (1980) 95-109.

[6] A. Pantokratoras, Laminar free-convection in glycerol with variable physical properties adjacent to vertical plate with uniform heat flux, Int J Heat Mass Transfer 46 (2003) 1675-1678.

[7] J. C. Patterson, S. W. Armfield, Transient features of natural convection in a cavity, J Fluid Mech 219 (1990) 469-497.

[8] G. C. Jeevaraj and J. C. Patterson, Experimental study of transient natural convection of glycerol-water mixtures in a side heated cavity, Int J Heat Mass Transfer 35 (1992) 1573-1587.

ISBN:978-84-692-9056-9/DL:T-2069-2009

[9] X. Feng, J. C. Patterson and C. Lei, Shadowgraph observation of the transition of the thermal boundary layer in a side-heated cavity, Exp Fluids 38 (2005) 770-779.

[10] A. Davaille, C. Jaupart, Transient high Rayleigh number thermal convection with large viscosity variation, J Fluid Mech 25 (1993) 141-166.

[11] J. E. B. Nelson, A. R. Balakrishnan, S. S. Murthy, Experimental on stratified chilled-water tanks, Int J Refrigeration 22 (1999) 216-234.

[12] R. J. Shyu, J. Y. Lin, L. J. Fang, Thermal analysis of stratified storage tanks, J Solar Energy Eng 111 (1989) 54-61.

[13] F. Chen and C. H. Wu, Unsteady convective flows in vertical slot containing variable viscosity fluids, Int J Heat Mass Transfer 36 (1993) 4233-4246.

[14] R. De. C. Oliveski, M. H. Macagnan, J. B. Copetti, A. M. Petroll, Natural convection in a tank of oil: experimental validation of a numerical code with prescribed boundary condition, Exp Thermal Fluid Sci 29 (2005) 671-680.

[15] J. C. Patterson and J. Imberger, Unsteady natural convection in a rectangular cavity, J Fluid Mech 100 (1980) 65-86.

[16] A. F. Emery and J. W. Lee, The effects of property variations on natural convection in a square enclosure, J Heat transfer 121 (1999) 75-82.

[17] J. M. Hyun, Effect of the Prandtl number on heatup of stratified fluid in an enclosure, ASME J Heat Transfer 107 (1985) 982-984.

[18] M.Ogawa, G. Schubert, A. Zebib, Numerical simulations of three-dimensional thermal convection in a fluid with strongly temperature-dependent visocity, J Fluid Mech 233 (1991) 299-328.

[19] M. A. Cotter E. C. Michael, Transient cooling of petroleum by natural convection in cylindrical storage tanks-II. Effect of heat transfer coefficient, aspect ratio and temperature -dependent viscosity, Int J Heat Mass Transfer 36 (1993) 2175-2182.

UNIVERSITAT ROVIRA I VIRGILI
NUMERICAL AND EXPERIMENTAL STUDY OF TRANSIENT LAMINAR NATURAL CONVECTION OF HIGH PRANDTL NUMBER FLUIDS IN A CUBICAL CAVITY
Obai Younis Taha Elamin
ISBN:978-84-692-9056-9/DL:T-2069-2009

[20] Y. S. Lin, R. G. Akins, An experimental study of flow patterns and heat transfer by natural convection inside cubical enclosures, ASME conference, Seattle, Washington, USA, July1983.

[21] V. F. Nicolette and K. T. Yang, Transient cooling by natural convection in two dimensional square enclosure, Int J Heat Mass Transfer 28 (1985) 1721-1732.

[22] W. Lin and S. W. Armfield, Direct numerical simulations of natural convection cooling in a vertical circular cylinder, Int J Heat Mass Transfer 42 (1999) 4117-4130.

[23] W. Lin, S. W. Armfield, Natural convection cooling of rectangular and cylindrical containers, Int J Heat Fluid Flow 22 (2001) 72-81.

[24] W. Lin, S. W. Armfield and J. C. Patterson, Cooling of $Pr \leq 1$fluid in a rectangular conatiner, J Fluid Mech 574 (2007) 85-108.

[25] H. A. Van Der Vorst, Bi-CGSTAB A fast and smoothly converging variant of Bi-CG for the solution on non-symmetric linear system, J Sci Stat comput 3 (1992) 631-644.

[26] J. Pallarès, F. X. Grau, F. Giralt, Flow Transitions in Laminar Rayleigh Bénard Convection in a Cubical Cavity at Moderate Rayleigh Numbers, Int J Heat Mass Transfer 42 (1999) 753-769.

[27] L. Valencia, J. Pallarès, I. Cuesta, F. X. Grau, Rayleigh Bènard Convection of water in a perfectly conducting cubical cavity : effects of temperature -dependent physical properties in laminar and turbulent regimes, J Num Heat Transfer, part A 47 (2005) 333-352 .

[28] I. Cuesta, Estudi Numeric de Fluxos Laminars i Turbulents en una Cavitat Cubica, Ph.D. Thesis, Universitat Rovira i Virgili, Tarragona, Spain, 1993.

[29] H. K. Versteeg, W. Malalasekera, An introduction to computational fluid dynamics, Pearson Prentice Hall, 1995.

[30] J. H. Ferziger, M. Perić, Computational methods fo fluid dynamics, Springer, 2002.

ISBN:978-84-692-9056-9/DL:T-2069-2009

[31] X. Feng, J. C. Patterson and C. Lei, An experimental study of the unsteady thermal flow around a thin fin on a sidewall of a differentially heated cavity, Int J Heat Fluid Flow 29 (2008) 1139-1153.

[32] W. Merzkirch, Flow visualization, Academic press, 1987.

[33] X. Feng, Transient natural convection in a differentially heated cavity with and without a fin on the sidewall, Ph.D. Thesis, James Cook University, Townsville, Australia, 2006.

[34] W. M. Kays, M. E. Crawford, Convective heat and mass transfer, McGraw-Hill International editions, 1993.

[35] E. L. Koschmieder, Bénard cells and Taylor vortices, Cambridge University press, 1993.

[36] J. Jeong, F. Hussain, On the identification of vortex, Journal of Fluid Mechanics 285 (1995) 69-94.

[37] C. Lei and J. C. Patterson, Natural convection in a reservoir sidearm subject to solar radiation: experimental observations, Exp Fluids 32 (2002) 590-599.

[38] H. E. Huppert, The propagation of two dimensional and axisymmetric viscous gravity currents over a rigid horizontal surface, J Fluid Mech 121 (1982) 43-58.